



**THESIS APPROVAL**  
**GRADUATE SCHOOL, KASETSART UNIVERSITY**

Master of Engineering (Civil Engineering)

DEGREE

Civil Engineering

FIELD

Civil Engineering

DEPARTMENT

**TITLE:** Effect of Infill Configurations on RC Frame Building under Earthquake Loading

**NAME:** Mr. Karma Tshering

**THIS THESIS HAS BEEN ACCEPTED BY**

THESIS ADVISOR

( Assistant Professor Piya Chotickai, Ph.D. )

THESIS CO-ADVISOR

( Associate Professor Trakool Aramraks, Ph.D. )

THESIS CO-ADVISOR

( Mr. Barames Vardhanabhuti, Ph.D. )

DEPARTMENT HEAD

( Associate Professor Korchoke Chantawarangul, Ph.D. )

APPROVED BY THE GRADUATE SCHOOL ON

DEAN

( Associate Professor Gunjana Theeragool, D.Agr. )

THESIS

EFFECT OF INFILL CONFIGURATIONS ON RC FRAME BUILDING UNDER  
EARTHQUAKE LOADING



KARMA TSHERING

A Thesis Submitted in Partial Fulfillment of  
the Requirements for the Degree of  
Master of Engineering (Civil Engineering)  
Graduate School, Kasetsart University  
2010

Karma Tshering 2010: Effect of Infill Configurations on RC Frame Building under Earthquake Loading. Master of Engineering (Civil Engineering), Major Field: Civil Engineering, Department of Civil Engineering. Thesis Advisor: Mr. Piya Chotickai, Ph.D. 111 pages.

Unreinforced masonry infills are commonly used as partitions in frame buildings. The infills are considered as non-structural element and not considered to resist the applied loads. Due to the complexity introduced by infill walls, it is generally kept unaccounted during the analysis and design of building. The effects of non-structural masonry infills on the earthquake responses of reinforced concrete (RC) frame structures were investigated by using RC building models with various configurations of masonry infills. The diagonal strut model was employed to represent masonry infills. The RC buildings with three different numbers of storeys, including 4-storey, 8-storey and 12-storey, designed as per Indian Standard were considered. The effects of infill configurations on the seismic responses were studied with static nonlinear pushover analysis.

A comparison of the structural responses was made between the bare frames and infilled frames with various infill configurations. The results indicated that infills contributed to a large increase in initial stiffness of low rise building but as the building height increased, the effect of infills on the initial stiffness of buildings decreased. Consequently, neglecting stiffness and strength of infills may have undesirable effects such as soft story failure of buildings. The presences of infills in the building increase the performance of the building especially in the low rise buildings. The effect of masonry infills should therefore be considered in the performance analysis to obtain an accurate estimate of the responses for the buildings with high area of masonry infills.

---

Student's signature

---

Thesis Advisor's signature

## ACKNOWLEDGEMENT

This research would not have been successful without the help, support and guidance rendered by many people who were directly or indirectly involved in this work. I would like to express my sincere gratitude and appreciation to my thesis advisor Assistant Professor Dr. Piya Chotickai for his invaluable guidance, encouragement and insight provided throughout the research period. My sincere appreciation is also due to Associate Professor Dr. Trakool Aramraks and Dr. Barames Vardhanabhuti for their invaluable suggestions.

I would like to express my gratitude to the Thailand International Cooperation Agency (TICA) for the scholarship awarded for the study. Thanks are also to all the staff of the International Graduate Program in Civil Engineering (IPCE), Kasetsart University, and specifically to Dr. Trakool Aramraks and Dr. Warakorn for providing all the support and help. I would like to take this opportunity to thank all my class mates in graduate program in IPCE for making my stay at the university a memorable one. Thanks are due for my friends at AIT, Kingmongkut University, and Chulaborn Research Institute. I would like to thank my friend Laksanavadee Jaturapat (Nun) for helping me and making my stay in Thailand a memorable one. I would also like to thank Mr. Kinzang Norbu, Thrompoen of PCC and other staff of PCC for their help. Thanks to my friend Ugyen Dorji at College of Science and Technology for his help in this work.

Last but not the least, I thank to my mother for everything she did, and still doing for me. I am also thankful to my beloved wife Karma and loving son Rigsel Tenzin Norday for their unwavering patience, encouragement and understanding and also for having applauded my success, supported my goals, and accepted my failures.

Karma Tshering

April 2010

## TABLE OF CONTENTS

	<b>Page</b>
TABLE OF CONTENTS	i
LIST OF TABLES	ii
LIST OF FIGURES	iii
LIST OF ABBREVIATIONS	vi
INTRODUCION	1
OBJECTIVES	5
LITERATURE REVIEW	6
RESEARCH METHODOLOGY	47
RESULTS AND DISCUSSIONS	63
CONCLUSIONS AND RECOMMENDATIONS	87
Conclusion	87
Recommendations	89
LITERATURE CITED	91
APPENDICES	97
Appendix A Design of Reinforced Concrete Frames	98
Appendix B Effective Width Calculation of Diagonal Strut	104
CURRICULUM VITAE	111

## LIST OF TABLES

<b>Table</b>	<b>Page</b>
1 Behavior modes of solid infilled panel components	17
2 Simplified force-deformation relationship for masonry infill walls	25
3 Effective stiffness values	31
4 Modeling parameters for nonlinear procedures – Reinforced concrete beam	34
5 Modeling parameters for nonlinear procedures – Reinforced concrete column	39
6 Structural member sizes and reinforcements used for the study	51
7 Fundamental periods of different building models	66
 <b>Appendix Table</b>	
A1 Seismic weight calculation of 8-storey building	100
A2 Distribution of lateral forces	102

## LIST OF FIGURES

Figure		Page
1	Seismic hazard map of Bhutan	3
2	Interactive behaviour of frame and infill; analogous braced frame	9
3	Failure modes of infill	10
4	Effect of infill	11
5	Knee braced frame model for sliding shear failure of masonry infill	18
6	Masonry failure with X-shaped cracks	18
7	Failure mechanism of infill frames	21
8	Equivalent diagonal compression strut model	23
9	Idealized force-displacement relations of infill walls	26
10	Strength envelop for masonry infill panel	28
11	Generalized load-deformation relations for structural components	29
12	Procedure to identify plastic hinge location in horizontal spanning components	32
13	Moment-Rotation relation for moment hinge used in pushover analysis	33
14	Strain distribution corresponding to points on interaction diagram	40
15	Equivalent SDOF system parameters	42
16	Lumped plasticity beam element	43
17	Force-deformation relation of a typical plastic hinge	45
18	Typical plan and elevation of the models	49
19	The infill configuration models	52
20	Vertical section plan and general beam & column sections	53
21	Force-deformation for a typical plastic hinge	56
22	Response spectrum for 5% damping	58
23	Variation of fundamental period with percent of infill area in the models	65

## LIST OF FIGURES (Continued)

Figure		Page
24	Variation of fundamental period with different compressive strength of masonry infill	67
25	Variation of axial force in column $C_T$	68
26	Variation of axial force in column $C_C$	69
27	Bending moment in column $C_T$	69
28	Bending moment in column $C_C$	70
29	Capacity curve of 8-storey building (Model-A)	72
30	Damage distribution and failure mechanism of 8-storey building (Model-A)	73
31	Capacity curve of 8-storey building (Model-B)	74
32	Damage distribution and failure mechanism of 8-storey building (Model-B)	75
33	Comparison of capacity curves of Model-A and Model-B of 8-storey building	76
34	Effect of infill area on initial stiffness of building models	78
35	4-storey building model showing soft storey mechanism (Mode-C)	79
36	Capacity curve of 4-storey building models	80
37	Capacity curve of 8-storey building models	80
38	Capacity curve of 12-storey building models	81
39	Capacity curves of 4-storey building models (Model-B) with different compressive strength of infill	82
40	Capacity curves of 8-storey building models (Model-B) with different compressive strength of infill	83
41	Capacity curves of 8-storey building models (Model-B) with different infill thickness	83
42	Capacity curve of 4-storey building (Model-B) with demand curves of different level of earthquake	85

**LIST OF FIGURES (Continued)**

<b>Figure</b>		<b>Page</b>
43	Capacity curve of 8-storey building (Model-B) with demand curves of different level of earthquake	86
44	Capacity curve of 12-storey building (Model-B) with demand curves of different level of earthquake	86
<b>Appendix figure</b>		
A1	Lateral load application on the structure	103
B1	Equivalent diagonal compression strut model	106
B2	Plot between displacement and shear force from calculation	110

## LIST OF ABBREVIATIONS

ACI	=	American Concrete Institute
ASCE	=	American Society of Civil Engineers
ATC	=	Applied Technology Council
BBC	=	Bhutan Building Code
DL	=	Dead load
EQ	=	Earthquake
FEA	=	Finite element analysis
FEMA	=	Federal Emergency Management Agency
IS	=	Indian Standards
LL	=	Live load
RC	=	Reinforced Concrete

## **EFFECT OF INFILL CONFIGURATIONS ON RC FRAME BUILDING UNDER EARTHQUAKE LOADING**

### **INTRODUCTION**

Masonry is one of the man's oldest building material and probably one of the most maligned and most certainly the least understood as far as its structural behavior is concerned (Schneider and Dickey, 1980). The behavior of masonry is not easy to predict because of its inherent brittle nature and variable material properties, and yet masonry is widely used in the reinforced concrete (RC) frame for infill walls functioning as partitions, exterior walls, walls around stairs, elevators' service shafts, and etc. In the construction of infill walls, masonry is easier, faster and even cheaper than other materials.

The infill panels are commonly considered to be non-structural and means of providing enclosure and internal partition to the building. This fact is far from reality, as the infill panel will definitely interact with the enclosing frame, especially under seismic forces. It is observed in common practice of construction that specific construction measure is not taken to account for the interaction of panels and frames in spite of high seismicity in the regions. Failures that can be ascribed to the behavioral change of frames due to tight infill panel are common, and its catastrophic has been reported all over the worlds in high seismic regions (Degefa, 2005).

It is a common misconception that masonry infills in reinforced concrete or structural steel frames can only enhance their lateral load performance and must therefore always be beneficial to the earthquake resistance of the structure (Hashmi and Madan, 2008; Rodrigues et al. 2008). Earthquake damage can be traced to structural modification of the basic frame by so-called non-structural masonry partitions and infill panels. Masonry infill can drastically alter the intended structural response, attracting forces to parts of the structure that have not been designed to resist them. The high shear forces generated in the infilled frames are transmitted

primarily by shear stresses in the panels. Shear failure commonly occurs with shedding of masonry into streets below, or into stairwells, posing great hazard to life.

As the consequence, of the reasons mentioned so far, this study aims at disclosing the facts related to seismic performance of infilled frames buildings which otherwise has been not considered by the practitioners in Bhutan.

In the urban and semi urban areas of Bhutan, the trend of building constructions has changed from the traditional building type to reinforced concrete frames, mainly due to its durability and high resistance against the earthquake. The other reason for the shift from traditional building to RC frames is due to high cost of land in the urban areas and limited space for horizontal expansion, hence making the vertical growth more economical and viable.

The buildings are infilled RC frame buildings mostly infilled with masonry. The infills mainly functions as exterior wall and partitioning as mentioned earlier, while some used as an architectural features for aesthetic reason. From the very wide range of masonry materials such as adobe, brick, stone and concrete blocks; the most widely used is the burnt clay brick. One of the main reasons why brick masonry were used is economy and ease of construction as it is locally available and not much skilled labour is needed. The material used as infill in Bhutan is mostly a handmade burnt clay bricks of typical size 220mm x 115mm x 70mm. The infill thickness is typically of 125mm including the plaster finishes.

### **Statement of the problem**

The brick infills serving as partitions and exterior walls in the reinforced concrete frame structures are widely used in Bhutan. Since they are normally considered as architectural elements, their presence is often ignored by the structural engineers. During the analysis and design, only the weight of infill is considered, while the strength and stiffness contributed by the infill is ignored.

However, the infills tend to interact with the surrounding frame when subjected to earthquake load, substantially changing the seismic responses of the building producing undesirable effects like torsional effect, dangerous collapse mechanism, soft storey, variation in the vibration period or favourable effect of increasing the seismic resistance capacity of the buildings (Girgin and Darilmaz, 2007). Ignoring the effect of the infill in stiffening and strengthening the surrounding frame is not always a conservative approach, since the stiffer the building, the higher seismic loads it attracts, which are sometimes higher than the capacity of the structural components that the components fails.

In view of the above reasons, it is very important to assess and evaluate the performance of the reinforced concrete infilled frame structures in Bhutan. Most existing reinforced concrete frame buildings in Bhutan are low to medium rise typically five storeys with regular plans. However, the situation is changing as many high rise buildings are being planned due to space constraints and zero horizontal growth in the urban areas. The fast increasing in urban population, scarcity of land, high cost of land and demands for more housing units compels people for vertical growth, which is more economical and viable.

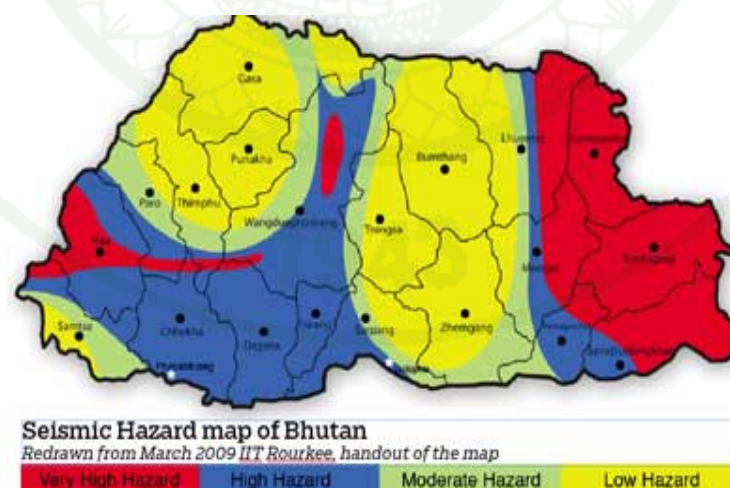


**Figure 1** Seismic Hazard Map of Bhutan

**Source:** Tenzin (2009)

Bhutan is situated on the foothills of Himalayan range, which according to the Indian system of categorization of seismic zones falls in a high-risk earthquake zone (zone V, where the zone factor is 0.36). Indian has divided its country into four seismic zones, viz. zone II (low seismic intensity), zone III (moderate seismic intensity) , zone IV (severe seismic intensity) and zone V (very severe seismic intensity) having zone factors 0.10, 0.16, 0.24 and 0.36, respectively. Bhutan recently has come up with a seismic hazard map as shown in Figure 1. The country is divided into four zones.

In the past, many earthquakes had hit the country and damaged many houses and buildings. The most recent earthquake measuring 6.3 on the Richter scale hit Eastern Bhutan on September 21, 2009, which killed 13 people, damaged 1100 traditional houses, 23 monasteries, 15 schools, and left many reinforced concrete frame buildings cracked (Choden, 2009).

Most of the low rise reinforced concrete infilled frame buildings in the second largest city of Bhutan, Phuentsholing, were built in the 1960s and 1970s before the introduction of seismic design code in Bhutan. These buildings are very much vulnerable to the earthquake. These buildings needs to be replaced with high rise buildings, as there is space constraint for horizontal growth. Furthermore, in the year 2001, a researcher, Roger Bilham of University of Colorado, USA published a report predicting a major earthquake of magnitude 8.1 and 8.3 on the Richter scale in Bhutan and the seismically active neighbouring areas of the Himalayan front 'very soon'.

Therefore, if any such major earthquake occurs as predicted, the consequences would be ravaging leading to loss of lives and properties. Hence, it is utmost important to evaluate the seismic response of reinforced concrete frames buildings designed as bare frame without considering the effect of the infill walls before a high rise buildings are built in Bhutan.

## OBJECTIVES

This study aims to investigate the response of unreinforced masonry infilled reinforced concrete moment resisting frame conventionally designed as a bare frame. The equivalent compression strut model was used based on the recommendation of FEMA 356 (2000) and researchers in recent past (Kiattivisanchai, 2001; Phatiwet, 2002; Inel M, et al., 2007; Baris B, et al., 2006) considering the important mechanical properties viz. compressive strength, modulus of elasticity and shear strength that affect the behavior of masonry wall. The specific objectives of the study are:

1. To study the nonlinear responses of infilled RC frame structure with different infill configurations under earthquake induced lateral load.
2. To study the effects on seismic performance of the structure due to infill wall on reinforced concrete frame subjected to various earthquake levels.
3. To study the effects on behaviour of building due to variation of infill wall thickness and infill compressive strength.

### Scope

The study will be mainly focused on the response behavior of infilled RC frame buildings with different infill configurations while other part will be on the response of RC buildings to different levels of earthquake. The scope of this study will be limited to three types of concrete frames of 4-storey, 8-storey and 12-storey with equal plan dimensions of length 20m with 4 bays and width 15m with 3 bays designed in accordance with the Indian Standards. A Nonlinear Static Pushover Analysis will be performed to evaluate the responses of structures with different infill configurations in accordance with the procedure given by ATC-40 (1996) and FEMA 356 while the modeling of the infills will be done as per the guidelines given in Chapter 9 of ATC-40 and FEMA 273/356.

## LITERATURE REVIEW

### 1. General Structural Forms

In the seismic design, one most important step is the conception of an effective structural system that needs to be configured with due regard to all important seismic performance objectives, ranging from serviceability considerations to life safety and collapse prevention. This step comprises the art of seismic engineering, since no rigid rules can, or should be imposed on the engineer's creativity to devise a system that not only fulfills seismic performance objectives but also pays tribute to functional and economic constraints imposed by the owner, the architect and other professionals involved in the design and construction of the building (Krawinkler and Seneviratna, 1998).

Also according to Smith and Coull (1991) the determination of the structural form of a building would ideally involve only the selection and arrangement of the major structural elements to resist most efficiently the various combinations of gravity and horizontal loadings. Usually the first and the foremost task of the designer is to select a structural system or forms of buildings that is most conducive to satisfactory seismic performance within the constraints dictated by the architectural requirements. The determination of structural systems of a building involves the selection of major structural elements to resist most proficiently the various combinations of gravity and lateral loads.

Generally speaking, typical multistory framed systems can be divided into three categories concerning their seismic behavior, namely reinforced concrete (RC) frames, masonry infilled frames, and wall- frame systems (Yong Lu, 2002). There are many types of frame structures. Following are the type of frame structures according to Smith and Coull, 1991. In this review only the masonry infilled frame was discussed in detail.

### 1.1 Braced - Frame Structures

The lateral resistance of the structure is provided by diagonal members that together with the girders form the web of the vertical truss with the column acting as the chords. The vertical shear on the building is resisted by the horizontal components because of the axial tensile or compression action in resisting lateral loads.

### 1.2 Rigid - Frame Structures

Rigid-Frame structures consist of columns and girders joined by moment resisting connections. Rigid-Frame construction is ideally suited for reinforced concrete buildings because of the inherent rigidity of reinforced concrete joints. It is also used for steel frame buildings but moment resisting connections in steel tends to be costly.

### 1.3 Wall - Frame Structures

When a shear walls are combined with rigid frames the walls tends to deflect in a flexural configuration while the frames tend to deflect in a shear mode. These actions are constrained to a common deflected shape by the horizontal rigidity of the girders and slabs. As a consequence, the walls and frames interact horizontally, especially at the top to produce a stiffer and stronger structure. The interacting wall-frame combination is appropriate for buildings in the 40 to 60 storey range, well beyond that of rigid frame.

### 1.4 Infilled Frame Structure

Infilled frame construction has been in use for more than 200 years. Basically infilled frames are associated with the construction of high rise buildings with the frame carrying the gravity loads and the infills providing enclosure and internal partitioning to the building. An original work on the investigation of the

interaction between the infill panels and frames began in 1950s in Russia (Polyakov, 1956). In the United States Benjamin and Williams (1958) reported the first research on the lateral load behavior of infilled frames. All the early studies were mostly concerned with the monotonic lateral strength capacity of the infilled frame systems.

The infill frame consists of a steel or reinforced concrete column and girder frame with infills of brickwork, concrete block work or cast in place concrete. They are usually provided as partitions, exterior walls, and wall around the stair, elevator and service shaft and treated as non structural element during the analysis and design. But it has been recognized by many researchers that it also serves structurally to brace the frame against horizontal in-plane loadings. The frame is designed for gravity loading only and in the absence of an accepted design method, the infills are presumed to contribute sufficiently to the lateral strength of the structure for it to withstand the horizontal loading. The simplicity of construction, and the highly developed expertise in building type of structure have made the infilled frame one of the most rapid and economical structural form for buildings. Absence of a well recognized method of design for infilled frames have restricted their use for bracing. So it has been more usual when designing an infilled frame structure to arrange for the frame to carry the total vertical and horizontal loading and to include the infills on the assumption that the infills do not act as part of the primary structure. On the other hand, it is evident from the frequently observed diagonal cracking of such infill walls that the approach is not always valid. The walls do sometimes attract significant bracing loads and in doing so, modify the structure's mode of behavior and the forces in the frame (Smith and Coull, 1991)

The use of masonry infill to brace a frame combines some of the desirable structural characteristics of each, while overcoming some of their deficiencies. The high in-plane rigidity of the masonry wall significantly stiffens the frame, while the ductile frame contains the brittle masonry, after cracking, up to loads and displacements much larger than it could achieve without the frame resulting in a relatively stiff and tough bracing system. The wall braces the frame partly by its in-

plane shear resistance and partly by its behavior as a diagonal bracing strut, as shown in the Figure 2a.

When the frame is subjected to lateral loading, the translation of the upper part of the column in each storey and the shortening of the leading diagonal of the frame cause the column to lean against the wall, as well as compress the wall along its diagonal. This is analogous to a diagonally braced frame as shown in Figure 2b.

The main three potential modes of failure of the infill wall arise as a result of its interaction with the frame. The first is shear failure stepping down through the joints of the masonry and precipitated by the horizontal shear stresses in the bed joints. The second is a diagonal cracking of the wall through the masonry along a line or lines parallel to the leading diagonal, and caused by tensile stresses perpendicular to the leading diagonal. The diagonal cracking is initiated at and spreads from the middle of the infill, where the tensile stresses are the maximum. In the third mode of failure, a corner of the infill at one of the ends of the diagonal strut may be crushed against the frame due to the high compressive stresses in the corner (Smith and Coull, 1991). These modes of failure are shown in Figure 3.

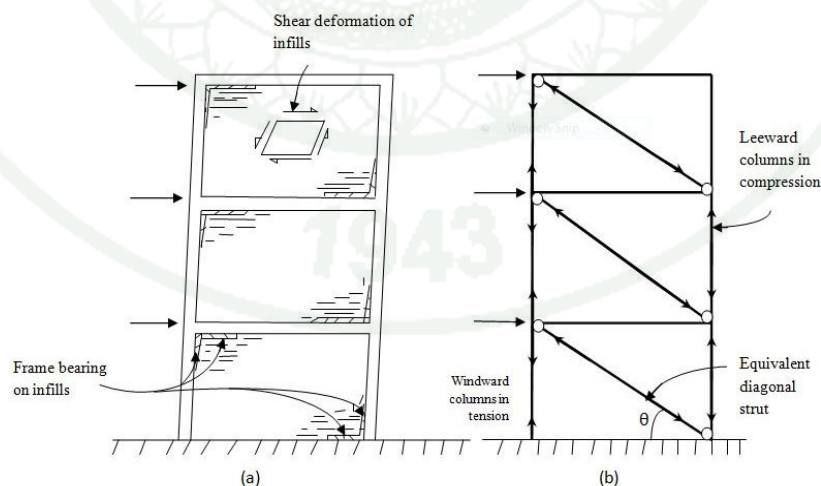


**Figure 2** a) Interactive behavior of frame and infill, and b) analogous braced frame

**Source:** Smith and Coull (1991)

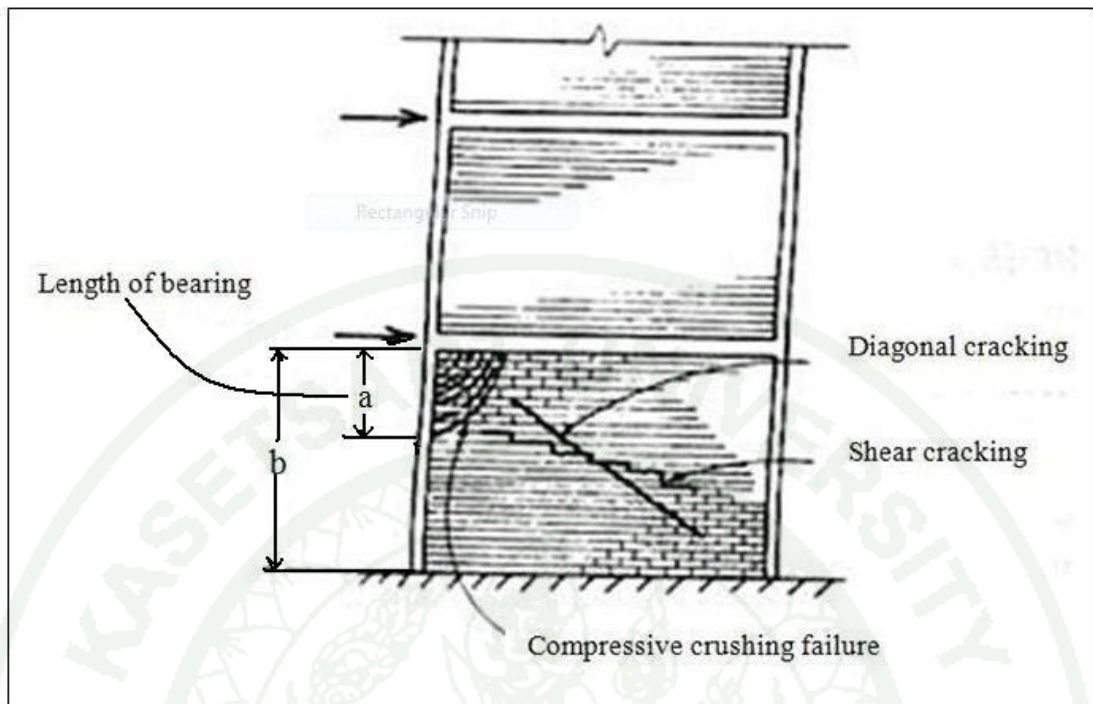


**Figure 3** Failure modes of infill

**Source:** Smith and Coull (1991)

The masonry infill might as well impart some deficiency to the RC frame structure. Irregularities, often unavoidable, contribute to complexity of structural behavior. The masonry infill can drastically alter the intended structural response, attracting forces to parts of the structure that have not been designed to resist them (Paulay and Priestley, 1992).

The behaviour of infill frames under lateral loading has been studied since the 1950s. Many researchers undertook the studies both experimentally and analytically to understand more about the behaviour of infilled frames under earthquake loads. The structural behaviour of an infill frame can be divided into two parts, in-plane and the out-of-plane. The simultaneous effect of in-plane and out-of-plane loading has usually been ignored in the research conducted to date, although in actual earthquake this effect will be present. Most of the studies have been carried out for in-plane loading due to stronger effect of infill wall in the in-plane direction.

Korkmaz et al (2007) studied the behaviour of a 3-storey RC frame building with different infill walls under the earthquake loading. The result demonstrated that the presence of infill walls modify the global behaviour of the building. The stability and integrity of RC frames are enhanced with infill walls. The building seems to have soft storey mechanism when there is irregular distribution of infill walls in elevation.

According to Das and Murty (2004), infilled frame tends to have less structural drift and more strength and stiffness compared to bare frames. The ductility is less and over strength is more for the infilled frames.

The presence of masonry infill affects the seismic behavior of building in the following ways (Tassios, 1984; Dowrick, 1987; Penelis and Kappos, 1997).

1. The stiffness of the building is increased, the fundamental period is decreased and therefore the base shear due to seismic action is increased.
  2. The distribution of the lateral stiffness of the structure in plan and elevation is modified.
  3. Part of seismic action is carried by infills, thus relieving the structural system.
  4. The ability of the building to dissipation energy is substantially increased.
- The more flexible the structural system, the greater the above effects of the infills.

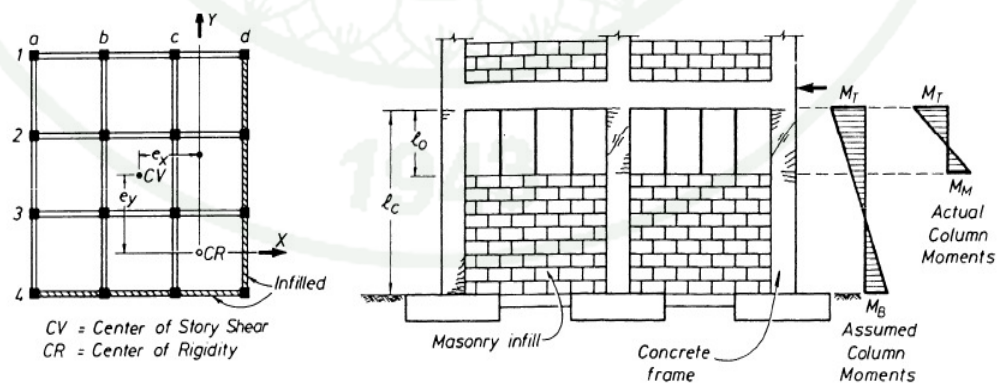


**Figure 4** Effect of infill

**Source:** Pauley and Priestley (1992)

For example, as shown in the left of Figure4, irregularities in placing of infill walls will cause change in the center of rigidity of the building thereby subjecting the building to seismic torsional response. The stiffness of infilled frames increase and consequently, the natural period of these frames will decrease and seismic force will correspondingly increase relative to other frames. Similarly, if the partial infill is provided as shown in the right, the infill will stiffen the frame, reducing the natural period and increasing the seismic force. The design level of shear force in the column will be given by:

$$V = \frac{M_T + M_B}{l_c} \quad (1)$$

Where

$V$  = Shear force of the structure for full column length

$M_T$  = Moment at the top of the column

$M_B$  = Moment at the bottom of the column

$l_c$  = Length of column

However, in reality, a structure will be subjected to shear force given by:

$$V^* = \frac{M_T + M_m}{l_o} \quad (2)$$

Where

$V^*$  = Shear force due to short column length

$l_o$  = Length of short column

$M_m$  = Actual moment at the start of short column

Shear failure can occur if the structure is not designed for the higher shear force given by Equation 2. Thus, if not taken in to account the effect of infill during analysis stage, infill might have some undesirable effect on the structure.

## 2. Model development of masonry infill and behavior modes

### 2.1 General

Masonry is a term covering a very wide range of material such as adobe, brick, stone, concrete blocks and etc. Each of these materials in turn varies widely in form and mechanical properties. It is a non-homogenous and anisotropic composite structural material, which can be used with or without reinforcement or in conjunction with other materials. Other than its use for primary structure, masonry is used for infill panels creating partitions, shafts and cladding walls.

Masonry structures of substantial size can be designed to perform adequately under major earthquakes, provided that careful design and detailing requirements are followed. By virtue of the form of construction, masonry has a large number of potential weak links than other materials. As masonry is a comparatively brittle material, it is generally necessary to design for higher seismic forces than that required for other materials. Its behavior is not perfectly elastic even in the range of small deformations. Even when lateral deformation of the wall is kept constant during a given time interval, changes in resistance and crack distribution can be observed during the test in the nonlinear range, which indicates the sensitivity of test results to the time history of lateral loads used for the simulation of seismic loads (Degefa, 2005).

When subjected to in-plane lateral forces, the infilled frames behavior is influenced by mechanical properties of the frame and infill materials, stress or lateral deformation levels, existence of openings in the infill, and the geometrical proportions of the systems. Existence of an initial gap between the frame and the infill also influences the behavior of the system. Usually it is assumed that the infills do not participate as a part of the primary structure in order to avoid load being transferred to them as a precaution. However, from the frequently observed diagonal cracking of infill walls, it is evident that the approach is not always valid. Hence, incorporation of modified mode of behavior for the frame and design of walls are required.

## 2.2 Historical Perspective

Since early 50's there have been numerous experimental and analytical researches to understand the influence of infill on the lateral strength and stiffness of frame structures. Masonry analysis has developed into a mature analytical field in the last half century as the guide rules are replaced by modern standards that are based on a mixture of proven empirical rules, extensive numerical and experimental research and finite element based analysis (Nichols, 2000). A rigorous analysis of infilled structure requires an analytical model of the force deformation response of masonry infills, and number of finite element models has been developed to predict the response of infilled frames (Asteris 2003; Shing *et al.* 1992; Dymiotis *et al.* 2001), such micro-modeling is too time consuming for analysis of large structures. Alternatively, a macro-model replacing the entire infill panel as a single equivalent-strut, by far has become the most popular approach.

Polyakov (1956) introduced the concept of equivalent diagonal strut and suggested that stresses from the frame to the infill are only transmitted in the compression zone of the infill, with a distribution more typical of a diagonally braced system than a shear wall.

Holmes (1961) proposed replacing the infill by an equivalent pin jointed diagonal strut of the same material and thickness with a width equal to one-third of its diagonal length. Later Stafford-Smith (1966) used the single strut to represent infill behavior followed by several multiple strut methods of analysis proposed (Chrysostomon *et al.*, 1988; Thiruvengadam, 1985; Pauley and Priestley, 1992; Mander *et al.*, 1994) for more accurate modeling of frame /panel interaction.

There are impediments to reliable modeling. The first being discontinuities of infill, resulting from soft stories or checkered patterns. The second is the large variation in construction practice over different regions and changes of materials over time. Early construction generally consisted of clay bricks (or stone masonry) with

iron/steel frames. With time, concrete frames become popular and concrete block units were used for the infill panels (Degefa, 2005).

Further research on the aspects of the static analysis of masonry was done by Dhanasekar (1985) and Ali (1987). Their work was instrumental in the development of the current code provisions related to the design of masonry structures for bi-axial loading, concentrated loads and in-plane loading of masonry. The early research mostly focused on developing improved seismic resistant design, analysis and construction techniques for new structures and little research was done on the response of existing structures which are designed only for gravity load with non-ductile detailing.

### 2.3 Components of Infilled wall

The infill panel and frame component are the main elements of the infilled frame structure system. The infill panels are usually categorized according to the material and geometric configuration. Among the different types of infill materials clay brick is one of the most common and traditional types of infill, mostly used all over the globe. Most of the masonry walls are unreinforced, except in the modern buildings where it may be reinforced, grouted-cavity wall construction (FEMA 306, 1998). The other form of infill wall like concrete masonry unit (CMU) is also the most common using hollow concrete blocks laid up with mortar. CMU may be left hollow or filled with grout with or without reinforcement.

The infills also have a wide range of geometric configurations. The aspect ratio (length/height) varies approximately from 1:1 to 3:1 with most ranging from 1.5:1 to 2.5:1. Based on the geometric configuration, there are two types of infilled panel components – solid panels and panels with openings. The openings are mostly used for functional requirements like doors, windows and ventilators.

## 2.4 Failure behavior modes

When the infilled frame is subjected to in-plane lateral forces its behavior is influenced by infill materials, stress or lateral deformation levels, existence of openings in the infill, geometrical proportion and even by the mechanical properties of the frames. The modes of failure of multistory infilled frames having reinforced concrete infill subject to dynamic load can be distinguished by the fact that whether or not connectors between the infill and the frames were provided. Models with solid infill failed by diagonal compression when there were no connectors, and failed by shear between the frame and the infill when there were connectors. Similarly, models with openings in the infill failed by bending in the lintel beams when there were no connectors, and they failed by shear in the lintel beams when there were connectors (T. C. Liaw, 1979).

Several potential failure modes for infill masonry walls are; firstly a horizontal sliding shear failure of masonry walls, second is the compression failure of diagonal strut, third is the diagonal tensile cracking which does not generally constitute a failure condition, as higher lateral forces can be supported, and lastly the tension failure mode (flexural) which is not usually a critical failure mode for infill wall (Paulay and Priestley, 1992).

Under small deformations the stiffness behavior is dominated by the panel stiffness characteristics (FEMA 306, 1998). As the deformation increases, the panel characteristics will be function of its element properties. Stair-stepped pattern of cracks through head and bed joints will result when the masonry units are strong relative to the mortar. When the mortar is stronger than the units, rather a rare case, cracks will develop through the units as well as the mortar. With the stair-stepped cracks, shear can continue to be resisted after cracking by the development of a compressive stress normal to the bed joints, characterized as a compression strut. If the mortar is weak relative to the units, an infill panel may crack along the bed joints instead of along the diagonal. When the infill panel is sufficiently strong in shear, the compressive stress at the compression corners will fail in crushing. The large forces

generated in this mode will be distributed to the beam and column members, and may result in either column or beam shear failures (Degefa, 2005).

**Table 1** Behavior modes of solid infilled panel components

Behavior mode	Description/Likelihood of Occurrence	Ductility
Bed-joint sliding	Occurs in brick masonry, particularly when length of panel is large relative to height. Aspect ratio is large and mortar strength is low	High
Diagonal cracking	Likely to occur in some form	Moderate
Corner compression	Crushing generally occurs with stiff columns	Moderate
Out-of-plane failure	More likely to occur in upper stories of buildings. However, out-of-plane “walking” is likely to occur in bottom stories, due to concurrent in-plane loading	Low

**Source:** FEMA 306 (1998)

Following are the failure modes (Table 1) recognized in masonry infilled frames.

i. Bed joint sliding: Bed-joint sliding or sliding shear failure is likely to occur when the bounding frame is strong and flexible (such as steel frames). A plane of weakness forms, usually near the mid-height level of the infill panel if the mortar beds are relatively weak compared to the adjacent masonry units. There is no limit to the displacement capacity of this behavior mode. If sliding shear failure of the masonry infill occurs, the equivalent structural mechanism changes from the diagonally braced pin-jointed frame to the knee-braced frame as shown in Figure 5.

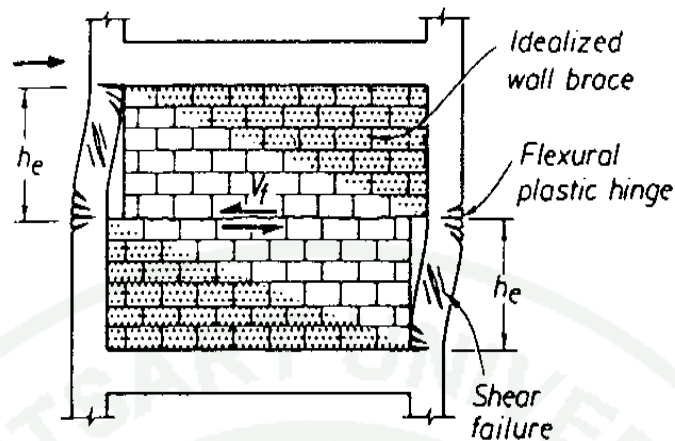


**Figure 5** Knee braced frame model for sliding shear failure of masonry infill

**Source:** Pauley and Priestley (1992)

ii. Diagonal Cracking: Transverse to the principle compression formed across the diagonal of an infill strains are tension strains. Diagonal cracks are formed as a result of the tensile strain exceeding the cracking strain of the infill material. These cracks commence in the center of the infill and run parallel to the compression diagonal. The cracks tend to propagate until they extend from one corner to the diagonally opposite corner. Diagonal cracking behavior usually signals the formation of a new diagonal strut behavior mode.

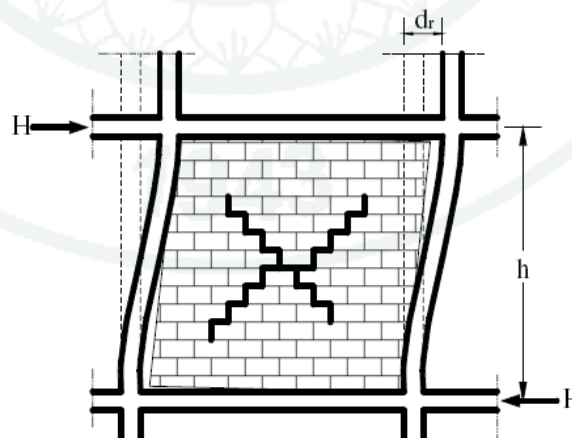


**Figure 6** Masonry failure with X-shaped cracks

**Source:** Penelis and Kappos (1997)

iii. Corner Compression: This is because of the high stress concentration at each corner of the compression diagonal. Corner crushing is located over a relatively small region for strong/stiff columns and beams; whereas for weaker frames, especially concrete frames, corner crushing is more extensive and the damage extends into the concrete frame itself.

iv. Out-of-plane failure: The failure is due to ground shaking perpendicular to the plane of a wall. Out-of-plane failure may occur in the upper stories of high rise buildings where the floor accelerations are basically resonances amplifications of prominent sinusoidal ground motion input. In the lower stories, when out-of-plane shear is combined with high in-plane story shears, infill panels tend to progressively “walkout” of the frame enclosure. Although complete out-of-plane failure is not common, there is some evidence that this behavior mode has occurred.

## 2.5 Modeling of masonry infill wall

Masonry infill walls are typically used in reinforced concrete buildings and are considered by engineers as nonstructural component. Though they are weak when compared to structural components, they can alter the response of the structures drastically (Kiattivisanchai, 2001; Phatiwet, 2002; Inel M, et al., 2007, Baris B et al., 2006). The presence of infill wall affects the lateral strength, stiffness and ductility of the structures. The effects of nonstructural masonry infills can modify the seismic behaviour of framed buildings to a large extent. The positive effect is that the panels can dramatically increase the global stiffness and strength of the structure, at least before the panels are severely damaged. Moreover, the presence of the panels results in a larger energy dissipation capacity of the structure. On the other hand, potentially negative effects that should be considered: torsional effects induced by in-plan irregularities or by failure of some of the panels, soft-storey effects induced by irregularities in elevation, short-column effects due to openings, concentration of forces in the elements of the frame due to interaction with the panels. Neglecting the effects of nonstructural infills does not, in general, result in a safe design, even though this is the practice suggested by most design codes (Negro and Colombo, 1997). For

these reasons, it is important to consider infill wall in analysis, design and evaluation of seismic response of buildings.

Masonry exhibits distinct directional properties, due to the influence of mortar joints acting as planes of weakness. Depending upon the orientation of the joints to the stress directions, failure can occur in the joints alone or simultaneously in the joints and blocks (Degefa, 2005).

At low level of in-plane lateral forces, the frame and infill wall panel will act in a fully composite fashion as a structural with boundary elements. With increase in lateral deformation, frames attempt to deform in a flexural mode but infill wall panel in shear mode. This leads to separation between frame and wall panel at the corners on the tension diagonals, and development of diagonal compression strut on the compression diagonal (Kiattivisanhai, 2001). As mentioned earlier the infill wall itself may fail in a variety of modes, most often involving some combination of bed joint sliding, corner crushing and diagonal cracking as shown in Figure 7.

Masonry walls are modeled using many methods and concepts. The two main methods are micro-modeling and macro-modeling. In the macro-modeling concept, the masonry wall is represented by an equivalent diagonal compression strut. Different researchers use different concept to model the equivalent diagonal compression strut in the macro-modeling methods.

a) FEMA-356 model

Masonry walls are modeled using equivalent compression strut concept based on recommendations of FEMA-273 and FEMA-356 by researchers in the recent past (Kiattivisanhai, 2001, Phatiwet, 2002; Inel M, et al., 2007; Baris B, et al., 2006) considering the important mechanical properties viz. compressive strength, modulus of elasticity and shear strength that affect the behavior of masonry wall. In addition, shear strength of un-cracked masonry wall is typically modeled with Mohr-Coulomb failure criteria relation as shown in Equation 3. Paulay and Priestly (1992)

recommends an average value of cohesive strength, ( $\tau_o$ ) of 4% masonry compressive strength, and a typical value of coefficient of friction, ( $\mu_f$ ) of 0.5.

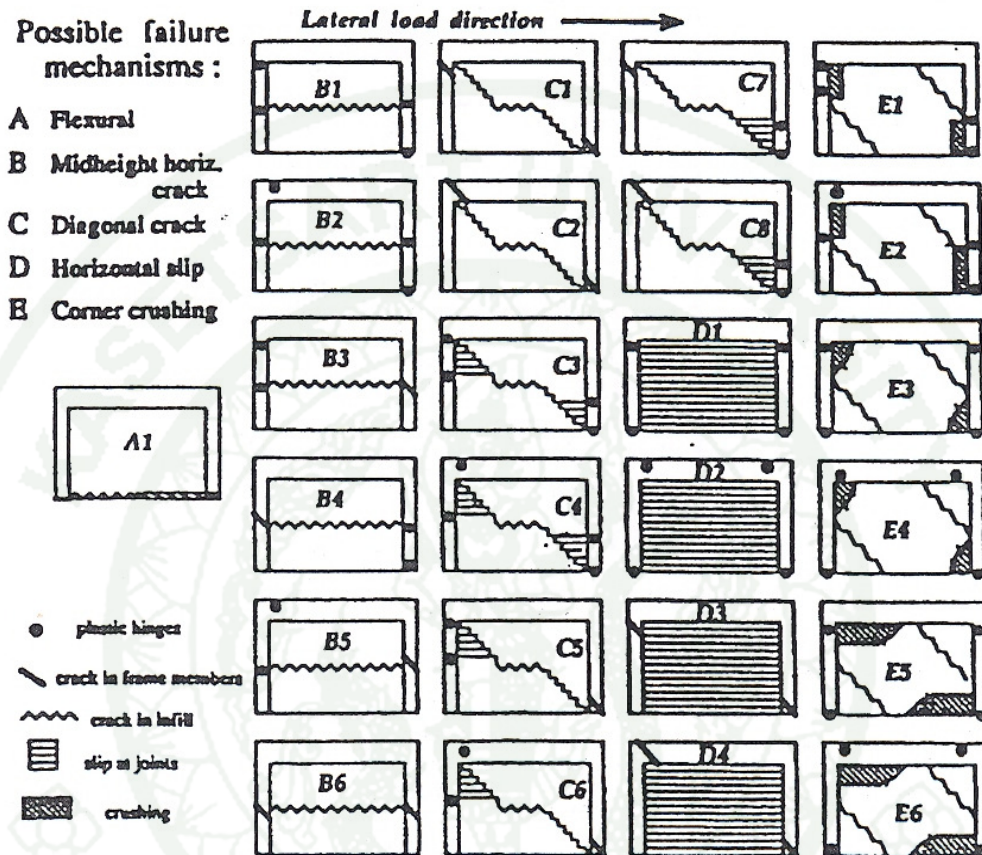


**Figure 7** Failure mechanisms of Infill Frames

Source: Phatiwet (2002)

These recommended values were used in the calculation of shear strength of masonry infill wall as follows

$$\tau_f = \tau_o + \mu_f \sigma_n \quad (3)$$

Where,

$\tau_o$  = cohesive capacity of the mortar beds

$\mu_f$  = sliding friction coefficient along the bed joint

$\sigma_n$  = vertical compression stress in the infill walls.

Applying the panel dimension, maximum horizontal shear force  $V_{ine}$  is assessed as follows.

$$V_{inf} = \tau_o t l_{inf} + \mu_f N \quad (4)$$

Where,

$t$  = infill wall thickness

$l_m$  = length of infill panel

$N$  = vertical load in infill walls.

In FEMA -306 (1988),  $N$  is determined to be the vertical load applied by vertical shortening strain in the panel due to lateral drifts.

$$N = l_{inf} t E_m r^2 \quad (5)$$

Where,

$E_m$  = Young's modulus of the masonry

$r$  = Inter story drift angle

However, the external vertical load is zero for the infill walls of the building and only the vertical component of the strut compression force is considered. Therefore, maximum shear force can be calculated as

$$V_{ine} = R_s \cos \theta \quad (6)$$

Where,

$R_s$  = Compressive strength of diagonal strut.

As stated earlier, the equivalent strut concept was used to model masonry infill wall. Based on the concept, the stiffness contribution of infill wall is presented by an equivalent diagonal compression strut as shown in Figure 8. The thickness and modulus of elasticity of strut are assumed to be same as those of infill walls. Furthermore, the width of equivalent strut 'a' is calculated using Equation 7, suggested by FEMA-273/356.

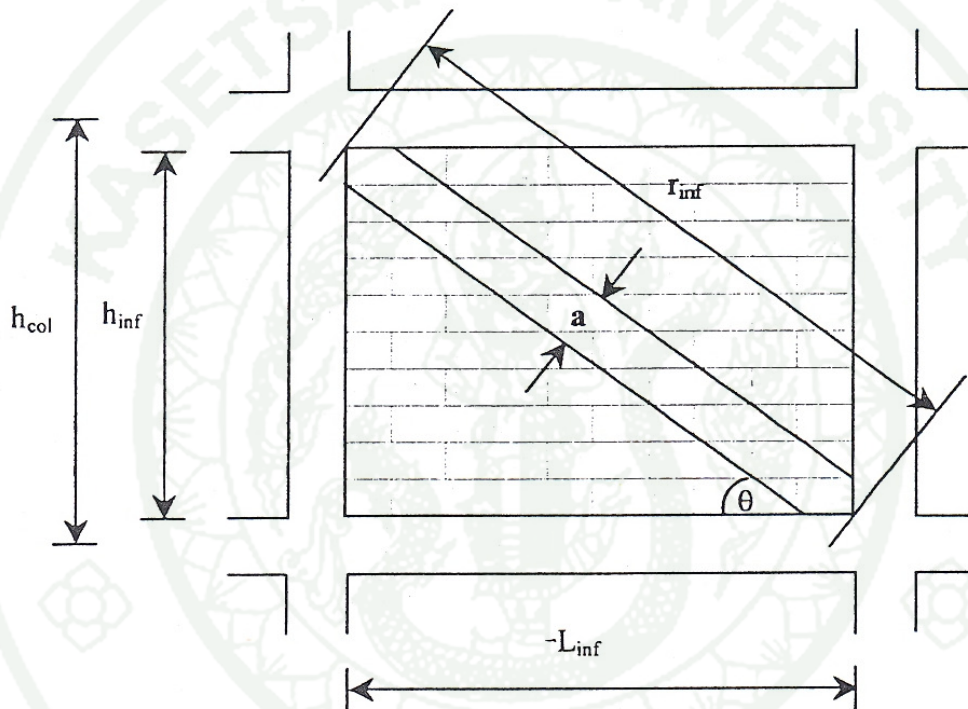


**Figure 8** Equivalent Diagonal Compression Strut Model

**Source:** Phatiwet (2002)

$$a = 0.175(\lambda h_{col})^{-0.4} r_{inf} \quad (7)$$

$$\lambda = \left[ \frac{E_{me} t_{inf} \sin 2\theta}{4E_{fe} I_{col} h_{inf}} \right]^{1/4} \quad (8)$$

Where,

$a$  = Diagonal strut width

$h_{col}$  = Column height between centerlines of beams

$I_{col}$  = Moment of inertia of column

$h_{inf}$  = Height of infill wall

$E_{fe}$  = Expected modulus of elasticity of frame material

$E_{me}$  = Expected modulus of elasticity of infill material

$L_{inf}$  = Length of infill panel, in.

$r_{inf}$  = Diagonal length of infill panel, in.

$t_{inf}$  = Thickness of infill panel and equivalent strut

In SAP2000, the equivalent diagonal compression strut is modeled as an axial element having a linear axial hinge along its length (Phatiwet, 2002). According to FEMA-356, idealized force displacement relations for infill wall are defined by a series of straight line segments shown in Figure 9. These relations are plotted between normalized force and story drift ratio. Variables  $d$  and  $e$  representing nonlinear deformation capacities of infill walls are expressed in terms of percentage story drift ratio as shown in Table 2. In absence of recommended values of  $c$  and  $e$ , these values are set equal to zero (Phatiwet, 2002; Inel M et al, 2006, Karchung, 2008). Finally, the load deformation relation of nonlinear axial hinge used in equivalent strut is as shown in Figure 9. In order to determine the expected strength of strut,  $R_s$ , the expected shear strength,  $V_{ine}$  was used.  $V_{ine}$  was calculated as the product of the net horizontal area of the infill wall panel, and the shear strength of the masonry infill wall was obtained from Equation 4. Therefore, the axial compression strength of equivalent strut  $R_s$ , (Equation 9) was obtained by solving Equation 4 and 6 simultaneously.

$$R_s = \frac{\tau_o}{[1 - \mu_f (\frac{h_{inf}}{L_{inf}})]} L_{inf} t_{inf} \quad (9)$$

$$\text{Where, } \sin\theta = \frac{h_{inf}}{r_{inf}} \quad \cos\theta = \frac{L_{inf}}{r_{inf}}$$

The axial yield deformation in strut is calculated directly from the axial stiffness of strut and  $R_s$ . In addition, the deformation capacities provided in Table 2 is transformed to represent the deformation in the axial direction of the equivalent diagonal compression strut.

**Table 2** Simplified force-deformation relationship for masonry infill walls

$\beta = V_{fre}/V_{ine}$	$L_{inf}/h_{inf}$	c	d (%)	e (%)	Acceptance Criteria	
					LS (%)	CP (%)
$0.3 \leq \beta < 0.7$	0.5	n.a.	0.5	n.a.	0.4	n.a.
	1.0	n.a.	0.4	n.a.	0.3	n.a.
	2.0	n.a.	0.3	n.a.	0.2	n.a.
$0.7 \leq \beta < 1.3$	0.5	n.a.	1.0	n.a.	0.8	n.a.
	1.0	n.a.	0.8	n.a.	0.6	n.a.
	2.0	n.a.	0.6	n.a.	0.4	n.a.
$\beta \geq 1.3$	0.5	n.a.	1.5	n.a.	1.1	n.a.
	1.0	n.a.	1.2	n.a.	0.9	n.a.
	2.0	n.a.	0.9	n.a.	0.7	n.a.

Source: FEMA-356 (2000)

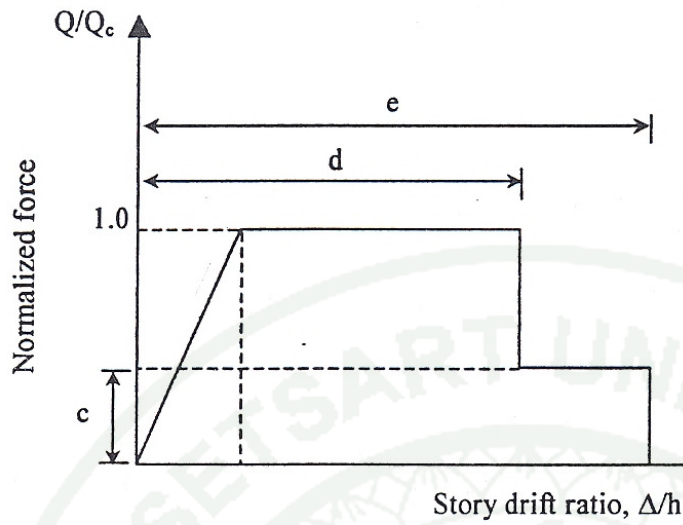


**Figure 9** Idealized Force-Displacement Relations of Infill Walls

**Source:** FEMA 356 (2000)

b) Madan's model

Considering the infill frame shown in Figure 8, the maximum lateral force  $V_m$  and corresponding displacement  $U_m$  in the infill masonry panel can be obtained as (Madan et al, 1997):

$$V_m \leq A_d f'_m \cos \theta \leq \frac{vtl_{inf}}{(1 - 0.45 \tan \theta) \cos \theta} \leq \frac{0.83tl_{inf}}{\cos \theta} \quad (10)$$

$$U_m = \frac{\epsilon'_m r_{inf}}{\cos \theta} \quad (11)$$

Where,

$f'_m$  = masonry prism strength

$\epsilon'_m$  = corresponding strain

$\theta$  =inclination of the diagonal strut

$v$  = basic shear strength of masonry

$A_d$  = area of the equivalent diagonal strut.

The shear strength obtained from the failure modes, sliding shear failure and diagonal compression failure may not exceed  $8.3 \text{ kg/cm}^2$  as recommended by ACI 530-88. Therefore, the corresponding shear strengths cannot be greater than the following value.

$$\frac{V_{\max}}{tl_{\text{inf}}} = 8.3 \text{ kg/cm}^2 \quad (12)$$

The monotonic lateral force-displacement curve is completely defined by the maximum force  $V_m$ , corresponding displacement  $U_m$ , the initial stiffness  $K_0$  and the ratio  $\alpha$  of the post yield to pre yield stiffness. The initial stiffness  $K_0$  of the infill masonry panel may be estimated using the Equation 13. (Madan et al, 1997; Murthy and Das, 2004; Mostafaei and Kabeyasawa, 2004):

$$K_o = 2\left(\frac{V_m}{U_m}\right) \quad (13)$$

The lateral yielding force  $V_y$  and displacement  $U_y$  can be calculated for the geometry in Figure 10.

$$V_y = \frac{V_m - \alpha K_o U_m}{1 - \alpha} \quad (14)$$

$$U_y = \frac{V_y}{K_o} \quad (15)$$

In this study, the FEMA 356 model was used as this model is readily available in SAP2000.

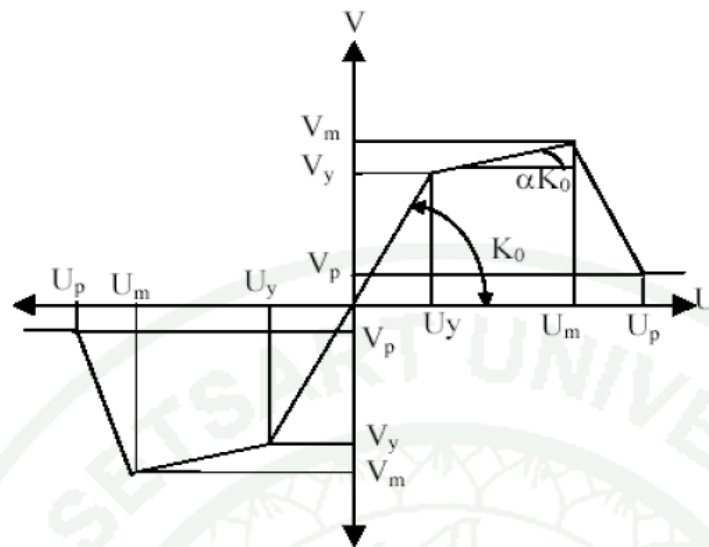


**Figure 10** Strength Envelop for Masonry Infill Panel

**Source:** Mostafaei and Kabeyasawa (2004)

### 3. Modeling of Structural Components

The beam and column components behavior has been modeled by past researchers using nonlinear load-deformation relations defined by a series of straight line segments. Figure 11 illustrates a typical representation of load-deformation relations for the structural components. In this figure,  $Q_c$  refers to the strength of the component and  $Q$  refers to the demand imposed by the earthquake. As shown in the Figure 11, point  $A$  corresponds to the unloaded condition and then the response is linear to an effective yield point  $B$ , followed by yielding, strain hardening for the structural components to point  $C$ . The drop in resistance, strength degradation from point  $C$  to point  $D$  represents initial failure of the components. It may be associated with the phenomena such as failure of longitudinal reinforcements, falling of concrete or sudden shear failure following the initial yield. The residual resistance from point  $D$  to point  $E$  is to represent the components that have lost their lateral force resistance but are still capable of sustaining gravity loads. Point  $E$  is a point defining the maximum deformation capacity. Deformation beyond this point should not be

permitted because gravity load no longer be sustained. Point  $D E$  is the post-failure capacity region.

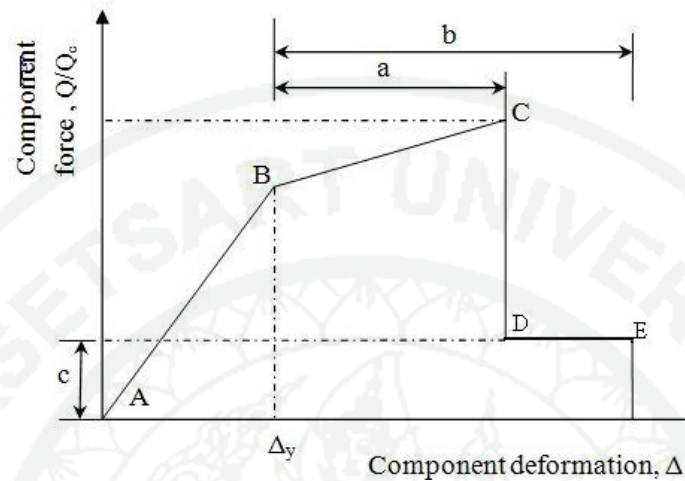


**Figure 11** Generalized Load-Deformation relations for Structural Components

**Source:** FEMA-356 (2000)

### 3.1 Component Initial Stiffness

Reinforced concrete component initial stiffness is represented by a secant value defined by the effective yield point of component, as shown by the initial slope in Figure 11. For flexure dominated components, the stiffness corresponds approximately to the fully cracked stiffness. For shear dominated components, the stiffness corresponds approximately to the un-cracked stiffness. The component stiffness value will affect the distribution of component forces and the hierarchy of formation of component yielding. There are many factors that affect the value of stiffness in each concrete component such as material properties, component dimensions, reinforcement's qualities, and boundary condition. Important variations in effective stiffness could occur even in similar conditions. As a result, it is impractical to calculate effective stiffness directly from the basic mechanics principles.

The recommended initial stiffness, corresponding to stiffness near yield, in many cases will be considerably less than the gross-section stiffness commonly used in conventional design practices. The effective stiffness for a given component will depend on the source of deformation and the anticipated stress levels.

Flexural stiffness can be calculated according to conventional procedures that take into account the variation of flexural moment and cracking along the component length. In the flexural theory, it is commonly assumed that the concrete in the tension zone carries no tension stress. However, in reality, cracking in the reinforced concrete components occurs at discrete locations, and significant tension stiffening is resulted from tension carried by concrete between the cracks (Park and Paulay, 1974; ATC-40, 1996). For shear-dominated components, the onset of shear cracking commonly results in a dramatic reduction in effective stiffness and may be considered to represent the end of elastic behavior for the component. Therefore, the effective initial stiffness may be based on the gross section properties. For an axial load-dominated component, the appropriate stiffness depends on whether the axial load is tensile or compressive under applicable load combination. Where it is compressive, the stiffness can be derived from the gross-section or un-cracked transformed-section properties. Where it is tensile, and has sufficient magnitude to crack, the stiffness should be based on the reinforcement only, although some adjustment to account for tension stiffening may be appropriate. However, it should be noted that tension stiffening tends to degrade under repeated loading. For many reasons, the approximate values of component initial stiffness are used instead of values calculated directly from the principles of mechanics. The approximate value of effective stiffness of each concrete component is given in ATC-40 & FEMA-273/356 as shown in Table 3 which was used in the study.

**Table 3** Effective Stiffness Values

Component	Flexural		
	Rigidity	Shear Rigidity	Axial Rigidity
Beams-nonprestressed	$0.5 E_c I_g$	$0.4 E_c A_w$	$E_c A_g$
Beams-prestressed	$E_c I_g$	$0.4 E_c A_w$	$E_c A_g$
Columns in compression	$0.7 E_c I_g$	$0.4 E_c A_w$	$E_c A_g$
Columns intension	$0.5 E_c I_g$	$0.4 E_c A_w$	$E_c A_g$
Walls-uncracked	$0.8 E_c I_g$	$0.4 E_c A_w$	$E_c A_g$
Walls-cracked	$0.5 E_c I_g$	$0.4 E_c A_w$	$E_c A_g$
Flat slabs-nonprestressed	-	$0.4 E_c A_g$	
Flat slabs-prestressed	-	$0.4 E_c A_g$	

Note:  $I_g$  for T-beams may be taken as twice the values of  $I_g$  of the web.

For shear stiffness, the quantity  $0.4 E_c$  has been used to represent the shear modulus  $G$

**Source:** ATC-40 (1996)

### 3.2 Beams

Following the guidelines of ATC-40, FEMA 273 and FEMA 356, beams have been modeled explicitly by the line elements having linear elastic properties along the length and the associated nonlinearities included in the moment rotation hinges at the ends where there is potential of yielding as shown in Figure 12 . Such type of modeling approach was adopted by Kiattivisanhai, 2001, also by Phatiwet, 2002; Shrestha, 2005 and Inel M, et al, 2007 and Karchung 2008. Attempts have been made to include the truly governing characteristics in these models for accurate analysis of the building like the anchorage slip of reinforcements (Barin et al, 2002). Many researchers have been conducted to simulate accurately the behavior of the

beams. New fiber models have been developed in which the element deformation is defined by the curvatures that develop at multiple locations along the length of the element which was lacking in the models used earlier. In such elements, inelasticity is allowed to spread along the length of the entire element.

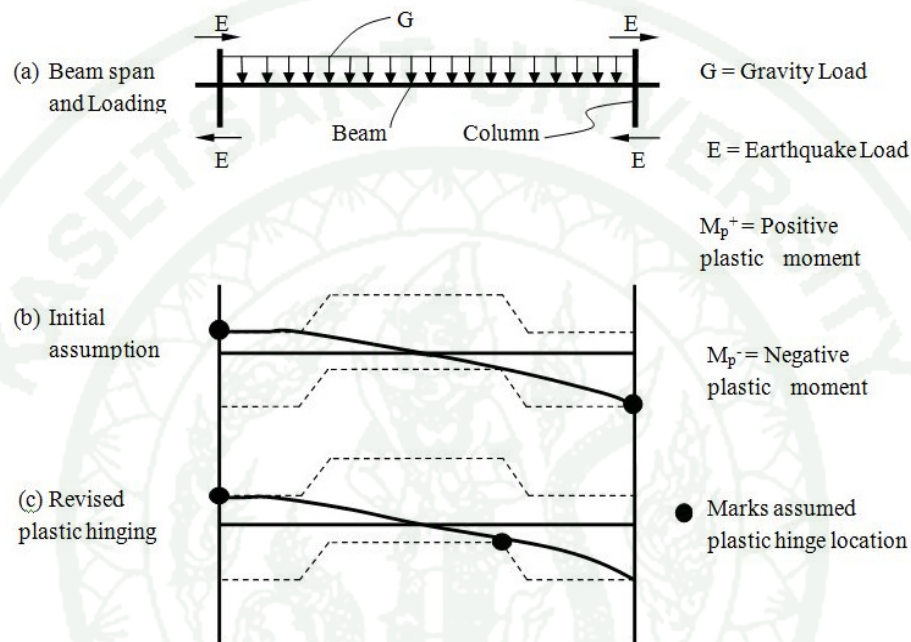


**Figure 12** Procedure to identify Plastic Hinge location in horizontal spanning Components

**Source:** ATC-40 (1996)

Beams are modeled as line element having linearly elastic properties along the length with nonlinear moment-rotation hinges at the locations where potential yielding can occur. The hinges used to represent flexural behavior of beams have the relationship between moment and plastic rotation as shown in Figure 13. The flexural strengths of beam component are calculated on the basis of assumed monotonic load behavior. It is assumed that the plane sections before bending remain plane after bending and strains vary linearly across the section. Stresses are assumed to be unique related to strain according to monotonic stress-strain relationship.

In the moment-rotation relation shown in Figure 13, point B is the point where reinforcement bars reaching first yielding with rotation  $\theta_y$  and moment  $M_y$ . Moment at point C shows the expected flexural strength that is defined as the mean maximum resistance expected over the range of deformations to which the component is likely to be subjected. In the calculation of expected flexural strength, expected material strength including strain hardening was taken into account in this study.

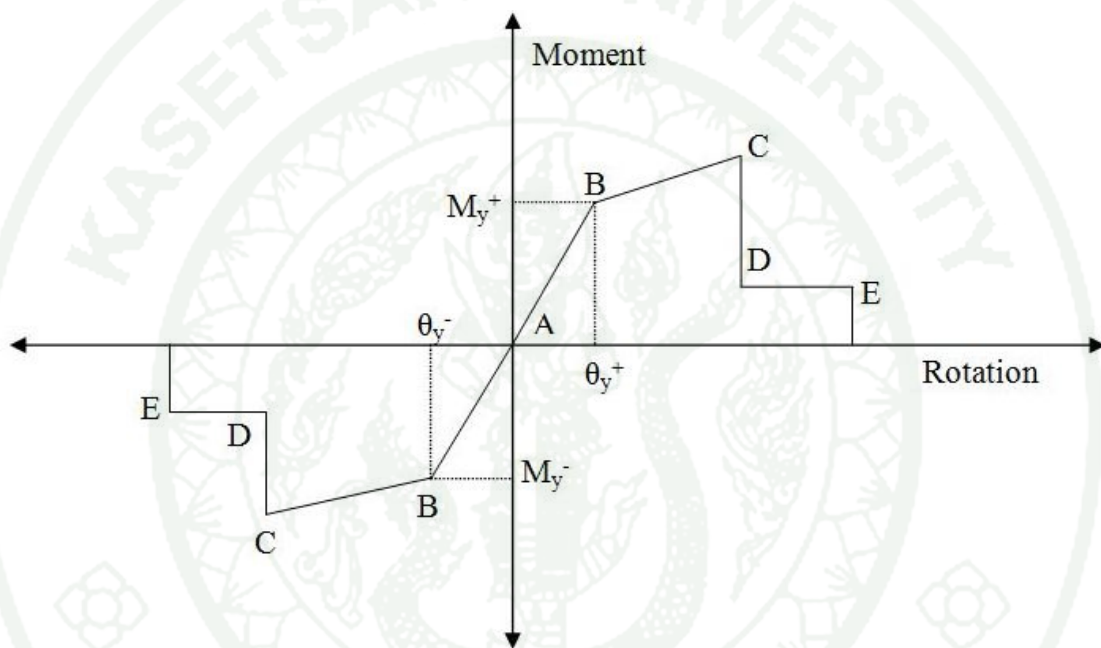


**Figure 13** Moment-Rotation relation for Moment Hinge used in Pushover Analysis

**Source:** Karchung (2008)

Furthermore, the plastic hinge rotation capacities at point C and E in Figure 13 may be derived from experiment or rational analysis considering the interaction between flexural and shear. As plastic hinge rotation increases, the widening of flexure-shear crack reduces the capacity for shear transfer by aggregate interlock and the shear strength reduces resulting in ductile shear failure.

ATC-40, however recommends the plastic hinge rotation capacity of reinforced concrete beams which take into account the important factors such as

reinforcement ratio, transverse reinforcements and design shear force of the beam components as shown in Table 4. Hence, these values were used in this study.

**Table 4** Modeling Parameter for Nonlinear Procedure- Reinforced Concrete Beam

<i>Component Type</i>	<i>Modeling Parameters</i> <sup>3</sup>				
	<i>Plastic Rotation Angle</i>		<i>Residual Strength</i>		
	<i>(rad)</i>		<i>Ratio</i>		
	<i>a</i>	<i>b</i>	<i>C</i>		
<b>1. Beams controlled by flexure</b> <sup>1</sup>					
$\frac{\rho - \rho'}{\rho_{bal}}$	<i>Transverse Reinforcement</i>	$\frac{V}{b_w d \sqrt{f'_c}}$ <sup>4</sup>			
≤ 0.0	C	≤ 3	0.025	0.05	0.2
≤ 0.0	C	≥ 6	0.02	0.04	0.2
≥ 0.5	C	≤ 3	0.02	0.03	0.2
≥ 0.5	C	≥ 6	0.015	0.02	0.2
≤ 0.0	NC	≤ 3	0.02	0.03	0.2
≤ 0.0	NC	≥ 6	0.01	0.015	0.2
≥ 0.5	NC	≤ 3	0.01	0.015	0.2
≥ 0.5	NC	≥ 6	0.002	0.01	0.2
<b>2. Beams controlled by shear</b> <sup>1</sup>					
Stirrup spacing ≤ d/2			0.0	0.02	0.2
Stirrup spacing > d/2			0.0	0.01	0.2
<b>3. Beams controlled by inadequate development or splicing along span</b> <sup>1</sup>					
Stirrup spacing ≤ d/2			0.0	0.02	0.0
Stirrup spacing > d/2			0.0	0.01	0.0
<b>4. Beams controlled by inadequate embedment into beam-column joint</b> <sup>1</sup>					
			0.015	0.03	0.2

**Source:** ATC-40 (1996)

As stated earlier, not only flexural failure mode but also shear failure mode should be considered. The shear strength of the reinforced concrete beam is considered to be the sum of shear forces carried by concrete,  $V_c$  and shear reinforcement  $V_s$ . ACI 318-2002 recommends that the contribution of concrete to shear strength of beam  $V_c$  can be calculated as follows:

$$V_c = 0.166 \sqrt{f'_c} b_w d \quad (16)$$

ACI 318-02 also suggests a value of  $V_c$  with more detailed calculation as below in Equation 17

$$V_c = \left( \sqrt{f'_c} + 120 \rho_w \frac{V_u d}{M_u} \right) \frac{b_w d}{7} \quad (17)$$

Where,

$V_c$  = Shear strength contribution attributed to concrete

$V_u$  = Factored shear force

$M_u$  = Factored moment of section

$f'_c$  = Concrete compressive strength

$b_w$  = Web width

$d$  = Effective depth

$\rho_w$  = Longitudinal steel ratio

This equation takes into account the effect of longitudinal steel ratio and also the shear span to depth ratio. However, it gives conservative value of  $V_c$  when longitudinal steel ratio ( $\rho_w$ ) is large and tends to overestimate when ( $\rho_w$ ) is small. Paulay and Priestley (1992) recommend that the shear strength provided by concrete may be taken as:

$$V_c = (0.07 + 10 \rho_w) \sqrt{f'_c} b_w d \leq 0.2 \sqrt{f'_c} b_w d \quad (18)$$

The major effects including shear resistance, tensile strength of concrete and longitudinal steel ratio are taken into account in this equation. It provides more accurate estimate of the value of  $V_c$  than the value in ACI. So, the Equation 17 was used in the calculation of shear resistance of beam component contributed by concrete in this study.

Apart from the shear strength presented by concrete, contribution of shear reinforcement prevents a shear failure resulting from diagonal tension. Because of reversal of shear forces in members due to earthquake, shear reinforcements in the form of stirrups are placed at right angle to the axis of the member. Accordingly the contribution of shear reinforcement to the total shear resistance based on truss model with 45 degree diagonal strut is as follows:

$$V_s = \frac{A_v \cdot f_{yt} \cdot d}{s} \quad (19)$$

Where,

$V_s$  = Shear strength contribution attributed to shear reinforcement

$A_v$  = Cross-sectional area of transverse reinforcement

$f_{yt}$  = Yield stress of reinforcing steel

$s$  = Longitudinal spacing of transverse reinforcement

This Equation was used to estimate the contribution of shear reinforcement to shear strength of beam in this study.

### 3.3 Columns

Columns are modeled in the same manner as beams to adequately represent important characteristics of reinforced concrete column components subjected to gravity and lateral loadings. Multiple failure modes, stiffness and strength degradation are considered. Similar to the beams, the columns are modeled as line element having linear elastic properties along its length with nonlinear moment-rotation hinges at the ends. However, there are significant axial force variations under the action of earthquake load that affect the variation of stiffness and strength properties of column components. As a result, the flexural yielding moment will depend mainly on the axial force level. Therefore, the interaction diagram showing the relationship between axial force and the flexural yielding is important and are used. Under each flexural yielding moment, the properties of nonlinear moment-rotation hinges of column components will be the same as those of beam components. In addition, ATC-40

recommends that the plastic hinge rotation capacities of reinforced concrete column considering the design shear force level as shown in Table 5 which was used in this study.

The flexural strength of column components can be calculated using the same procedures and assumption as in beam components by considering axial force levels as shown in Figure 13. In this relationship between flexural yielding moments and axial force, point *A* represents pure axial compression where concrete in compression reaches its ultimate compressive strain,  $\varepsilon_{cu}$  set at 0.003. Point *B* corresponds to crushing of concrete at one face and zero tension at another. Point *C* corresponds to a strain distribution with a maximum compression strain  $\varepsilon_{cu}$  on one side of section and tensile strain  $\varepsilon_y$ , the yielding strain of reinforcement at the level of tension steel.

This represents balanced failure in which crushing of concrete and yielding of tension steel develop simultaneously. Point *D* represents pure bending where axial load equal to zero and the calculation of flexural strength of column at this point is exactly the same as beams. Point *E* represents pure axial tension where all reinforcements reach their yielding strain.

As in the beams, column shear strength is also sum of the shear strength of concrete and steel reinforcements. ACI 318-02 recommends the calculation of shear strength in concrete by using the following Equations:

For axial compression

$$V_c = 0.3\sqrt{f'_c}b_wd\sqrt{1+\frac{0.3N}{A_g}} \quad (20a)$$

For axial tension

$$V_c = \left( 1 + \frac{0.3N}{A_g} \right) \frac{\sqrt{f'_c}}{6} b_w d \geq 0 \quad (20b)$$

However, this codified shear strength method of design cannot be considered as predictive equations since they are intended to provide conservative and safe lower bound of strength and as such will not be used in this study. ATC-40, 1996 recommends that column shear strength carried by concrete in existing construction on the available test data may be computed using the following Equation.

$$V_c = 0.29\lambda \left( k + \frac{N}{14A_g} \right) \sqrt{f'_c} b_w d \quad (21)$$

Where,

$N$  = Axial force

$A_g$  = Gross cross-sectional area

$\lambda$  = 0.75 for light-weight concrete

1 for normal weight- concrete

$K$  = 1 in region of low ductility demand

0 in region of high ductility

**Table 5** Modeling Parameters for Nonlinear Procedure-Reinforced Concrete Columns

Component Type	Modeling Parameters <sup>4</sup>		
	Plastic Rotation Angle	Residual Strength	
	<i>a</i>	<i>b</i>	<i>C</i>
<b>1. Columns controlled by flexure<sup>1,3</sup></b>			
$\frac{P}{A_g f'_c}$ <sup>5</sup> Transverse Reinforcemen	$\frac{V}{b_w d \sqrt{f'_c}}$ <sup>6</sup>		
≤ 0.1 C	≤ 3	0.02	0.03
≤ 0.1 C	≥ 6	0.015	0.025
≥ 0.4 C	≤ 3	0.015	0.025
≥ 0.4 C	≥ 6	0.01	0.015
≤ 0.1 NC	≤ 3	0.01	0.015
≤ 0.1 NC	≥ 6	0.005	0.005
≥ 0.4 NC	≤ 3	0.005	0.005
≥ 0.4 NC	≥ 6	0.0	0.0
<b>2. Columns controlled by shear<sup>1,3</sup></b>			
Hoop spacing ≤ d/2, or $\frac{P}{A_g f'_c}$ <sup>5</sup> ≤		0.0	0.015
Other cases		0.0	0.0
<b>3. Columns controlled by inadequate development or splicing along the clear</b>			
Hoop spacing ≤ d/2		0.01	0.02
Hoop spacing > d/2		0.0	0.01
<b>4. Columns with axial load exceeding 0.70P<sub>o</sub><sup>1,3</sup></b>			
Conforming reinforcement over the entire length		0.015	0.025
All other cases		0.0	0.0

Source: ATC 40 (1996)

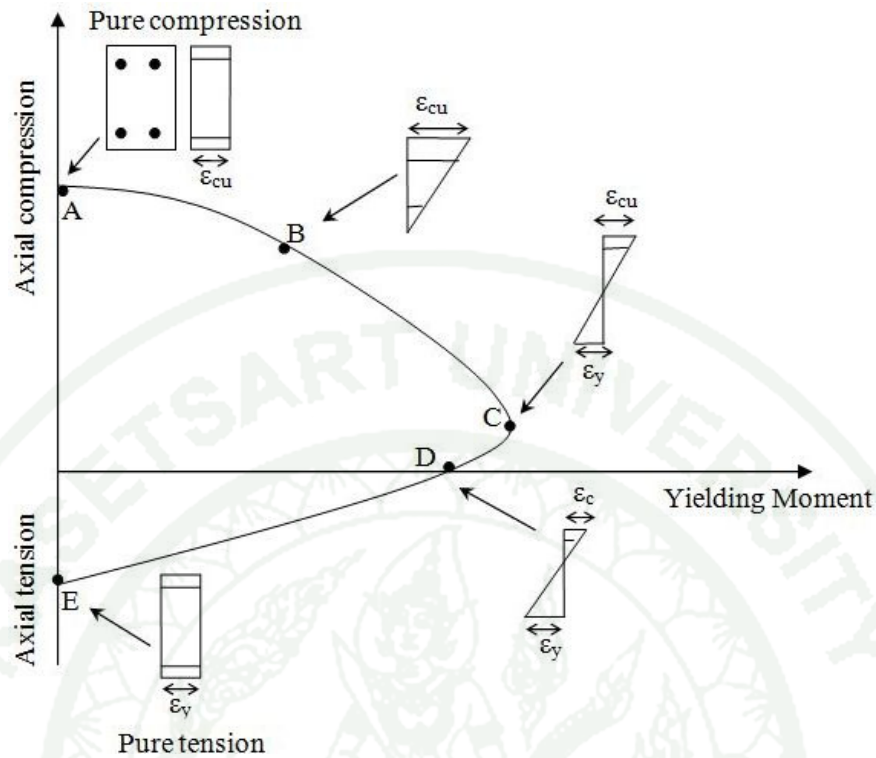


**Figure 14** Strain distributions corresponding to points on Interaction Diagram

**Source:** Karchung (2008)

Besides, the contribution of shear reinforcements to shear strength is based on truss mechanism with  $30^\circ$  strut. So, when the shear reinforcements is perpendicular to axis of column, shear strength carried by shear reinforcement can be calculated by using the following equation which will be used to estimate the shear strength of column member in this study.

$$V_s = \frac{A_v \cdot f_{yt} \cdot d}{0.6s} \quad (22)$$

Equation 21 and 22 were used in this study to estimate shear strength of column components.

#### 4. Nonlinear Static Pushover analysis

For the analysis of new and existing buildings various analysis methods are available, both elastic (linear) and inelastic (nonlinear). Although, an elastic analysis gives a good indication of the elastic capacity of structures and indicates where first yielding will occur, it cannot predict failure mechanisms and accounts for redistribution of forces during progressive yielding (ATC-40, 1996). So, to know the actual behaviour of the building after post-yielding, it is necessary to do the nonlinear analysis. A Nonlinear analysis is the most powerful method of analysis, able to trace the complete response of a structure from the elastic range, through cracking and crushing, up to complete failure (Lourance, 2002)

Though, Nonlinear Time History Analysis is the most basic and complete inelastic analysis but it is considered most complex, time consuming and impractical for the general use (ATC-40, 1996; Penelis and Kappos, 1997). Hence, the simplest option for estimating the strength capacity in the post-elastic range is the inelastic static pushover analysis that can provide valuable information with less effort but with a similar degree of confidence like that of detailed and rational evaluation methods based on inelastic time-history analysis of the whole structure. The technique may be also used to highlight potential weak areas in the structure.

Pushover analysis can be described as applying lateral loads in patterns that represent the relative inertial forces generated at each floor level and pushing the structure laterally under lateral loads to target displacement (maximum displacement) with expected earthquake ground motion ( Zou and Chan, 2005; D.G. Lee et al, 2006; Kadid and Boumrkik, 2008). The target top displacement may be the deformation expected in the design earthquake in case of designing a new structure, or the drift corresponding to structural collapse for assessment purposes. The method allows tracing the sequence of yielding and failure on the member and the structure levels as well as the progress of the overall capacity curve of the structure (Mwafy and Elnashai, 2000).

Pushover analysis is performed, subjecting the structure to monotonically increasing lateral forces with invariant distribution until a target displacement is reached; both the force distribution and target displacement are hence based on the assumption that the response is controlled by a fundamental mode that remains unchanged throughout (Pinho et al, 2007). The assumption that the seismic response of the building is dominated by a single mode and the mode shape remains unchanged throughout the analysis has enabled to relate the response of multi-degree of freedom (MDOF) building with response of an equivalent single-degree freedom (SDOF) system as illustrated in Figure 15 (Mohamed, 2007).

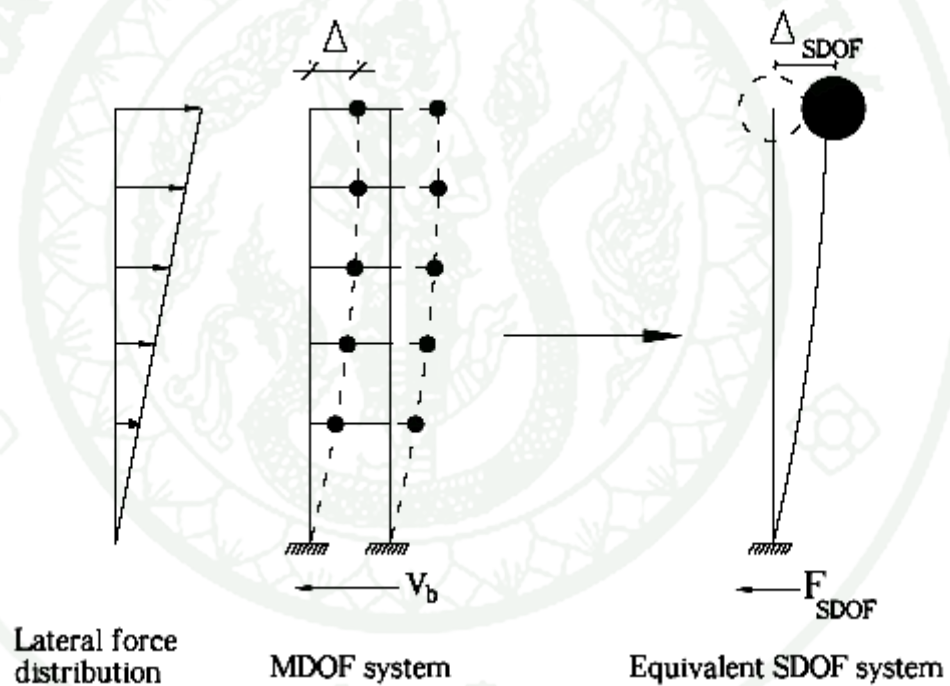


**Figure 15** Equivalent SDOF system parameters

**Source:** Mohamed (2007)

The pushover analysis provides a base shear vs. displacement relationship and indicates the inelastic limit as well as lateral load capacity of the structure. The change in slope of this curve gives an indication of yielding of various structural elements (Armagan et al, 2003). The predetermined pattern of load (inverted

triangular or uniformly distributed) is applied incrementally into frame work structures until a plastic collapse mechanism is reached. The analysis method generally adopts a lumped-plasticity approach that tracks the spread of inelasticity through formation of nonlinear plastic hinges at the frame element's ends during the incremental loading process.

The lumped plasticity approach is a good compromise between accuracy and simplicity. Using a lumped plasticity model (Figure 16) the parts of the member which are likely to undergo plastic deformations have to be identified through a preliminary analysis. For frame structures this is a simple process because plastic hinges generally form at the ends of the members (Galli, 2006).

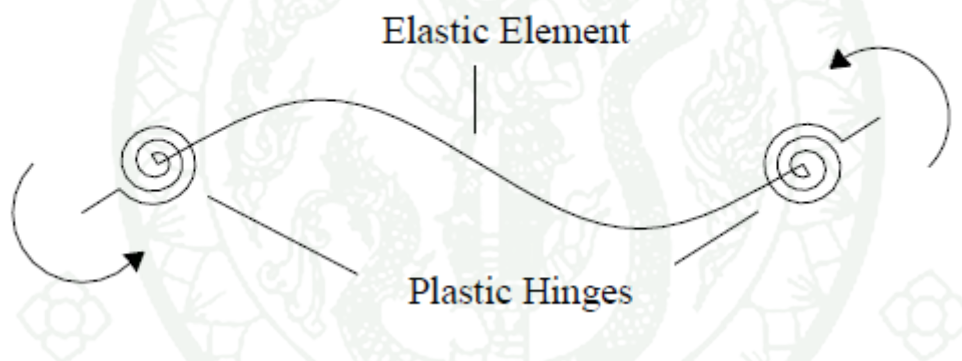


**Figure 16** Lumped plasticity beam element

**Source:** Galli (2006)

The purpose of the pushover analysis is to evaluate the expected performance of a structural system by estimating its strength and deformation demands in design earthquakes by means of a static inelastic analysis, and comparing these demands to available capacities at the performance levels of interest. The evaluation is based on an assessment of important performance parameters, including global drift, inter-story drift, inelastic element deformations (either absolute or normalized with respect to a yield value), deformations between elements, and element and connection forces (for elements and connections that cannot sustain inelastic deformations). The nonlinear static pushover analysis can be viewed as a method for predicting seismic force and

deformation demands, which accounts in an approximate manner for the redistribution of internal forces occurring when the structure is subjected to inertia forces that no longer can be resisted within the elastic range of structural behavior. The pushover is expected to provide information on many response characteristics that cannot be obtained from an elastic static or dynamic analysis (Krawinkler and Seneviratna, 1997).

In nonlinear static pushover analysis, the magnitude of the structural loading is incrementally increased in accordance with a certain predefined pattern. With the increase in the magnitude of the loading, weak links and failure modes of the structure are found. The loading is monotonic with the effects of the cyclic behavior and load reversals being estimated by using a modified monotonic force-deformation criteria and with damping approximations. Nonlinear static pushover analysis is an attempt by the structural engineering profession to evaluate the real strength of the structure and it is useful and effective tool for performance based evaluation (Karchung, 2008).

The FEMA-273, FEMA-356 and ATC-40 documents have developed modeling procedures, acceptance criteria and analysis procedures for pushover analysis. These documents define force-deformation criteria for hinges used in pushover analysis. As shown in Figure 17, five points labeled A, B, C, D, and E are used to define the force deflection behavior of the hinge and three performance levels Immediate Occupancy (IO), Life Safety (LS) and Collapse Prevention (CP) are used to define the acceptance criteria for the hinge.

For performing the pushover analysis, SAP2000, a state-of-the-art, general purpose, 3-dimensional structural analysis program was used as a tool. The pushover analysis capabilities, which are fully integrated into the program, allows quick and easy implementation of the pushover procedures prescribed in the FEMA-356 and ATC-40 documents for both two and three dimensional model of the building.

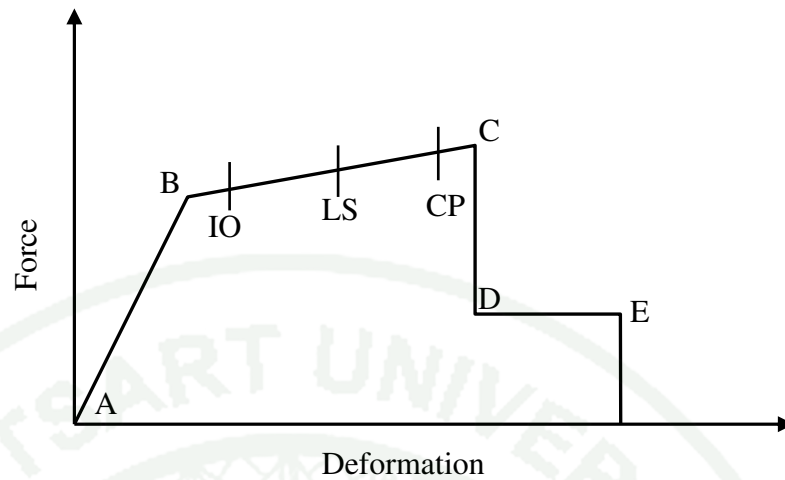


**Figure 17** Force-Deformation relationship of a typical Plastic Hinge

**Source:** Karchung (2008)

The building was created using a finite element model as stated in the previous section. The graphical interface of SAP2000 makes this a very quick and easy task. The properties and acceptance criteria for pushover hinges are accordingly defined using plastic hinge properties in accordance with ATC-40 and FEMA-356 in the nonlinear static pushover analysis. In defining the loading cases, the first pushover load case was the gravity load and then subsequent lateral pushover load cases were specified to start from the final conditions of the gravity pushover. The pushover load cases can be force-controlled, that is pushed to certain force level and displacement-controlled is one which is pushed to certain specified displacement called target displacement. The gravity load pushover is force-controlled while lateral load pushovers are displacement-controlled.

Pushover analysis is based on two basic assumptions: 1) the response is controlled by the fundamental mode of the structure which can be related to the response of an equivalent single degree-of-freedom (SDOF) system. 2) The mode shape remains unchanged after the structure yields (Gupta and Krawinkler, 1999, Kunnath and Gupta, 2000, Goel and Chopra, 2005, Jianmeng et al, 2008). It is clear that both assumptions are incorrect but pilot studies carried out by several investigators have indicated that these assumptions lead to rather good predictions of

the maximum seismic response of multi degree-of-freedom (MDOF) structures, provided their response is dominated by a single mode. Therefore, it is very difficult to apply pushover analysis for the high rise buildings as the pushover does not account for the contribution of higher modes to the structural response.

A nonlinear static pushover provides a graphical representation of the global force-displacement capacity curve of the structure commonly known as pushover curve. The pushover curve provides a relationship between shear vs. displacement and indicates the inelastic limit as well as lateral load capacity of the structure. The change in slope of this curve gives an indication of yielding of various structural elements. The main aim of the pushover analysis is to determine member forces and global and local deformation capacity of a structure. The information can be used to assess the integrity of the structure.

## RESEARCH METHODOLOGY

For this thesis work, the resources were completely dependent on literatures and some material data from Bhutan. Therefore, literature review and material data were vital for this research. Thus, the methodology for the study was as described below.

### 1. Literature review

To familiarize with the theoretical part, journals and articles on the effect of masonry infill on steel or reinforced concrete moment resisting frames were reviewed. In addition books, relevant design codes, and guidelines of different countries were studied. The main purpose of literature review was to gain firsthand knowledge on the methods of studies adopted, which was used as a guideline for this study. Further, the review of past studies had also provided some idea of the modeling techniques and parameters used for different materials like reinforced concrete and brick masonry.

### 2. Data Collection

The study was done with the prevalent construction materials being used in Bhutan. Thus, the required experimental and material data necessary to make the analytical model of the brick masonry infill were collected from The College of Science and Technology, Rinchending, Phuentsholing, Bhutan and Standard and Quality Control Authority, Thimphu, Bhutan. The Bhutan Building Code (BBC) and Indian Standards Codes were collected from the Phuentsholing City Corporation, Ministry of Works and Human Settlement, Bhutan.

### 3. Methodology adopted

As mentioned earlier, the present practice of structural analysis is to treat the masonry infill as non-structural element and the analyses as well as design were carried out by using only the mass but neglecting the strength and stiffness contribution of infill. Thus, the structures were modeled as bare frame, and considered fixed at base. In Bhutan, building structures were analyzed for seismic loading as per Bhutan Building Code 2003 and IS 1893(Part 1): 2002 Criteria for Earthquake Resistant Design of Structures (Part 1: General Provisions and Buildings). The buildings were modeled as the 3-dimensional finite element model to get the area of steel reinforcement to be used but the analysis has been carried out for the 2-dimensional models only. The frame structure has moment resisting joints. The beams and columns were modeled as a frame element which has the capability to deform in axial, shear, bending and torsion. The effect of RC slab for rigid floor diaphragm action to resist lateral force was taken into account.

#### 3.1 Selection of Building

For the present study, a hypothetical 4-storey, 8-storey and 12-storey apartment type buildings with typical floor plan and elevations as shown in Figure 18 were considered to get the area of reinforcement for analysis. These buildings represent the typical RC frame buildings in Bhutan that were designed and constructed according to Indian standards with seismic consideration of zone V, with zone factor of 0.36. The buildings were symmetrical in plan with respect to two orthogonal axes and the plan dimensions of the buildings were 20 m in length, 15 m in width and the total heights of the buildings were 13.8 m for 4-storey, 26.6 m for 8-storey and 39.4 m for 12-storey. The grid spacing along both axes was 5 m. Thus there are 5 grids along X-axis and 4 grids along Y- axis. The typical floor height is 3.2 m with foundation of 1 m for all three types of building. For this study, only 2-dimensional models were used. The models used were along the Y-axis and different infill configurations were shown in Figure 19.

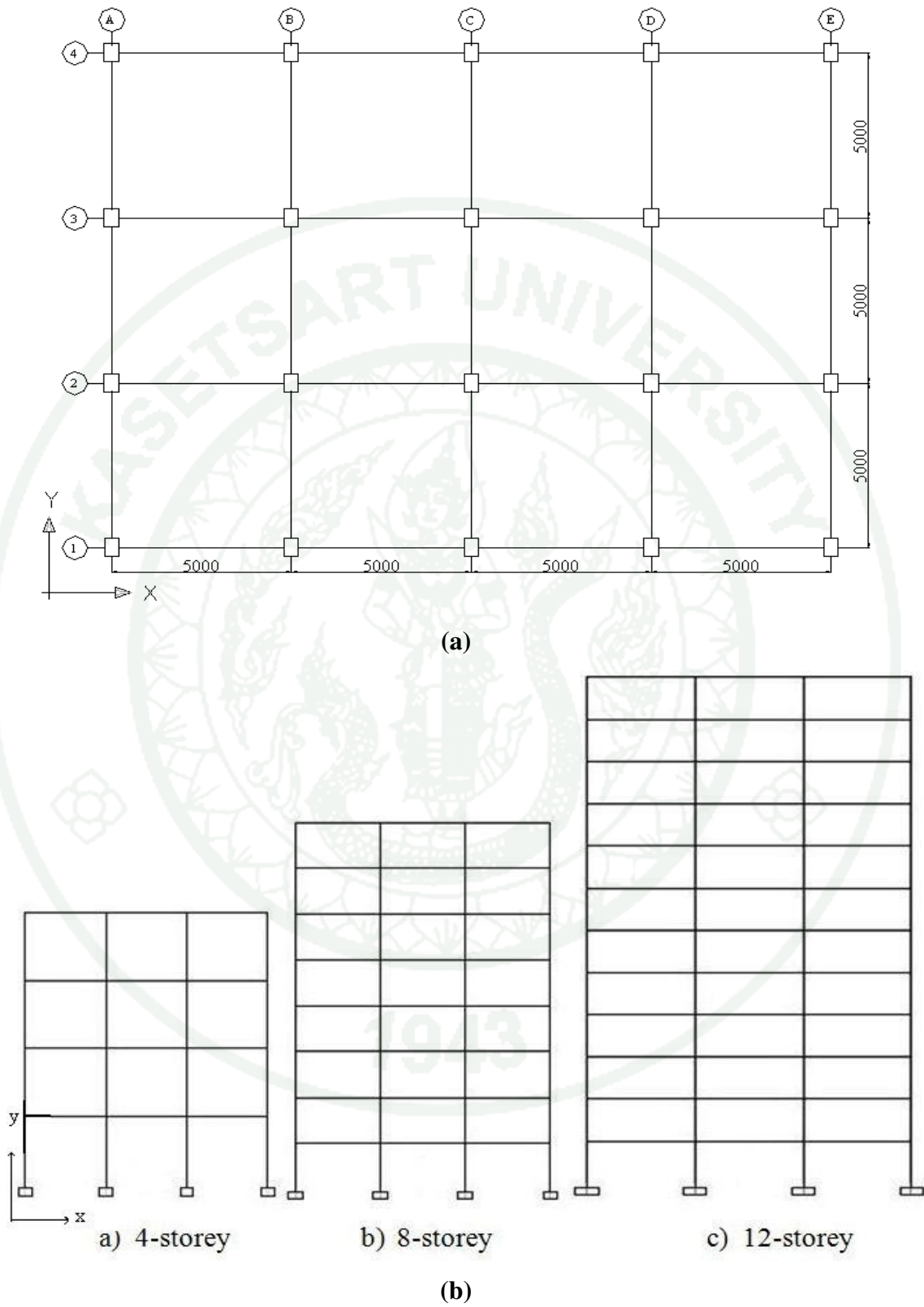


**Figure 18** Typical plan and elevation of the models

The buildings were designed according to Indian standards. The beam-column joints reinforcement, anchorage and lapping length of the reinforcement were provided according to Indian standard.

### 3.2 Description of the Models

To investigate the effect of infill walls in the reinforced concrete buildings, five different models were used as shown in Figure 19. These models included, a bare frame (Model-A), a fully infill frame (Model-B), an infill frame with open ground storey (Model-C), an infill frame without infill in middle bay (Model-D) and an infill frame with infill only in middle bay (Model-E). These models have been chosen for the study as most of the building stock in Bhutan has similar configurations. The bare frame and fully infilled frame were the most extreme cases in this study and were considered as the reference models. The building configurations used in the study were simple and regular. A two dimensional structural models were sufficient to capture the structural behaviour of the building. The vertical plans with beam and column sections of the models are shown in Figure 20. The beam sections shown in the figure is the typical section use in Bhutan.

Only the masonry surrounded by beams and columns were considered as infills. For walls in other location, only the weight contribution is considered. Minor details that were less likely to significantly affect the analysis were deliberately left out from the models. The main purpose was to compare the overall behavior of the structure, but not the behavior of infill panel or on the behavioral effect due to minute details. All the five different models were shown in Figure 19. Model-A has 0% infill, Model-B has 100% infill, Model-C has 75% infill, Model-D has 66.7% infill and Model-E has 33.3% infill. The member sizes are shown in Table 6.

**Table 6** Structural member sizes and reinforcements used for this study

Type of Structure	Sections	Sizes (mm)	Reinforcements *
4-storey	C1-1	400 x 300	10 $\square$ 20 (3141.6 mm <sup>2</sup> )
	C1-2	400 x 300	6 $\square$ 22 (2280.8 mm <sup>2</sup> )
	C2-1	500 x 300	12 $\square$ 20 (3769.9 mm <sup>2</sup> )
	C2-1	500 x 300	8 $\square$ 20 (2472mm <sup>2</sup> )
	B1	400 x 250	3 $\square$ 25 + 3 $\square$ 20 (2415 mm <sup>2</sup> )
	B2	350 x 250	3 $\square$ 20 + 2 $\square$ 16 (1335 mm <sup>2</sup> )
8-storey	C1-1	600 x 400	14 $\square$ 20 (4523 mm <sup>2</sup> )
	C1-2	600 x 400	10 $\square$ 20 (2973 mm <sup>2</sup> )
	C1-3	600 x 400	6 $\square$ 22 (2107 mm <sup>2</sup> )
	C2-1	650 x 450	14 $\square$ 22 (5042 mm <sup>2</sup> )
	C2-2	650 x 450	12 $\square$ 20 (3355 mm <sup>2</sup> )
	C2-3	650 x 450	8 $\square$ 20 (2500 mm <sup>2</sup> )
	B1	500 x 300	3 $\square$ 25 + 2 $\square$ 25 (2454 mm <sup>2</sup> )
	B2	450 x 300	4 $\square$ 20 + 2 $\square$ 20(1840 mm <sup>2</sup> )
12-storey	C1-1	700 x 500	12 $\square$ 26 (6542 mm <sup>2</sup> )
	C1-2	700 x 500	8 $\square$ 26 (4148 mm <sup>2</sup> )
	C1-3	700 x 500	8 $\square$ 20 (2400 mm <sup>2</sup> )
	C2-1	600 x 500	14 $\square$ 28 (7731 mm <sup>2</sup> )
	C2-2	600 x 500	10 $\square$ 25 (4956 mm <sup>2</sup> )
	C2-3	600 x 500	6 $\square$ 25 (2800 mm <sup>2</sup> )
	B1	550 x 400	3 $\square$ 25 + 3 $\square$ 20(2415 mm <sup>2</sup> )
	B2	500 X 400	3 $\square$ 25 + 2 $\square$ 25(1418 mm <sup>2</sup> )
	B3	450 X 350	3 $\square$ 20 + 4 $\square$ 16 (1746 mm <sup>2</sup> )

\*  $F_y = 415$  MPa

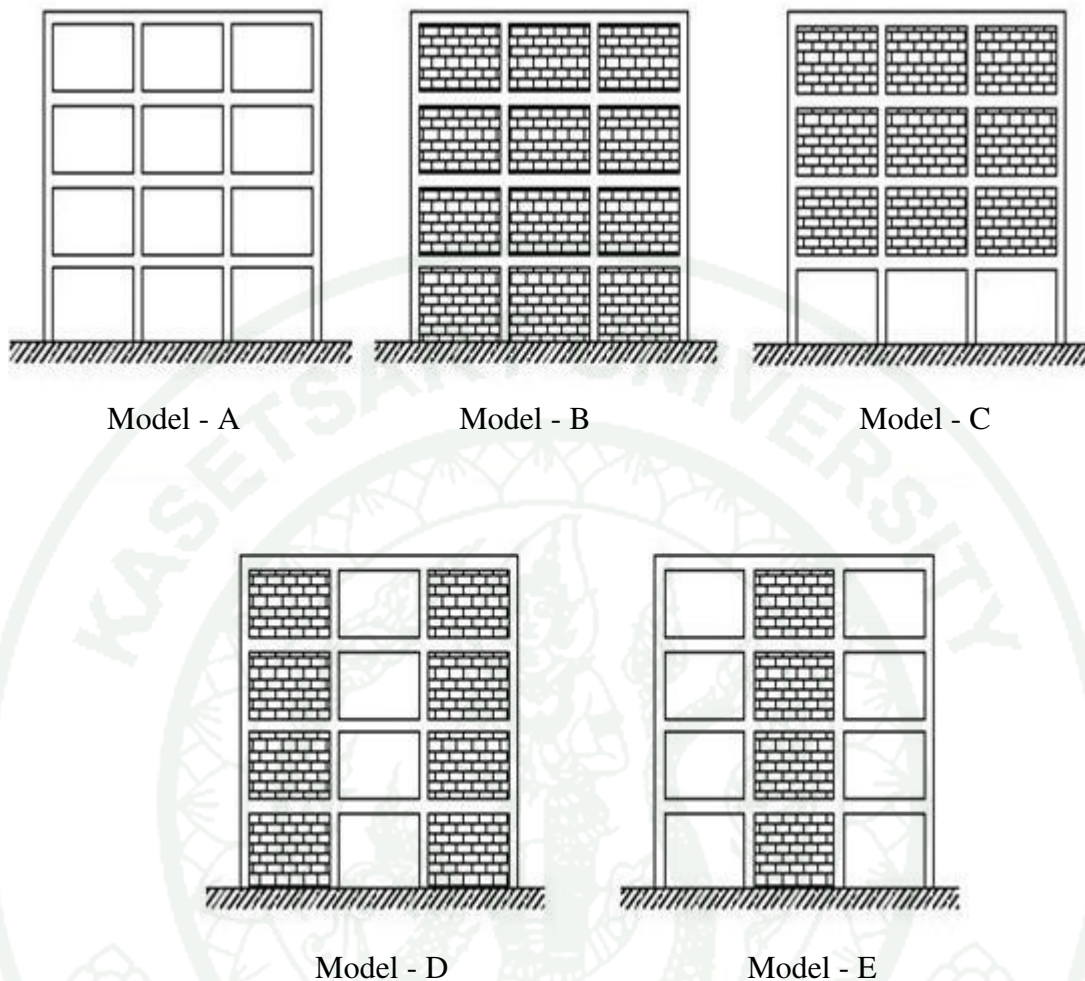


**Figure 19** The infill configuration models (a) Bare frame, (b) Fully infilled, (c) first soft storey, (d) weak middle bay, (e) strong middle bay being studied

The initial dimensioning of the beams and columns were made on the basis of bare frame design for full wall case with earthquake load as per IS1893-2002 code such that the structure met the strength and ductility requirements of Indian code, with a limitation that the lateral displacement limit exceeded the allowable value. The same sections were used for the other cases of infill. Further, it was assumed that the infill panels were neither integral nor bonding with the frame.

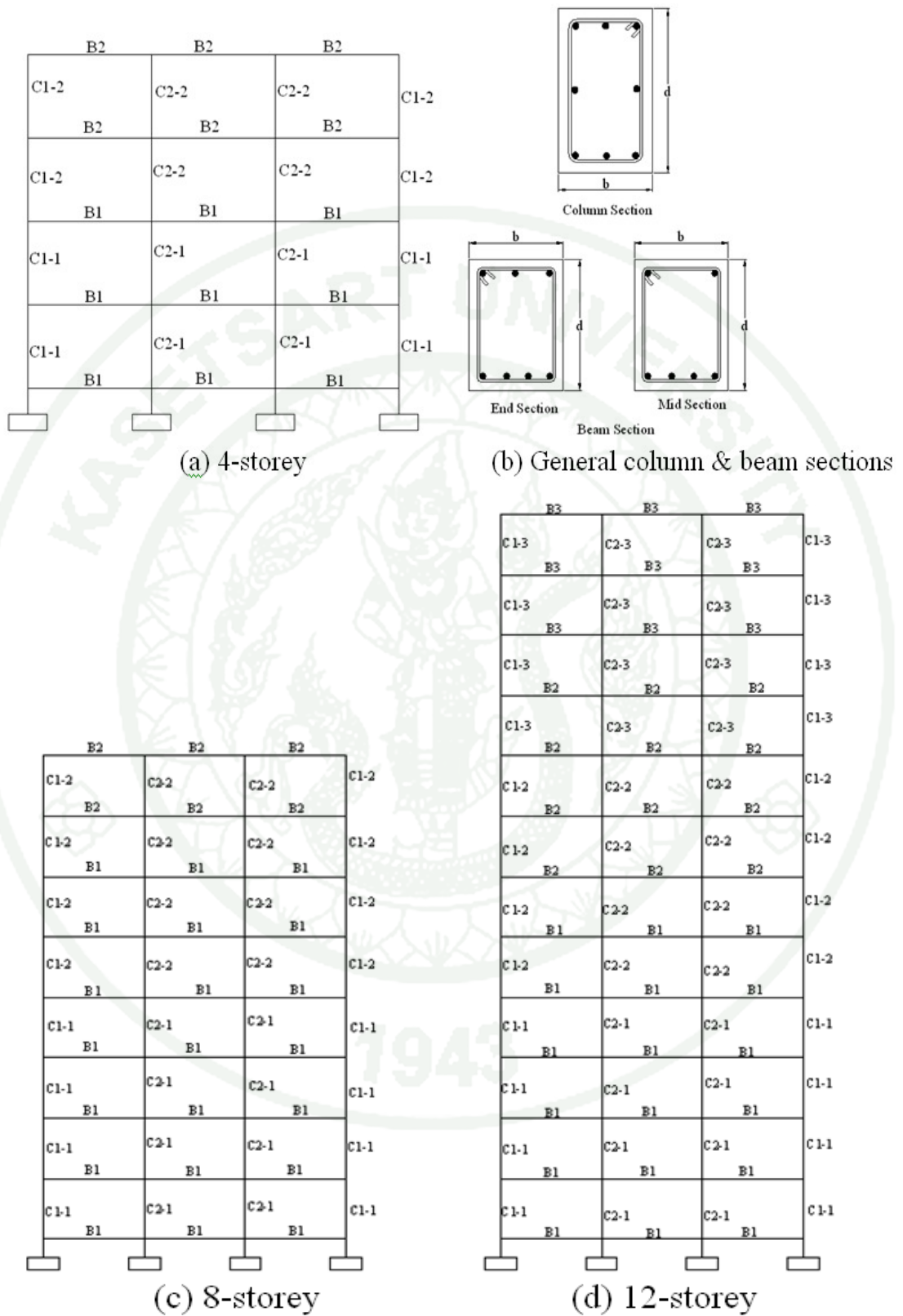


**Figure 20** Vertical section plan and general beam and column sections

#### 4. Modeling of the Building

Mathematical model of the building was created as mentioned in Chapter 2 to analyze and predict the actual elastic and inelastic response of the structure under lateral loading. Different models with different infill configurations were developed to analyze and to investigate the effect of infill wall on seismic response of the typical structures. For each infill case, bare frame and infill frame models was developed. The common approaches used for modeling the infill frames are as follows:

i) Bare Frame Method

This is the commonly accepted method of structural analysis and design for buildings with infill panel all around the globe. The only contribution of masonry infill is their masses in the form of non-structural element. Consequently, analysis of the structure is based on the bare frame. In this, the beam and columns are modeled as frame element and the beam-column joints were modeled as rigid. Since infills are not considered, their contributions to the lateral stiffness and strength may invalidate the analysis and the proportioning of structural members for seismic resistance on the basis of its results. However, this method is still being widely used in the world even in the earthquake prone areas, including Bhutan and is considered for the comparison in the present study.

ii) Equivalent Diagonal Strut Method

There are two main method of modeling the infill panel; micro-model and macro-model. In the micro-model method the infill panel is modeled using the shell element and the interaction between wall and the frame is modeled using the interface element. Though micro-model gives a very good result including the frame-wall interaction, however, it's too time consuming for the large structure. Hence, alternatively, a macro-model replacing the entire infill panel as a single equivalent-strut by far has become the most popular approach for analyzing infilled frame systems. In this method, the brick infill is idealized as a pin jointed diagonal strut and

the RC beams and columns are modeled as three-dimensional beam elements with 6 degrees of freedom at each node. The idealization is based on the assumption that there is no bond between frame and infill. The brick masonry infill is modeled as a diagonal strut member whose thickness is same as that of the masonry and the length is equal to the diagonal length between compression corners of the frame. The effective width of the diagonal strut depends on various factors, such as contact length, aspect ratio of the infill and the relative stiffness of frame and the infill.

The macro modeling approach takes into account only the equivalent global behavior of the infill in the analysis and does not permit the study of local effects such as frame-infill interaction within the individual infilled frame subassemblies, which needs detailed micro modeling. However, the macro-modeling approach allows for adequate evaluation of the force-deformation response of the structure and individual components under seismic loading (Madan *et al.* 1997) and may be used to assess the overall response to a sufficient degree of accuracy. Thus, the proposed macro model is better suited for representing the behavior of infills of complex structures with multiple components particularly in cases where the focus is on evaluating the response.

In this work, all the members were modeled as reinforced concrete elements with sections given in the design for nonlinear analysis. The mass that was considered for the analysis include dead load and 25 percent of live load (IS 1893:2002). Live load of 3 kN/m<sup>2</sup> was considered in the design. The nonlinearities in the beam and columns will be introduced using lumped plasticity by defining plastic hinges at both ends of the beams and columns.

In SAP2000, plastic hinge properties were defined in accordance with ATC-40 and FEMA-356. The five points leveled A, B, C, D and E in Figure 21 defines the force-deformation behavior of a plastic hinge whose values depends on the type of elements, material properties, longitudinal and transverse reinforcements.

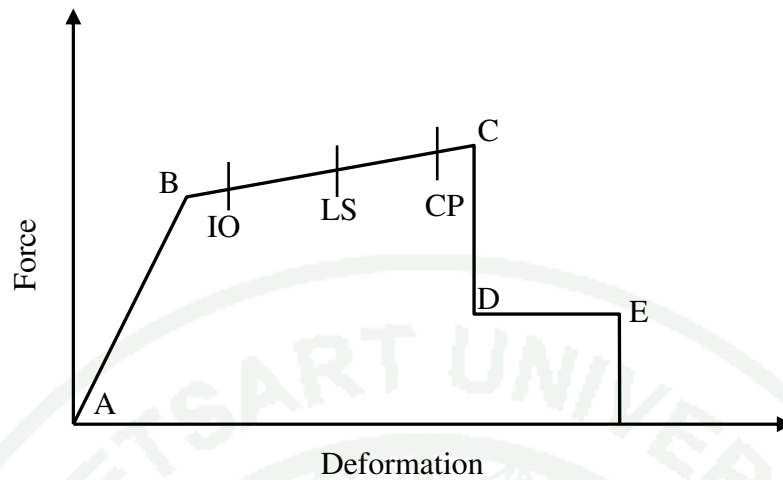


**Figure 21** Force-deformation for a typical plastic hinge

**Source:** Karchung (2008)

#### 4. Modeling Assumptions

Following assumptions were made in creating model of the building for seismic analysis in this study.

1. Lateral loads were assumed to act only at floor level. This is justified because of the fact that the inertia forces depend on the mass and the most of the masses are at floor level.
2. The diaphragm was assumed to be rigid. The floor was assumed to be rigid in the plane of diaphragm, but flexible in bending. In other words, all the horizontal components displacements at the same floor level were assumed identical.
3. The joints were assumed rigid as joint reinforcements needs to be provided according to the Indian standards.
4. Footings are assumed fixed. The seismic effect below the ground level is neglected.

## 5. Application of Loads

a. Dead load: The unit loads to be used in this study was based on Bhutan Building Code (2003). This Bhutan Building code for Unit Weight of Materials adopts the Indian Code IS:875 (Part 1) – 1987 Code of Practice for Design Loads (Other than Earthquake) for Buildings and Structures, Part 1, Dead Loads-Unit Weights of Building Materials and Stored Materials, (Second Revision).

b. Live Load: The live load to be used in this study was based on Bhutan Building code (2003) which adopts the Indian Code IS:875 (Part 2) - 1987 Code of Practice for Design Loads (Other than Earthquake) for Buildings and Structures, Part 2 Imposed Load, (Second Revision).

c. Earthquake Load: The code used for the earthquake design in Bhutan is Bhutan Building code (2003) which adopts Indian Standard IS1893 (Part 1): 2002, Criteria for Earthquake Resistant design of Structure, Part 1: General Provisions and Buildings (fifth revision). In this study IS 1893(Part 1):2002 was used. Static analysis using equivalent lateral force procedure is restricted to regular buildings having height less than 40 m and irregular buildings having height less than 12 m in seismic Zone V which is the most severe zone. Seismic weight of a structure is computed from total dead load and reduced (25%) live load and is multiplied by a coefficient from the response spectrum plot shown in Figure 22. The equivalent base shear method is formulated with the assumption that the first mode of vibration governs, which is true for short period structures. Hence, the equations for equivalent base shear method are derived on the assumption that the horizontal displacement of the first mode of vibration increases either linearly or quadratically with height (FEMA-450, 2003), the IS 1893 employs the quadratic variation of displacement. Since, the building under study is regular in both horizontal and vertical axis and the height is less than 40 m, the seismic coefficient method was used which is defined as follow:

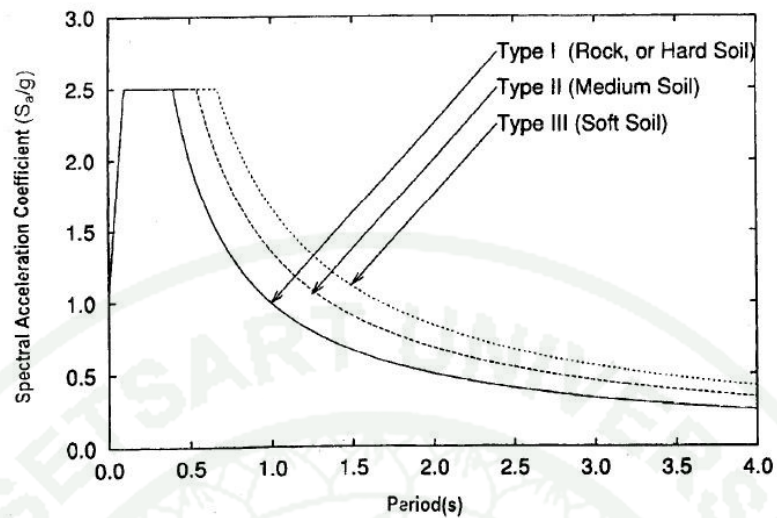


**Figure 22** Response spectrums for 5% damping

**Source:** IS 1893 (2002)

The design base shear  $V_B$  which is the total lateral force at the base of a structure is computed in accordance with the clause 7.5.3 of the code which states,

$$V_B = A_h W \quad (23)$$

Where,

$$A_h = \frac{Z}{2} \frac{I}{R} \frac{S_a}{g} \quad (24)$$

Provided that for any structure with  $T < 0.1$  sec,  $A_h$  is not less than  $(Z/2)$  whatever be the value of  $(I/R)$ .

Where,

$Z$  = Zone factor = 0.36

$I$  = Importance factor = 1

$R$  = Response reduction factor = 5

$S_a/g$  = Average response acceleration coefficient from Figure 22 which depends on the fundamental time period of the building

$W$  = Seismic weight of building, which is the total dead load plus appropriate amount of imposed load.

The approximate fundamental natural period of vibration ( $T_a$ ), in seconds, of a moment resisting frame building may be estimated by the empirical expression:

$$T_a = 0.075h^{0.75}; \text{ For RC frame building} \quad (25a)$$

$$T_a = 0.085h^{0.75}; \text{ For steel frame building} \quad (25b)$$

$$T_a = 0.09h/\sqrt{d}; \text{ For RC frame building with brick infill panels.} \quad (25c)$$

Where,

$h$  = Height of building in meter

$d$  = Base dimension of the building at the plinth level, in meter, along the considered direction of the lateral force.

The design base shear ( $V_B$ ) computed above was distributed along the height of the building as per the following expression:

$$Q_i = V_B \frac{W_i h_i^2}{\sum_{j=1}^n W_j h_j^2} \quad (26)$$

Where,

$Q_i$  = design lateral force at floor  $i$

$W_i$  = seismic weight of floor  $i$

$h_i$  = height of floor  $i$  measured from base

$n$  = number of story in the building, is the number of levels at which the masses are located

## 6. Material Properties used

For this study, the material property used for concrete, reinforcing bar and brick masonry panels were as follows:

Yield strength of reinforcing bar  $f_y = 415 \text{ N/mm}^2$  (Fe 415)

For Concrete:

Unit weight =  $24 \text{ kN/m}^3$

Characteristic compressive strength,  $f_{ck} = M20 = 20 \text{ N/mm}^2$

Tensile strength (flexural strength),  $f_{cr} = 0.7\sqrt{f_{ck}} = 3.13 \text{ N/mm}^2$

Shear strength,  $\tau_c = 3.5 \text{ N/mm}^2$

Young's modulus of elasticity,  $E_c = 5000\sqrt{f_{ck}} = 22360.68 \text{ N/mm}^2$

Poisson's ratio,  $\nu_c = 0.15$

Shear modulus,  $G_c = \frac{E_c}{2(1+\nu_c)} = 9722.03478 \text{ N/mm}^2$

For Brick Masonry Panel

Size of brick =  $200 \text{ mm} \times 100 \text{ mm} \times 60 \text{ mm}$ ,  $h_b = 60 \text{ mm}$

Horizontal mortar thickness,  $j = 15 \text{ mm}$

1 course of brick + mortar =  $75 \text{ mm}$

Mortar ratio = 1:5

Compressive strength of hand molded burnt clay brick,  $f_{cb} = 7N/mm^2$

Compressive strength of 1:5 mortar,  $f_j = 5N/mm^2$

Tensile strength of brick,  $f_{tb} = 0.1f_{cb} = 0.7 N/mm^2$

The compressive strength of masonry prism,  $f_m$  was calculated by the relation given by Paulay and Priestley (1992):

$$f_m = \frac{f_{cb}(f_{tb} + \alpha f_j)}{U_u(f_{tb} + \alpha f_{cb})} = \frac{7(0.7 + 0.061 \times 5)}{1.5(0.7 + 0.061 \times 7)} = 4.16N / mm^2$$

$$\text{Where, } \alpha = \frac{j}{4.1h_p} = \frac{15}{4.1 \times 60} = 0.061 \text{ and,}$$

$U_u$  = stress non-uniformity coefficient = 1.5

Young's modulus of elasticity,  $E_m = 550f_m = 2288 N/mm^2$

Poisson's ratio,  $\nu_c = 0.12$

## 7. Analysis of Building

A nonlinear static pushover analysis as stated in the literature review was performed using SAP2000 version 14 to obtain the response of the structure with different infill configurations as shown in Figure 19 and three different earthquake levels, serviceability earthquake (SE), design earthquake (DE) and maximum earthquake (ME).

The pushover analysis was carried out using two dimensional building models (Figure 18) in the principle Y-direction (along grid-1 frame) without considering the P- $\Delta$  effects.

## RESULTS AND DISCUSSIONS

In the preceding topics, all the information that was necessary for the study of effect of masonry infill walls on the seismic behaviour of reinforced concrete frame buildings were thoroughly discussed. The bare frame and infill frames of various configurations were studied analytically. A nonlinear static pushover analysis was performed to study the effect of masonry infill walls on the seismic behaviour of reinforced concrete buildings. A parametric study was carried out and the influence of masonry infills on the seismic behaviour of RC buildings was studied.

### 1. Modal Analysis

Modal analyses were carried out to obtain the fundamental period of the bare frame models and infilled frame models. The empirical formulae available in codes do not specify the extent of infill usage in the frame system. Thus, the current study determined the periods of various infill configurations in the infilled frame system with infills without openings.

The sources of mass were from the dead load of infill walls and the frame elements. The dead load from the infill walls were applied as the uniformly distributed load along the beams. The equivalent diagonal strut's mass is not included but its stiffness was included in the analysis since the models were studied under the in-plane loads. The mass and stiffness of entire structures were taken into consideration.

#### 1.1 Fundamental Period

The structural responses of a building under an earthquake excitation were dependent on inherent properties like mass and stiffness of the building structure as well as the earthquake ground motion. Infill walls, which were usually considered as a non-structural component, have been proven to enhance the initial strength and stiffness of the frame system under lateral loads by past researchers. Nevertheless,

very little consideration of infill has been made in the current codes, especially the Indian code IS 1893-2002 which is currently used in Bhutan. To compute the lateral seismic coefficient, the current Indian code uses design spectrum which is dependent on the fundamental period of the structures. The code uses empirical formulae to approximate the fundamental period of both bare frame building and infilled frame building as given by equations below.

$$T_a = 0.075h^{0.75} \quad (\text{For RC bare frame buildings}) \quad (27)$$

$$T_a = \frac{0.09h}{\sqrt{d}} \quad (\text{For RC infilled frame buildings}) \quad (28)$$

Where,  $T_a$  = Approximate fundamental natural period of vibration (sec)

$h$  = Height of building (m)

$d$  = Base dimension of the building at the plinth level in the direction under consideration (m)

It was found that the fundamental period of the bare frame model was comparable to the fundamental period obtained from the code equation but the period of infilled frame models were of significant difference as shown in Table 7.

Figure 23 shows the variation of fundamental periods of different models with number of storeys or height of the building models. It can be seen from the figure that infill has significant effect on the fundamental periods of the buildings. There was a significant difference between the fundamental period of the bare frame models and the infilled frame models. This indicated that the infills have significant influence or effect on the structural behaviour of the buildings. The fundamental periods of 4-storey, 8-storey and 12-storey bare frames (Model-A) were 0.57 seconds, 1.09 seconds and 1.55 seconds, respectively while for fully infill frames (Model-B) were 0.3 seconds, 0.67 seconds and 1.08 seconds, respectively. The difference in fundamental periods of bare frame models and fully infilled frame models was 90% higher for bare frame models for 4-storey building models, 62.69% higher for bare frame models for 8-storey building models and 43.52% higher for bare frame models for 12-storey building models. When the area of infill was decreased, the difference in fundamental period between the bare frame models and infill frame models decreased

as expected. The difference in fundamental periods between model-A (bare frame) and model-E (infilled frame with least area of infill) was 35.71% higher for Model-E for 4-storey building models, 25.29% higher for Model-E for 8-storey building models and 16.54% higher for Model-E for 12-storey building models. It was also observed, when the height of building was increased, the difference in percentage of difference decreased.

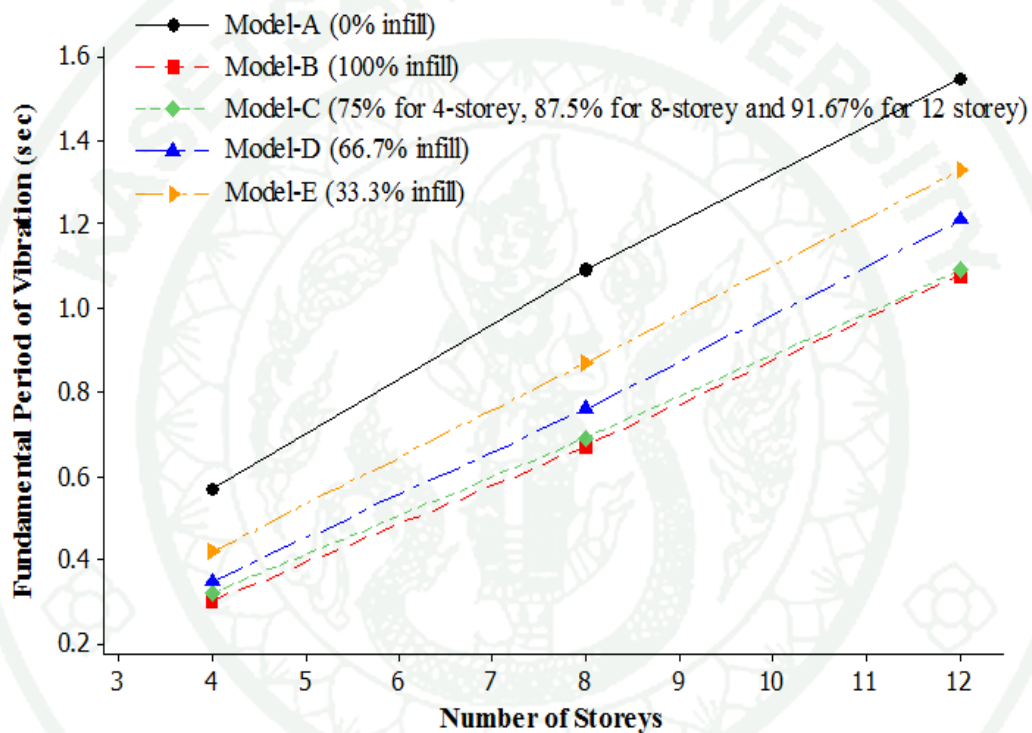


**Figure 23** Variation of Fundamental Period with Percent of Infill Area in the Models

In the study, the difference in fundamental periods calculated from the code equation and analysis was also studied. It was found that the difference between codes calculated fundamental periods and modal analysis fundamental periods were not much in both bare frame and infilled frame. However, as the height of the building was increased, the difference in period increased. In case of fully infilled frame models (Model-B), a difference of 3.45% higher for analysis for 4-storey building models, 15.52% higher for analysis for 8-storey building models and 22.73% higher for analysis for 12-storey building models were observed.

**Table 7** Fundamental periods of different building models

No. of Storeys	Infill configuration	Fundamental Time Period From Analysis (sec)	Time Period From IS: Code 1893-2002 (sec)
4	Model - A	0.57	0.51
	Model - B	0.30	0.29
	Model - C	0.36	0.29
	Model - D	0.35	0.29
	Model - E	0.42	0.29
8	Model - A	1.09	0.85
	Model - B	0.67	0.58
	Model - C	0.69	0.58
	Model - D	0.76	0.58
	Model - E	0.87	0.58
12	Model - A	1.55	1.16
	Model - B	1.08	0.88
	Model - C	1.09	0.88
	Model - D	1.21	0.88
	Model - E	1.33	0.88

The variation of fundamental periods of the buildings with changed in compressive strength of the brick masonry infill walls were also studied. It can be seen from the Figure 24 that the changed in compressive strength of the masonry infill walls changed the fundamental period of the building models. The increase in compressive strength of masonry infill walls decreased the fundamental period slightly. It was found that when the compressive strength was increased from 3 MPa to 5 MPa, the fundamental periods decreased by 13.5% for 4-storey building models, 13% for 8-storey building models and 11% for 12-storey building models. The decrease in fundamental period with increase in compressive strength of masonry infill is due to increase stiffness of the infills. The stiffness was increased due to

increase in modulus of elasticity of masonry infill, which is directly related to compressive strength of the infills. It may be concluded here that not only the inclusion of masonry infill walls in the building changes the fundamental period of the building but even the compressive strength of the masonry infills was of slight influence on the dynamic behaviour of the buildings.

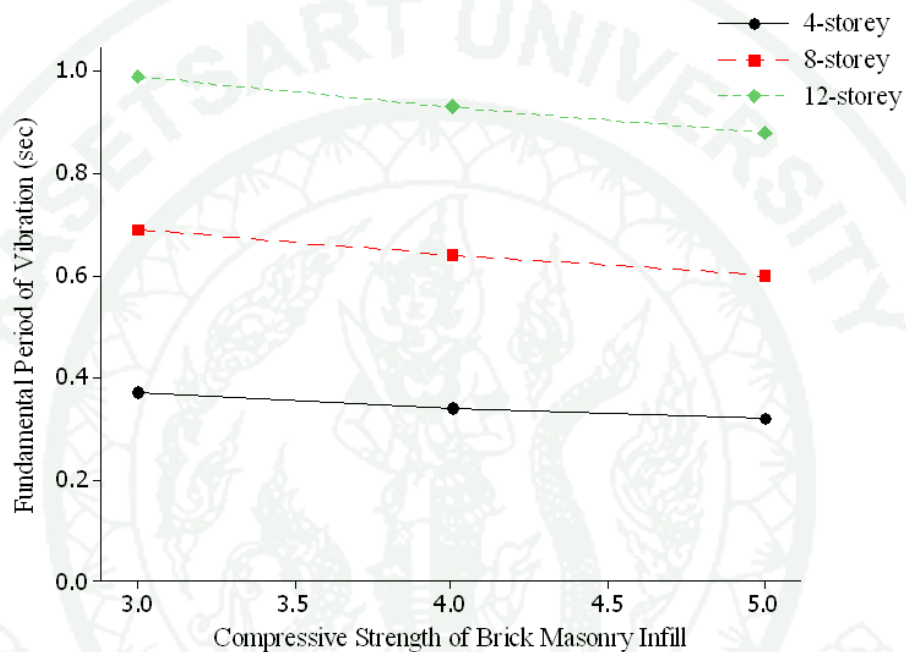


**Figure 24** Variation of fundamental period with different compressive strength of masonry infill (Model-B)

## 2. Axial Force and Bending Moment Distribution

In this study the effect of masonry infills on the distribution of column axial forces and bending moments were also investigated. Figures 25 and 26 show the typical variation of axial forces along the height of the exterior columns  $C_T$  and  $C_c$  under combined gravity and earthquake load (lateral load).  $C_T$  represents column on tension side (lateral loading side) of the building when earthquake loads were applied along positive X direction. Similarly,  $C_c$  represents columns on compression end. It was observed from the figures that axial forces due to earthquake got increased and

bending moment got reduced in columns in infilled frame building models for a particular level of earthquake (base shear force of 615.98 KN). These column axial forces in infilled frame due to earthquake forces were found to be large enough to cause net tension in columns on the tension side and failure of columns occurred due to tension. Similarly, on compression side, the column axial load increased due to presence of infills. This increase in axial load resulted in the failure of columns at a lower moment. This may also result in yielding of columns prior to yielding of beams. The change in behaviour was due to change in load transfer mechanism of the building models from frame action to truss action, due to presence of masonry infill walls.

Figure 27 and 28 shows the bending moment distribution along the height of the same columns that of axial forces. It can be seen from the figures that there is reverse bending moments and the magnitude of bending moments are less for infilled frame models. This is a truss action mechanism in the infilled frame models. Therefore, the bending moment in the columns reduced accordingly

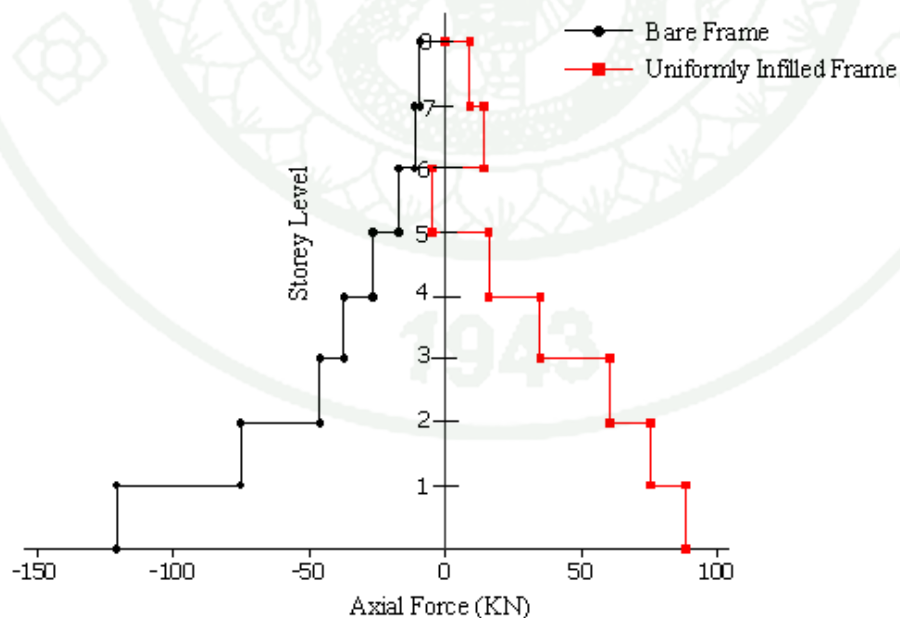


**Figure 25** Variation of axial force in column  $C_T$

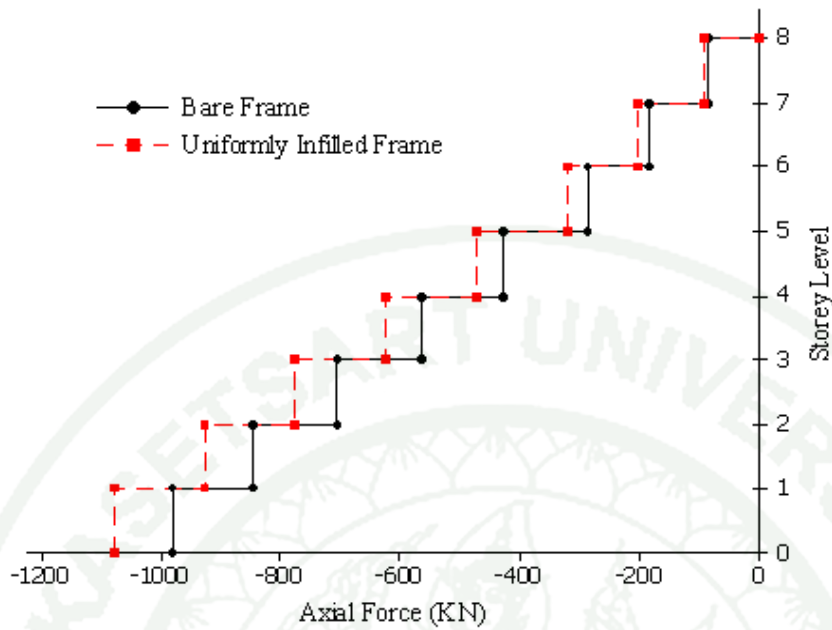


**Figure 26** Variation of axial force in column  $C_c$

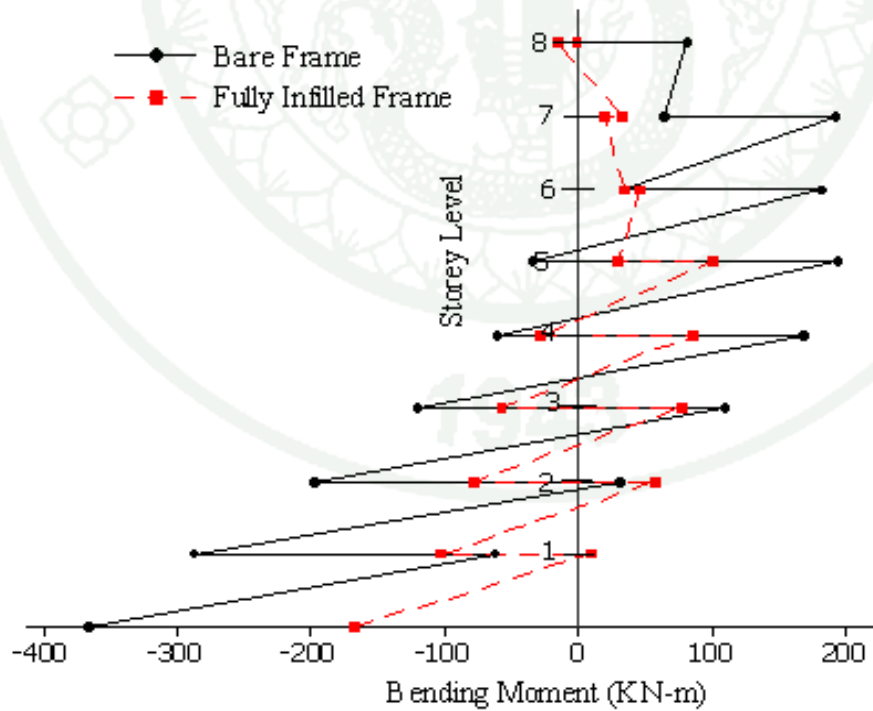


**Figure 27** Bending moment in column  $C_T$

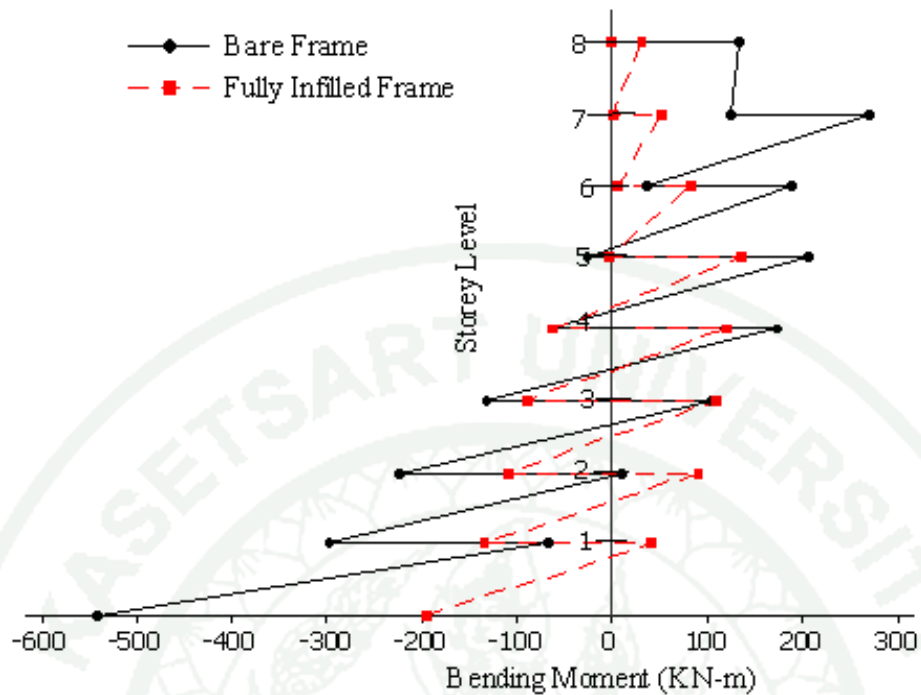


**Figure 28** Bending moment in column  $C_c$

### 3. Pushover Analysis

In the preceding section, all the dynamic information that was necessary for evaluating seismic behaviors of the building were thoroughly discussed. In this section, nonlinear static pushover analysis results of the three selected reference buildings were presented. The parameters which are normally neglected in the analysis and design of the building such as effect of infill walls, compressive strength of infill materials and thickness of infill walls on the lateral capacity of the building were presented.

### 3.1 Notation

In this study, lateral capacity of the selected 8-storey building was presented in the form of capacity curves which were plotted between base shear vs. roof displacement. Significant events in the pushover analysis were duly noted on the curves. Due to limitation of space, abbreviations were introduced to describe the response of the structure during pushover analysis. The general format used in this study was as “YY-Y(Y)”. First two characters represent the damage type of the building components, next character represents name of the building components and the last character represents the location (storey level) of the components in the building. For example, flexural failure of beam B1 (refer Figure 20 for notation) at third floor was represented as FF-B1 (3). The abbreviations FF (flexural failure), FY (flexural yielding) and BW (brick work) were used throughout in the succeeding discussions.

### 3.2 Capacity Curves of the Building

Nonlinear static pushover analysis was performed using two-dimensional frames in the Y-direction of the building plan. The capacity curves were plotted between base shear versus roof displacements and their failure mechanism were presented. To investigate the effect of infill walls, building models without and with infill walls were analyzed but however only the result of 8-storey building model was presented in this section as the failure mechanism and results of 4-storey and 12-storey models were similar with 8-storey models. Furthermore, to investigate the effect of variation in strength of materials on the structure, all the three different buildings were analyzed by varying the compressive strength of brick masonry infill and the thickness on infills.

Building was first analyzed without infill walls along the Y-direction. Capacity of the building without infill wall is as shown in Figure 29, and the damage distribution due to plastic hinge formation is shown in Figure 30.

The capacity curve of the 8-storey building without infill walls (Model-A) showed that after yielding of beams (B1) at second, third, fourth, fifth and sixth floor levels, the overall lateral stiffness of the structure declined. The base shear-roof displacement curve changed slope, i.e. the curve deviated from the initial straight line as shown in the Figure 29. From the point the capacity curve changed its slope to the maximum strength, yielding of all the beams occurred with yielding of some columns. The curve flattened as the yielding spread to the other components and dropped down when the component B1 at third floor failed. The curve continued dropping down as the failure of beams spread to other spans in third floor and other floors. Capacity dropped sharply when column C1-1 at fourth floor failed in flexure. The overall capacity further dropped sharply when column C1-1 and C2-1 at fourth floor failed in flexure. It was noted that all the beams fail at the right end. The reason was, under the combination of gravity and lateral loads, the negative moment demand at right end is much higher than the positive moment demand at left (near loading) end.

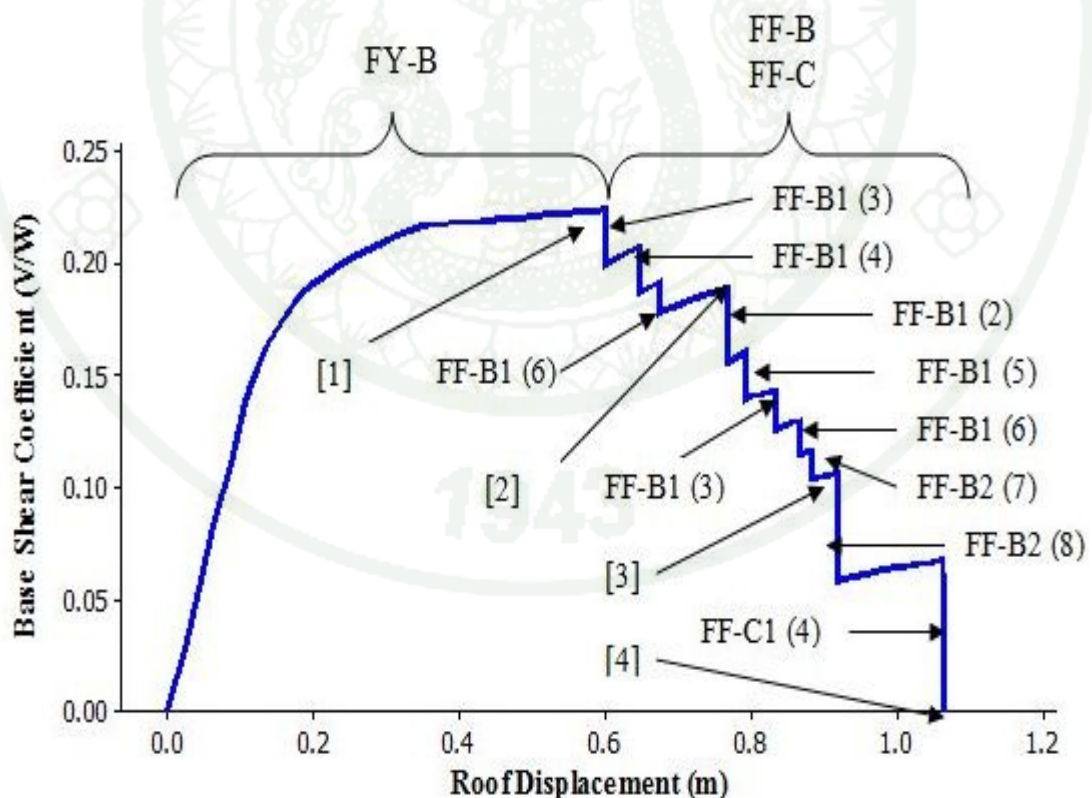


**Figure 29** Capacity Curve of 8-storey Building model (Model-A)

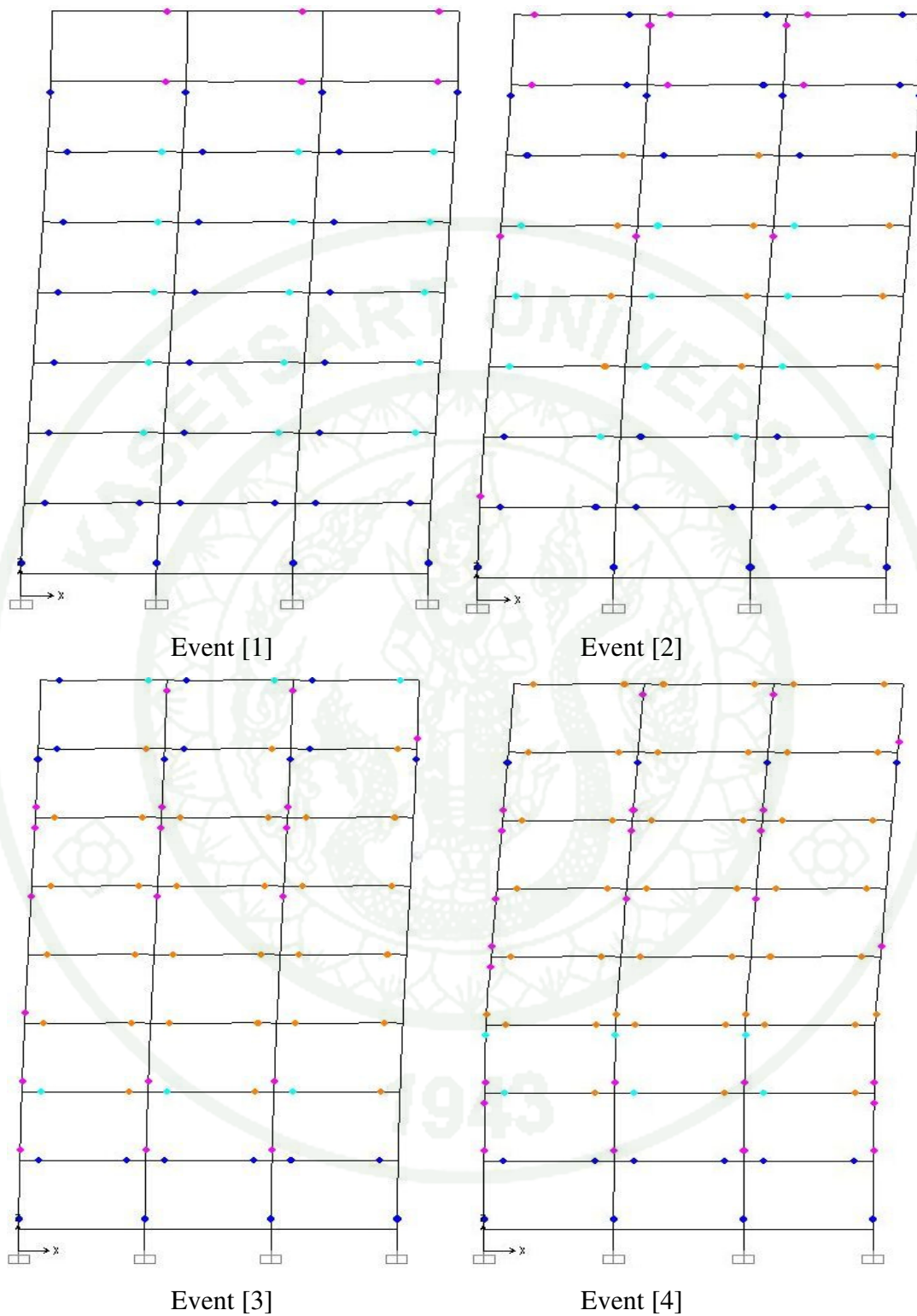


**Figure 30** Damage distribution and failure mechanism of 8-storey building (Model-A)

The capacity curve of 8-storey building model with infill wall (Model-B) showed that after cracking of infill walls, slope deviated from the original straight line. With the failure of walls and yielding of beams B1 at third floor and then followed by rest of the floor, the capacity curve with infill walls became like the capacity curve without walls as shown in Figure 31. In between Event [1] and Event [2], flexural yielding of beam B1 occurred at all the levels while yielding of some columns occurred at the same time. The failure sequence of the building components was similar to that of building without infill walls after the failure of brick masonry walls. The damage distribution and failure mechanism of building with infill walls is shown in Figure 32.

The comparison between the capacity curves with and without infill walls was made. It can be observed from Figure 33 that the infill walls increased the lateral stiffness of the structure but not increased the strength of the building. After the failure of infill walls at first, second, third and fourth floor, the capacity curve of the structure with infill walls came in line with the capacity curve without infill walls and ultimately failed in the same manner as structure without infill walls as shown in Figure 31.

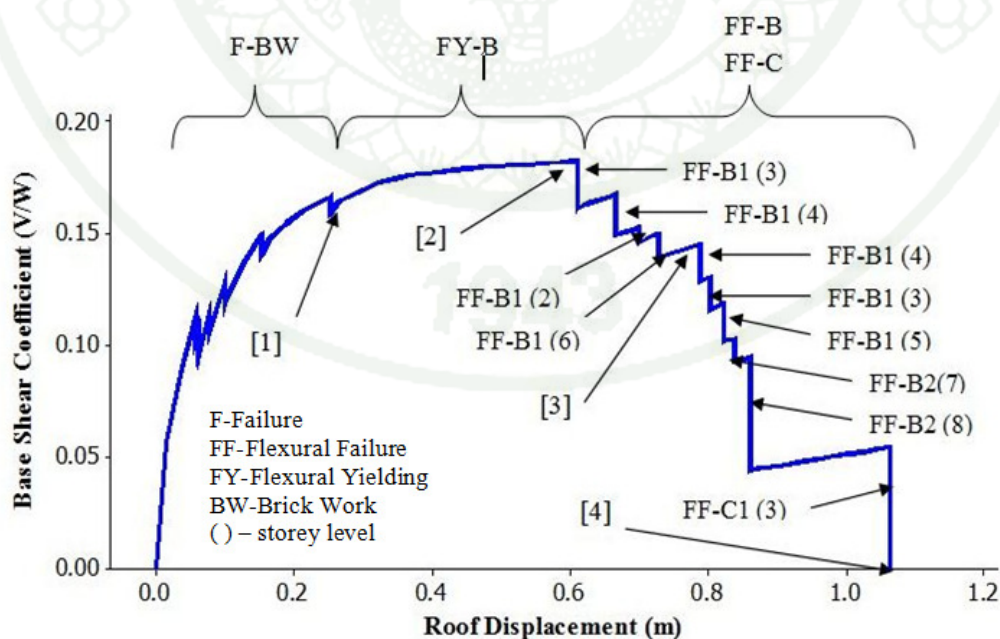


**Figure 31** Capacity curve of 8-storey building model (Model-B)

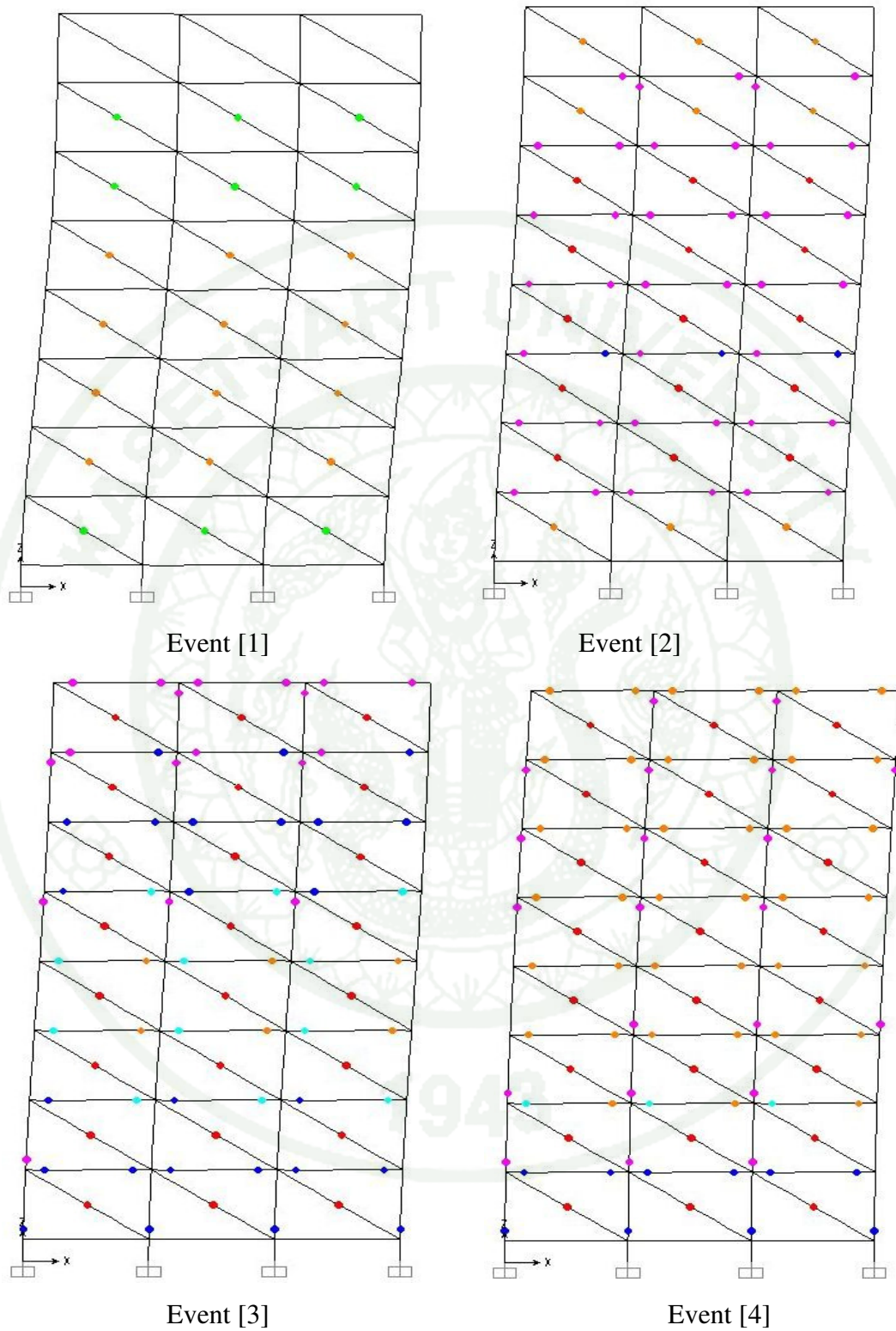


**Figure 32** Damage distribution and failure mechanism of 8-storey building  
(Model-B)

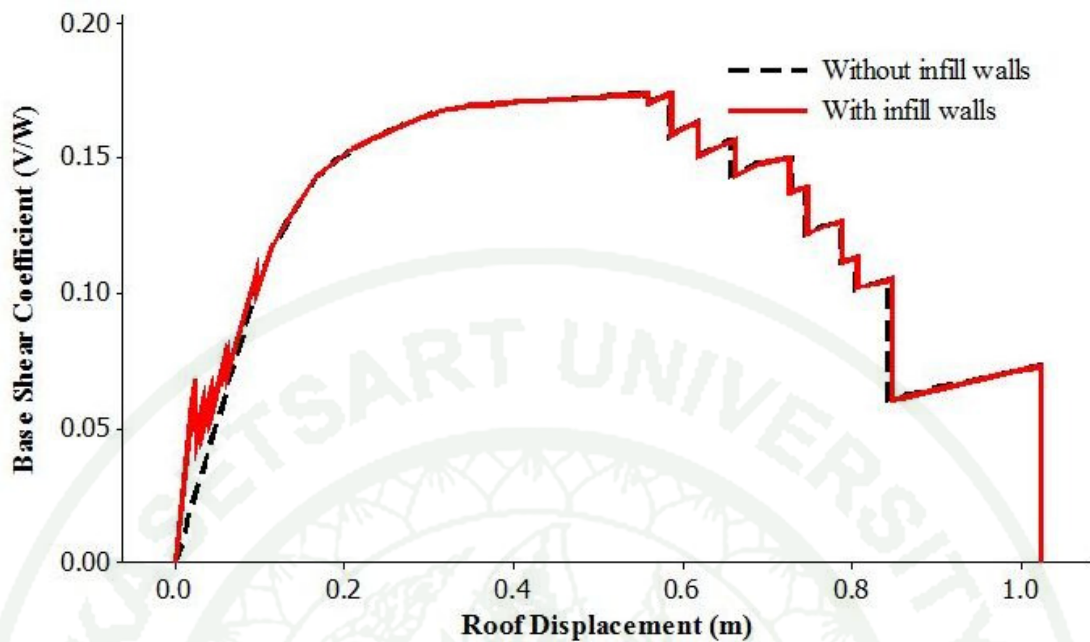


**Figure 33** Comparison of Capacity Curves of Model-A and Model-B of 8-storey building models

### 3.3 Effect of different infill configurations

The study was also done to find out the effect of infill with different configurations, as shown in Figure 19. A comparative study was made for different building models with respect to their capacity curves and initial stiffness from linear equivalent static method. The capacity curve was divided into four stages. First cracking and failure of masonry infills, second maximum capacity, third failure of beams and finally collapse of the building structures. In the elastic range of the curve, there was an increased in initial stiffness before the cracking and failure of masonry infills occurred.

The stiffness of building models shown in Figure 34 was obtained using the linear equivalent static method. From the results of equivalent static method analysis, both roof displacement and base shear of the building models were obtained. The stiffness of the building models were calculated using the relation  $K = P/U$  (stiffness

= Force / Displacement). It can be noted from Figure 34 that the initial stiffness for Model-A (0% infill) was 4618.2 KN/m, 3649.43 KN/m and 3214 KN/m for 4-storey, 8-storey and 12 storey building models, respectively while for Model-B (100% infill) the initial stiffness was 14667.24 KN/m, 12416.67 KN/m and 9213.77 KN/m for 4-storey, 8-storey and 12-storey building models, respectively. The increased in initial stiffness was 217.6% for 4-storey building models, 240.23% for 8-storey building models and 186.67% for 12-storey building models. It can also be observed from Figures 34 to 36 that presence of masonry infill walls increased the stiffness and the strength of the buildings in the elastic range but the ultimate strength of the building remained unaffected. The increased in initial stiffness decreased with increased in height of the buildings. Hence, it indicated the effect of masonry infill walls were more in 4-storey buildings compared to 12-storey buildings.

The different infill configurations also affect the lateral load carrying capacity of the building in the elastic range. It was observed that the lateral load carrying capacity of the building models before the failure of infill walls were 85.5%, 84.3%, 73.2% and 61.16% of the total load carrying capacity of the building for Model-B, Model-C, Model-D and Model-E respectively for a 4-storey building models. However, for the same displacement, the load resisting capacity of Model-A (Bare frame) was only 48% of the total load carrying capacity of the building. Similarly for 8-storey building models, the affect on the load carrying capacity was 70%, 69%, 64.68% and 47% for Model-A, Model-B, Model-C and Model-E respectively, of the maximum load carrying capacity of the 8-storey building while it was only 44% for Model-A for same displacement. For 12-storey buildings, the affect on load resisting capacity of the building for same displacement was 65.55% for Model-B, 65.35% for Model-C, 63.7% for Model-D, 54% for Model-E and 52% for Model-A of the maximum load resisting capacity of 12-storey building. It was noted that the presence of infill wall increases the load resisting capacity of the building in the elastic range. The effect on the load resisting capacity of the building due to infill was observed to be more in the lower storey building and the effect decreases as the height of the building increases.

With different infill configurations, only the initial behaviour of the building is changed. In the elastic range of the pushover curve, the change in behaviour like stiffness, strength and deformation capacity takes place. The models with different infill configurations have different variation in stiffness, strength and deformation capacity. The variation in the above behaviour was dependent on percentage of area of infill present in the models.

It was witnessed that the increase in stiffness of the buildings were depended on the area of percentage of infills (Figure 34) while failure of building models were depended on the vertical configurations of infills. When the ground storeys were kept open (Model-C) for the functional requirements, the buildings models tend to have a soft storey mechanism, as plastic hinges formed first in columns in the ground storey (Figure 35). The other configurations (Model-D and Model-E) have not much effect on the failure modes but initial stiffness changed as the area of infill changed.

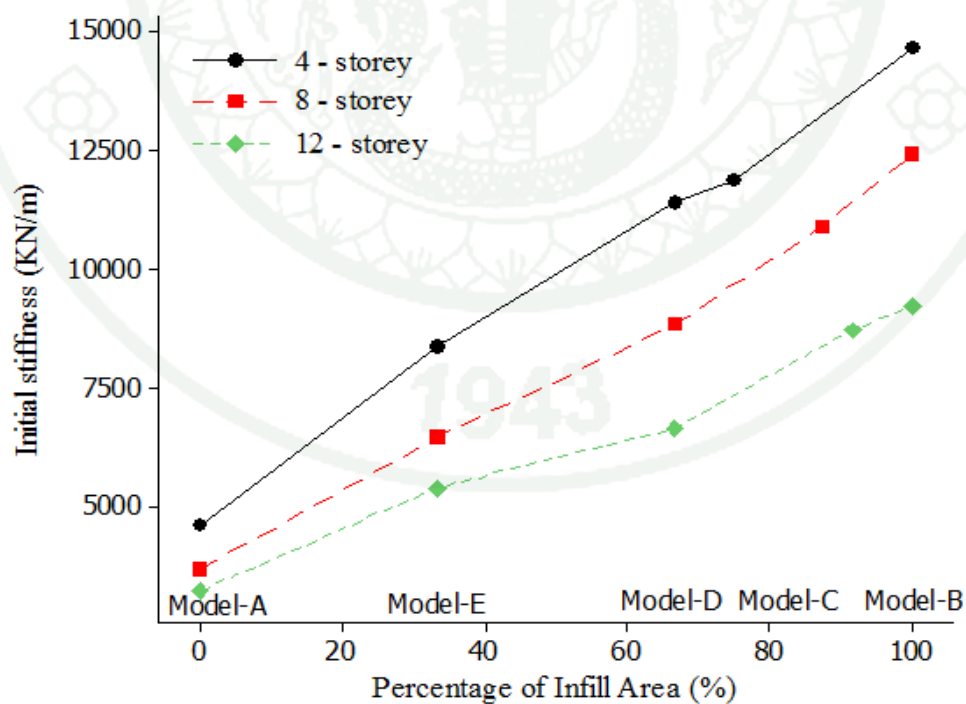


**Figure 34** Effect of infill area on initial stiffness of building models

It can be seen from Figure 36 to 38 that Model-A and Model-B were the two extreme cases while the other models falls in between these two models as expected. The effect of infill walls depend on percentage of infill area in the model and not much on the horizontal locations or configurations. The failure behaviour depends on the vertical location of the infill walls specially the vertical configurations. There was soft storey mechanism when infill walls in the first floor were removed (Model-C). In all the models it was observed that there was no increased in the ultimate strength.

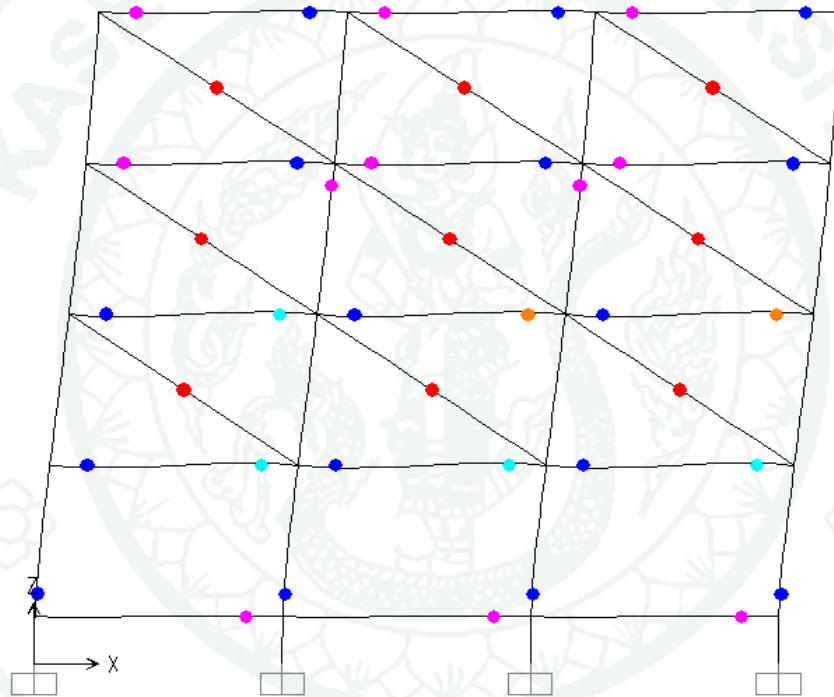


**Figure 35** 4-storey building model showing soft storey mechanism (Model-C)

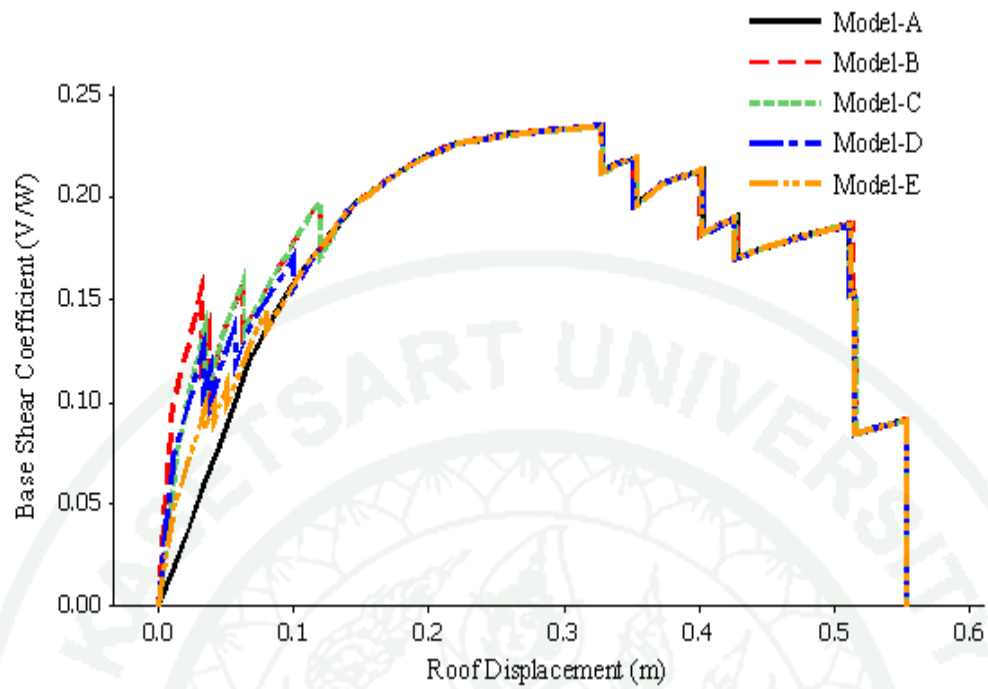


**Figure 36** Capacity curves of 4-storey building models

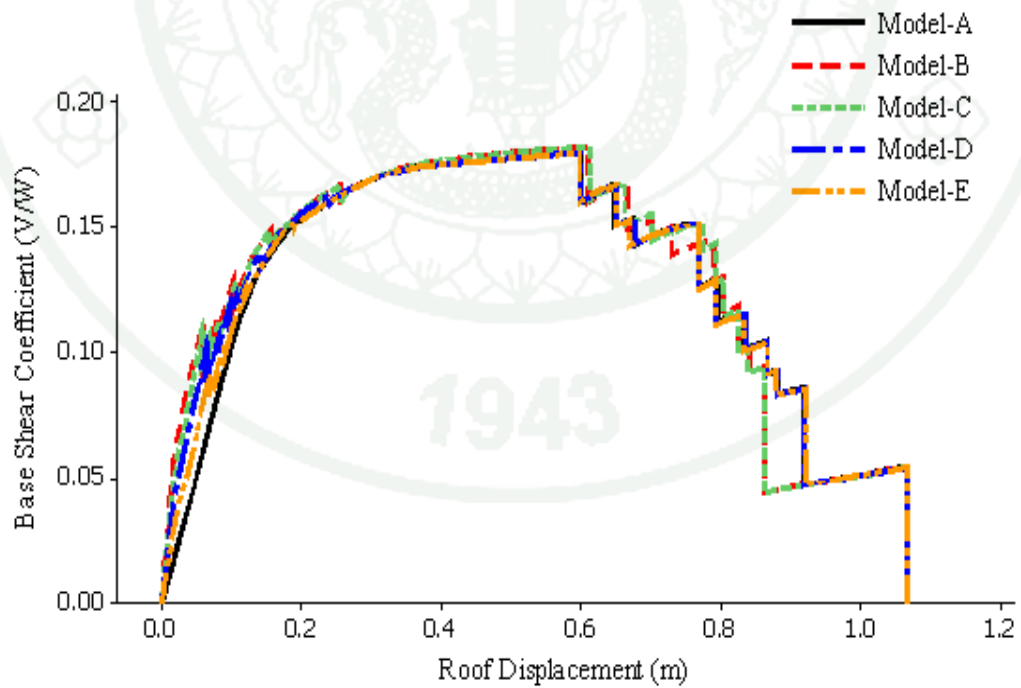


**Figure 37** Capacity curves of 8-storey building models

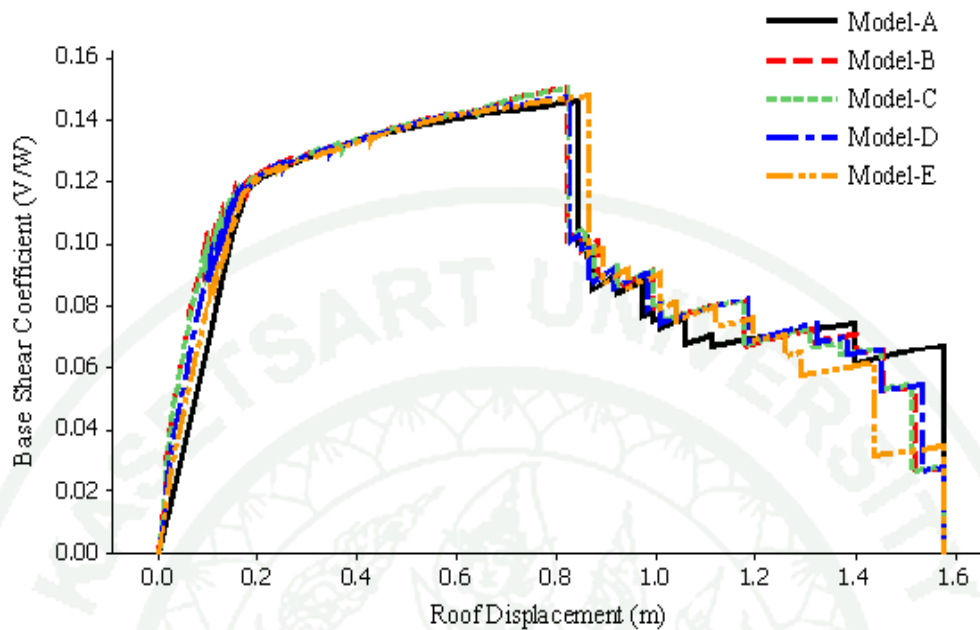


**Figure 38** Capacity curves of 12-storey building models

### 3.4 Effect of compressive strength and thickness of infill walls

Other than the configurations of the infill, compressive strength of the infill material and the thickness of the infill walls were investigated. Figure 39 and 40 show the effect of compressive strength of brick infill wall on a 4-storey and 8-storey building models. It was observed that when the compressive strength was increased from 3 MPa to 5 MPa, there was increased in initial stiffness from 10562.4 KN/m to 13692 KN/m for 4-storey building models and from 13674.4 KN/m to 17092.8 KN/m for 8-storey building models. The increased in percentage of initial stiffness was 29.63% and 25% for 4-storey and 8-storey building models, respectively. It can be seen that the increased in initial stiffness decreased with increased in height of the building.

The study on the effect of thickness of infill wall was also done in this study. When the thickness of the infill wall was increased, the initial stiffness and strength of the building models increased. It can be seen from Figure 41 that the initial strength of the building model with infill thickness of 300 mm was almost greater or equal to the ultimate strength of the building model. It was observed that there was drastic increased in strength of the building model in the elastic region until the failure of infill walls.

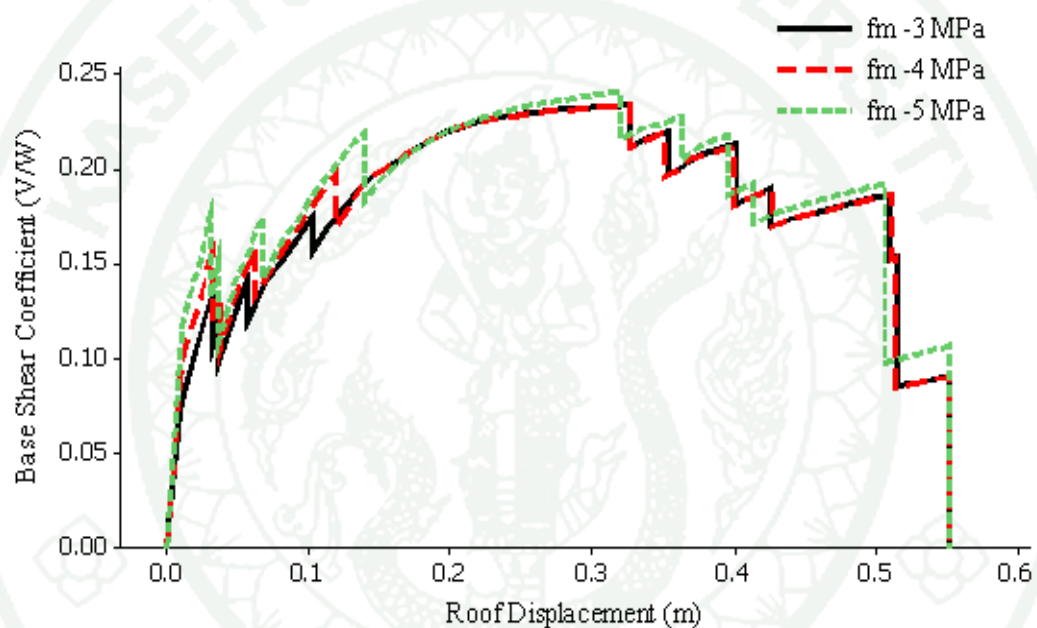


**Figure 39** Capacity curves of 4-storey building (Model-B) with different compressive strength of infill

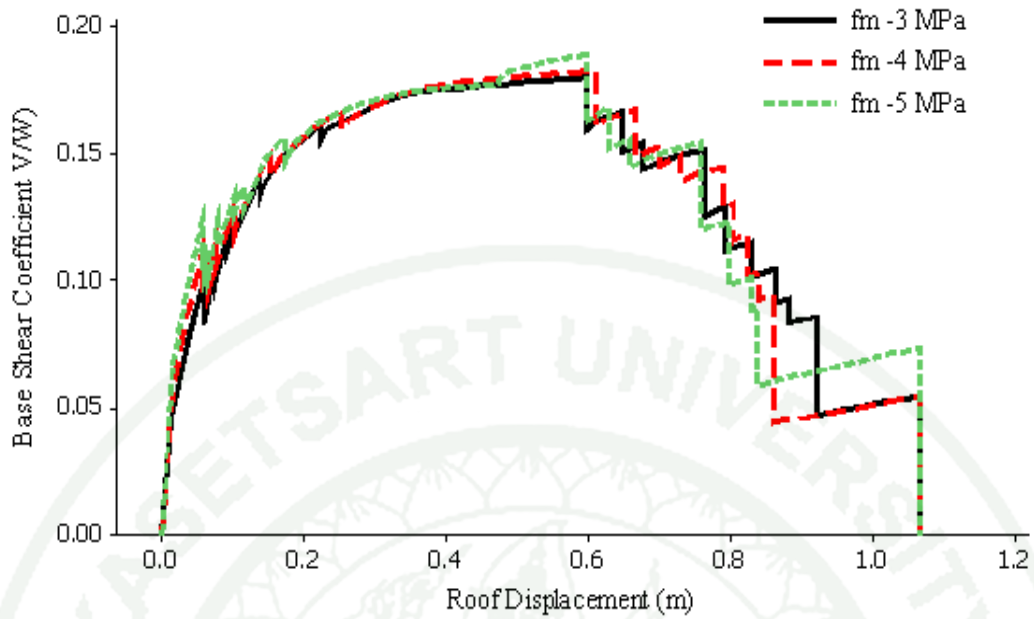


**Figure 40** Capacity curves of 8-storey building (Model-B) with different compressive strength of infill

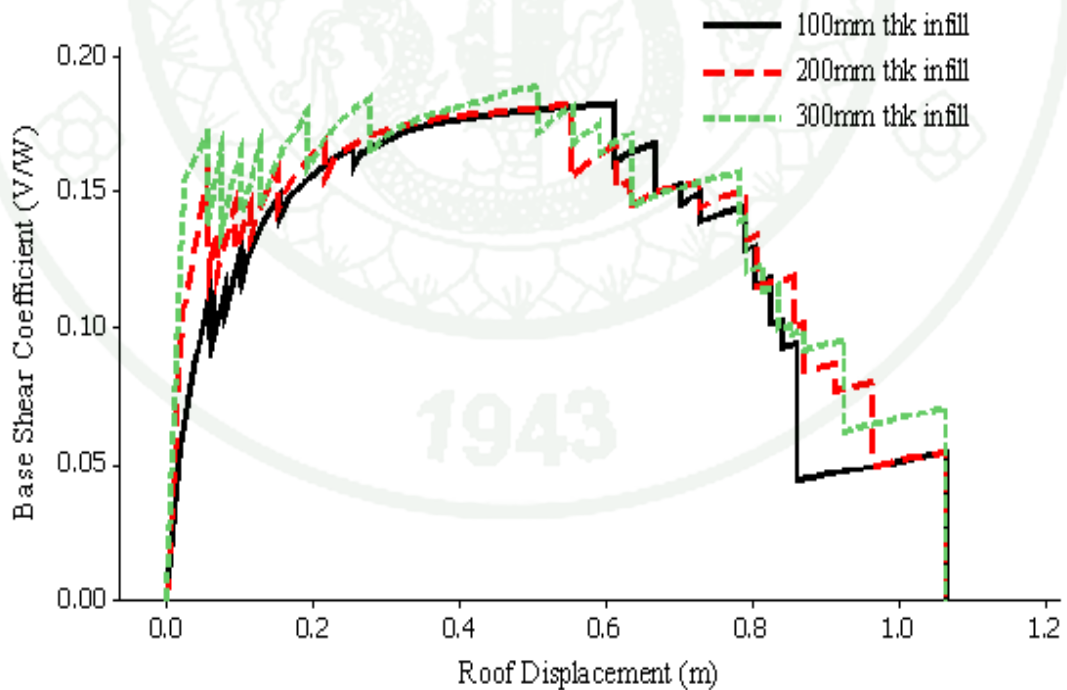


**Figure 41** Capacity curves of 8-storey building (Model-B) with different infill thickness

#### 4. Different earthquake levels

The study was also done on the behaviour of fully infilled building models under different earthquake levels. The study on three levels of earthquakes viz. serviceability earthquake (SE), design earthquake (DE) and maximum earthquake (ME) were done to find out the capacity of the fully infilled building models to resist these levels of earthquakes. The aim was to find out if masonry infill walls can withstand the minimum level of earthquake force (serviceability earthquake). The three earthquake levels can be defined as (ATC-40, 1996):

The serviceability earthquake (SE) is defined as the level of ground shaking that have a 50 percent probability or chance of being exceeded in a 50 year period. This type of ground shaking is typically about 0.5 times the level of ground shaking of the design earthquake.

The design earthquake (DE) is defined probabilistically as the level of ground shaking that have a 10 percent chance of being exceeded in 50 year period.

The maximum earthquake (ME) is defined as the level of earthquake ground shaking that has a 5 percent probability of being exceeded in a 50 year time period. It can also be defined as deterministically the maximum level of earthquake ground shaking which may ever be expected at the building site.

In this research study, the fulfillment for immediate occupancy criterion was studied for the infilled building models under the serviceability earthquake. Immediate occupancy, means the post-earthquake damage state in which only very limited structural damage has occurred. The basic vertical and lateral-force-resisting systems of the building retain nearly all of their pre-earthquake strength and stiffness. The risk of life-threatening injury as a result of structural damage is very low, and although some minor structural repairs may be appropriate, these would generally not be required prior to re-occupancy (ATC-40, 1996).

It can be observed from Figure 42 (4-storey building Model-B) that the infill walls withstand the serviceability level of earthquake with out failure though damage might have occurred but this was not the case with 8-storey (Model-B) and 12-storey (Model-B) building models (Figure 43 and 44). The infills were collapsed or damaged before their capacity reached the serviceability earthquake level while all the main structural elements were capable of withstanding the design level of earthquake and not the maximum level.

It was found that all the three types of buildings with infill walls have the capacity to resist the design level of earthquake forces without any complete failure of their structural components. A minor crack or damage might have occurred but no complete failure of structural element was observed. The yielding of the beam components reached up to the level of immediate occupancy or life safety performance level for the design earthquake force for all the three types of building models with fully infilled masonry walls. Hence, conclusion can be made that good detailing and designed should be done to make reinforced concrete frames with infill walls an earthquake resistant building.

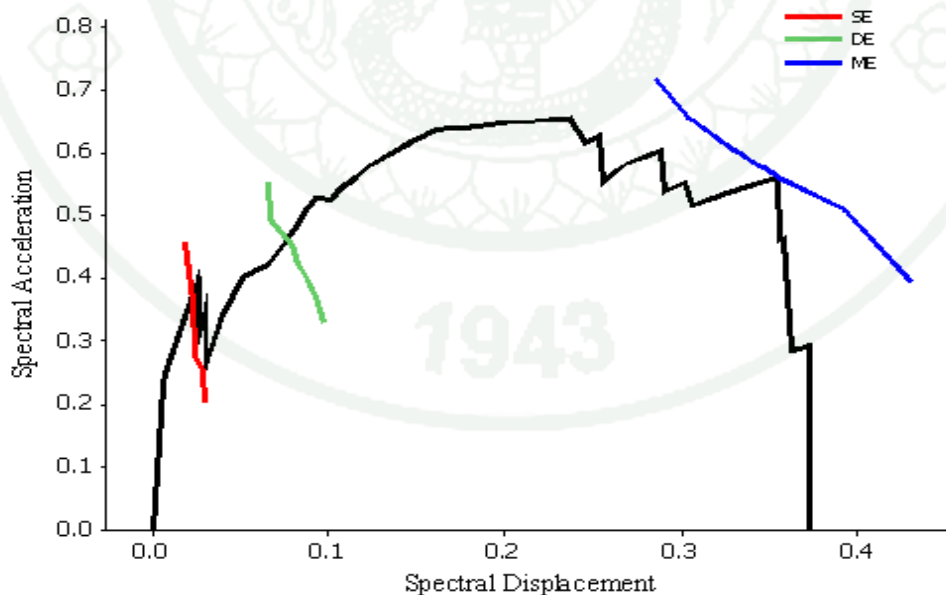


**Figure 42** Capacity curve of 4-storey building (Model-B) with demand curves of different level of earthquake

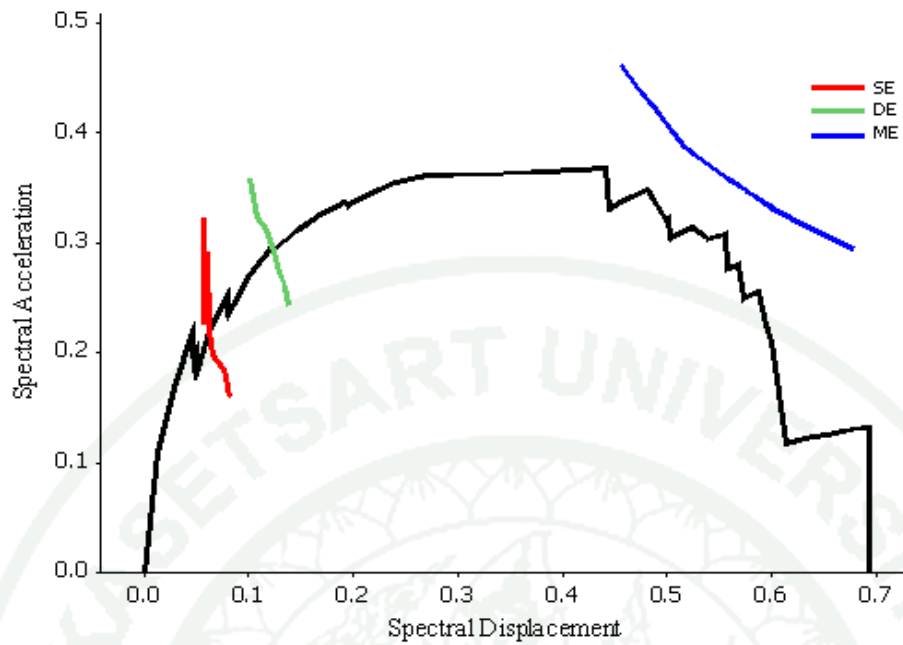


**Figure 43** Capacity curve of 8-storey building (Model-B) with demand curves of different level of earthquake

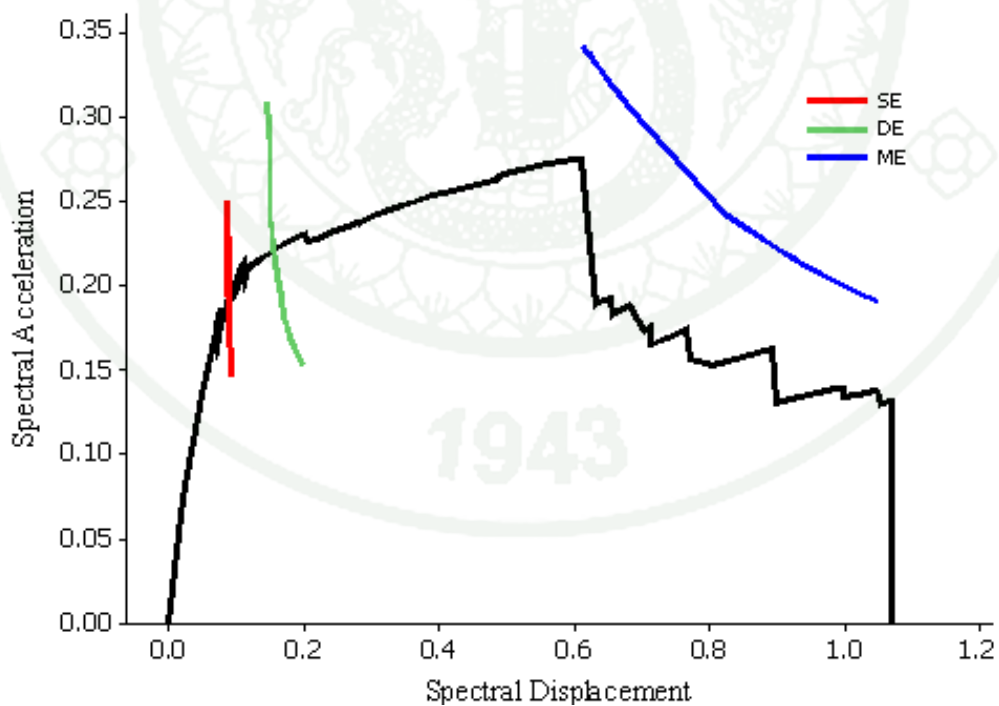


**Figure 44** Capacity curve of 12-storey building (Model-B) with demand curves of different level of earthquake

## CONCLUSIONS AND RECOMMENDATIONS

A study on effect of masonry infill walls on behaviour of reinforce concrete frame buildings under seismic force was studied using different infill patterns or configurations. The infill walls were usually considered as non-structural elements and were not included in the analysis and design. However, the fact is far from reality as the infill walls would definitely interact with the enclosing frame especially under seismic forces.

The effect of masonry infills on seismic behaviour of RC frame buildings with different heights, designed as per current Indian codes of practice was studied by utilizing nonlinear static pushover analysis. The infill walls were modeled as compressive equivalent diagonal strut having nonlinear hinge at the mid-span. The dimensions of diagonal strut were calculated as per the guidelines given in ATC-40 and FEMA- 356. Columns and beams were modeled as line element having nonlinear hinges lumped at the ends. Five different models for each building type were studied. The parametric study on thickness of infill, fundamental period and compressive strength of infill walls were also done.

### Conclusions

The results from the different models on fundamental periods were discussed here. It was observed that masonry infill walls had significant effect (increases the time period) on the dynamic characteristics like fundamental period of the buildings. The fundamental periods were dependent on the area of infill walls. It was also observed that the IS: 1893-2002 gave highly conservative time period formula for infilled frame buildings compared to analysis.

The results of analysis demonstrated that masonry infill walls highly increased the stiffness and strength of a structure in the elastic region as long as the seismic

demands did not exceed the deformation capacity of the infills. After that, both the global stiffness and the strength fall back to the same value of bare frame. It was also observed that different configurations of infills did not have much effect on the stiffness if the area of percentage of infills remained same. However, the vertical locations of infills could have an effect on the collapse mechanism, especially for the buildings with open ground storey. This effect was confirmed by the results of 4-storey building model (Model-C).

The other parametric study that was done was infill wall thickness. The results indicated that the structural responses were affected with infill thickness. The increased in infill thickness decreased the fundamental period and roof displacement stiffness. This occurred due to increase in lateral stiffness of the models with increased in infill thickness. The increase in lateral stiffness occurred only in the elastic range of the capacity curve. The increase in thickness of infill wall also increased the initial strength of the building model in the elastic range. However, the ultimate strength of the building model remains unchanged with changed in the infill wall thickness.

The compressive strength of infill wall has a role in the global behaviour of the building models and its performance too. The structural responses such as roof displacement and fundamental period decreased with increased in compressive strength. This happened due to increased in lateral stiffness and strength of the building models in the elastic range of the capacity curve. Hence, it is important to choose the right material for infill and consider it in the analysis and design.

The final study that was done to study the behaviour of the infilled reinforced concrete frame was on different earthquake levels. Three different levels of earthquakes were applied to building models (Model-B) of all three types of buildings having full infill walls. From the capacity curve it was observed that all the building models have the capacity to resist both SE and DE levels of earthquake but not the

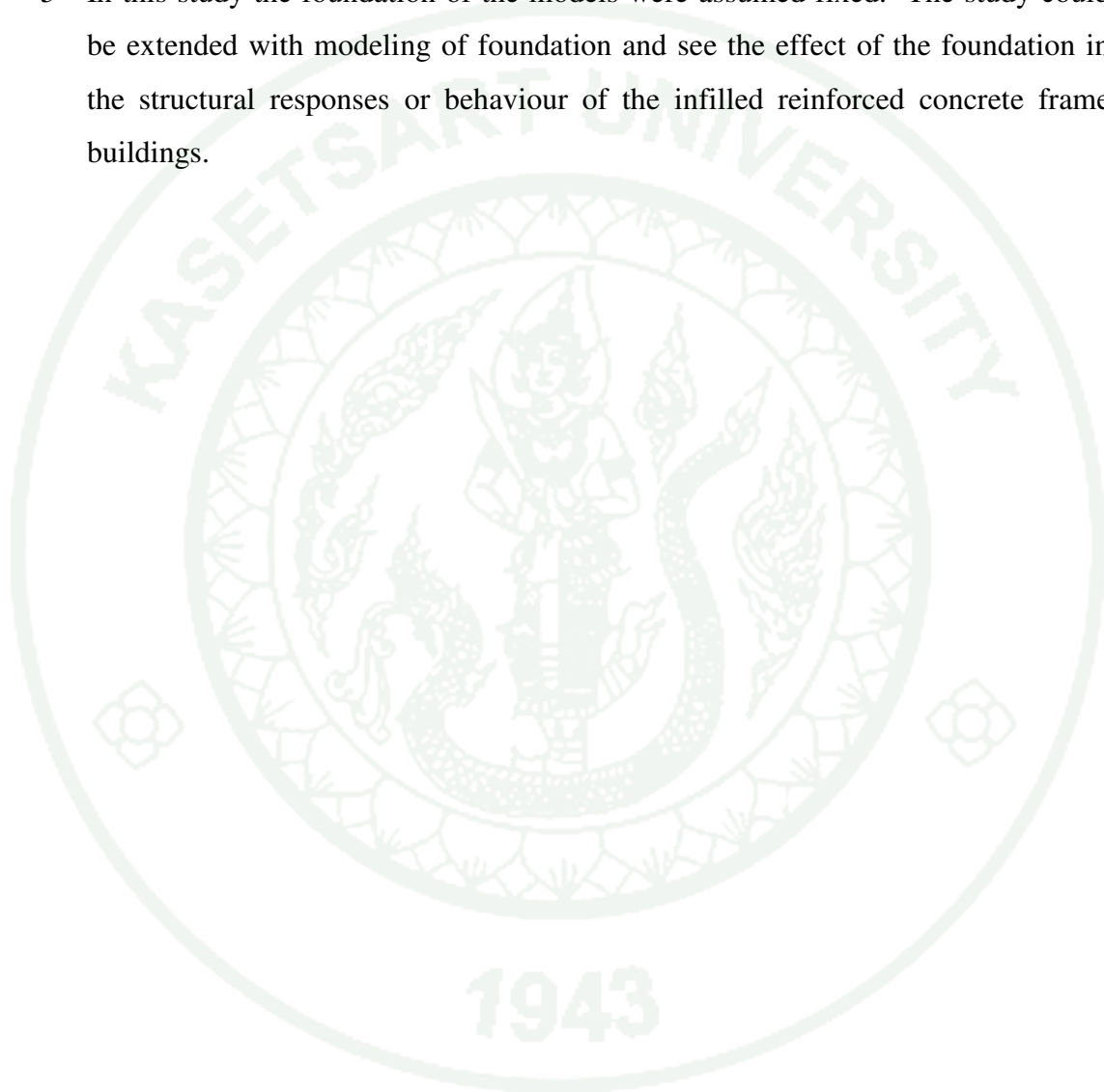
ME level of earthquake. It can be assumed that masonry infill walls help in increasing the performance of the building models at SE level especially in the low rise buildings (4-storey building).

### **Recommendations**

The multi-storey buildings in most of the countries around the world consist of moment resisting reinforced concrete frames. This reinforced concrete frames have infill walls in the vertical space created by reinforced concrete beams and columns. However, this masonry infill walls were not considered as an integral part of the moment resisting structure and not included in the analysis and design. Nevertheless, the fact is that these masonry infill walls interact with the reinforced concrete members during the earthquakes leading to an unexpected failure of the structure. To understand the effects of masonry infill walls, a small effort was made in this study. Three different building with analytical models of both bare frame and infill frame were studied using non linear static pushover analysis. Following were made for further study.

1. The empirical formulae given by the codes to compute the fundamental natural period depends on height and width of the building only. A further study could be done to find the effect of number of span, span length and orientation of column for rectangular columns.
2. The present study was carried out for fully infill frame without openings. This could be extended to infill walls with openings and partial infills.
3. The study was carried out using macro-modeling approach which takes into account only the global behaviour of the infill in analysis. To capture the local conditions within the infill in detail, further study could be carried out using micro-modeling approaches.

- 4 The present study was limited to two dimensional models only. Further study could be carried out using three dimensional models to capture the true behaviour of the building structures including torsion.
- 5 In this study the foundation of the models were assumed fixed. The study could be extended with modeling of foundation and see the effect of the foundation in the structural responses or behaviour of the infilled reinforced concrete frame buildings.



## LITERATURE CITED

- Applied Technology Council. 1996. **Seismic evaluation and retrofit of reinforced concrete buildings, ATC-40 report**. California Seismic Safety Commission, California, USA
- American Concrete Institute. 2002. **Building code requirement of beam-column joints in monolithic reinforced concrete structures (ACI352R-91)**. Michigan, Farmington Hills, USA
- Arshad K. Hashmi and Alok Madan. 2008. Damage forecast for masonry infilled reinforced concrete framed buildings subjected to earthquakes in India. **Current Science** 94(1): 35 - 42
- Barin B. and Pincheira J.A. 2002. **Influence of Modeling Parameters and Assumptions on the Seismic Response of Existing Buildings**. M.Eng. Thesis, University of Wisconsin.
- Baris, B., Guney, O. and Ramazan, O. 2006. Analysis of FRP composite for seismic retrofit of infill walls in RC frames. **Engineering Structures**, 38: 575-583.
- Binay Charan Shrestha, 2008. **Effect of unreinforced full and partial infilled brick masonry wall in RC frame under seismic loading**. M.Eng. Thesis, Kasetsart University
- Chao Hsun Huang, Yungting Alex Tuan and Ruo Yun Hsu, 2006. Nonlinear pushover analysis of infilled concrete frames. **Earthquake Engineering and Engineering Vibration** 5(2):1671-3664.
- Dowrick, D.J., 1987. **Earthquake Resistant Design for Engineers and Architects**. John Wiley & Sons, New York.

- FEMA 273. 1997. **NEHRP Guidelines for the Seismic Rehabilitation of Buildings**. Building Seismic Safety Council, Federal Emergency Management Agency, Washington (DC).
- FEMA 306/307. 1998. **Evaluation of Earthquake Damaged Concrete and Masonry Wall Buildings, Basic Procedures Manual**. Applied Technology council, Federal Emergency Management Agency, Washington (DC).
- FEMA 356. 2000. **Prestandard and Commentary for the Seismic Rehabilitation of Buildings**. American Society of Civil Engineers, Federal Emergency Management Agency, Washington (DC).
- FEMA 450. 2003. **NEHRP Recommended Provisions for Seismic Regulations for New Buildings and other Structures**. Building Seismic Safety Council, Federal Emergency Management Agency, Washington (DC).
- Ghassan Al-Chaar, Mohsen Issa, and Steve Sweeney, 2002. Behavior of Masonry-Infilled Non-ductile Reinforced Concrete Frames. **Journal of Structural Engineering** ASCE, 128(8): 0733-9445.
- Girgin K. and Darilmaz K. 2007. Seismic response of infilled framed buildings using pushover analysis. **ARI. The Bulletin of the Istanbul Technical University**, 54(5): 23-30.
- Han-Seon Lee and Sung-Woo Woo. 2002. Effect of masonry infills on seismic performance of a 3-storey reinforced concrete frame with non-seismic detailing. **Earthquake Engineering and Structural Dynamics**. 31: 353–378
- Helmut Krawinkler and G. D. P. K. Seneviratna, 1998. Pros and cons of a pushover analysis of seismic performance evaluation. **Engineering Structures**. 20: 452-464

Holmes, M. 1961. Steel Frames with Brickwork and Concrete Infilling. **Proceedings of Institution of Civil Engineers**.19: 473-478.

Hossein Mostafaei and Toshimi Kabeyasawa, 2004. Effect of infill masonry walls on the seismic response of reinforced concrete buildings subjected to the 2003 Bam Earthquake strong motion: A Case Study of Bam Telephone Center. **Bulletin of the Earthquake Research Institute**. University of Tokyo, Vol. 79: 133-156

Inel, M. and Ozmen, B.H. 2006. Effect of plastic hinge properties in nonlinear analysis of RC building. **Engineering structures**. 28: 1494-1502.

Inel, M., Ozmen, B.H. and Bilgin, H. 2007. Re-evaluation of building damage during recent earthquakes in Turkey. **Engineering structures**. 30: 412-427.

Kadid, A. and Boumrkik, A. (2008). Pushover analysis of reinforced concrete frame structures. **Asian Journal of Civil Engineering (Building and Housing)**. 9(1): 75-83.

Kasim Armagan Korkmaz, Fuat Demir and Mustafa Sivri, 2007. Earthquake Assessment of R/C structures with Masonry Infill Walls. **International Journal of Science and Technology**. 2 (2): 155-164.

Kiattavisanchai, S. 2001. **Evaluation of seismic performance of an existing medium rise reinforced concrete frame buildings in Bangkok**. M.Eng. Thesis, Asian Institute of Technology

Konuralp Girgin and Kutlu Darilmaz, 200. Seismic Response of Infilled Framed Buildings Using Pushover Analysis. **ARI The Bulletin of the Istanbul Technical University**. 54 (5): 33-41.

- Lakshmanan, N. 2006. Seismic Evaluation and Retrofitting of Buildings and Structures. **ISSET Journal of Earthquake Technology**.43: 31-48
- Lee, D.G.; Choi, W.H.; Cheong, M.C.; Kim, D.K., 2006. Evaluation of seismic performance of multistory building structures based on the equivalent responses. **Engineering Structures**. 28: 837–856
- Lourance, P.B., 2002. **Guidelines for analysis of Historical Masonry Structures**. Finite Elements in Civil Engineering Applications. Hendriks & Rots(eds); Swets & Zeitinger, Lisse. 90: 509-530
- Madan, A., A.M. Reinhorn, J.B.Mander and R.E.Valles, 1997. Modeling of Infill Panels for Structural Analysis. **Journal of Structural Engineering ASCE**, 123 (10): 1295-1302.
- Mekonnen Degefa, 2005. **Response of Masonry Infilled RC Frame under Horizontal Seismic Force**. M.Eng. Thesis, Addis Ababa University
- Mohemed Nourel-din Abd-alla, 2007. **Application of Recent Technique of Pushover for Evaluating Seismic Performance of Multistory Buildings**. M.S. Thesis, Cairo University.
- Mizam Dogan, 2009. Damage of open ground storey during earthquakes. **Proceedings of World Academy of Science, Engineering and Technology**. 38: 2070-3740
- Mwafy, A.M. and Elnashai, A.S., 2001. Static pushover versus dynamic collapse analysis of RC buildings. **Engineering Structures**. 23: 407–424
- Paolo Bazzurro, Fabrizio Mollaioli, Adriano De Sortis and Silvia Bruno. 2006. Effects of Masonry walls on the seismic risk of reinforced concrete frame buildings. **The Proceedings of 8<sup>th</sup> US National Conference**

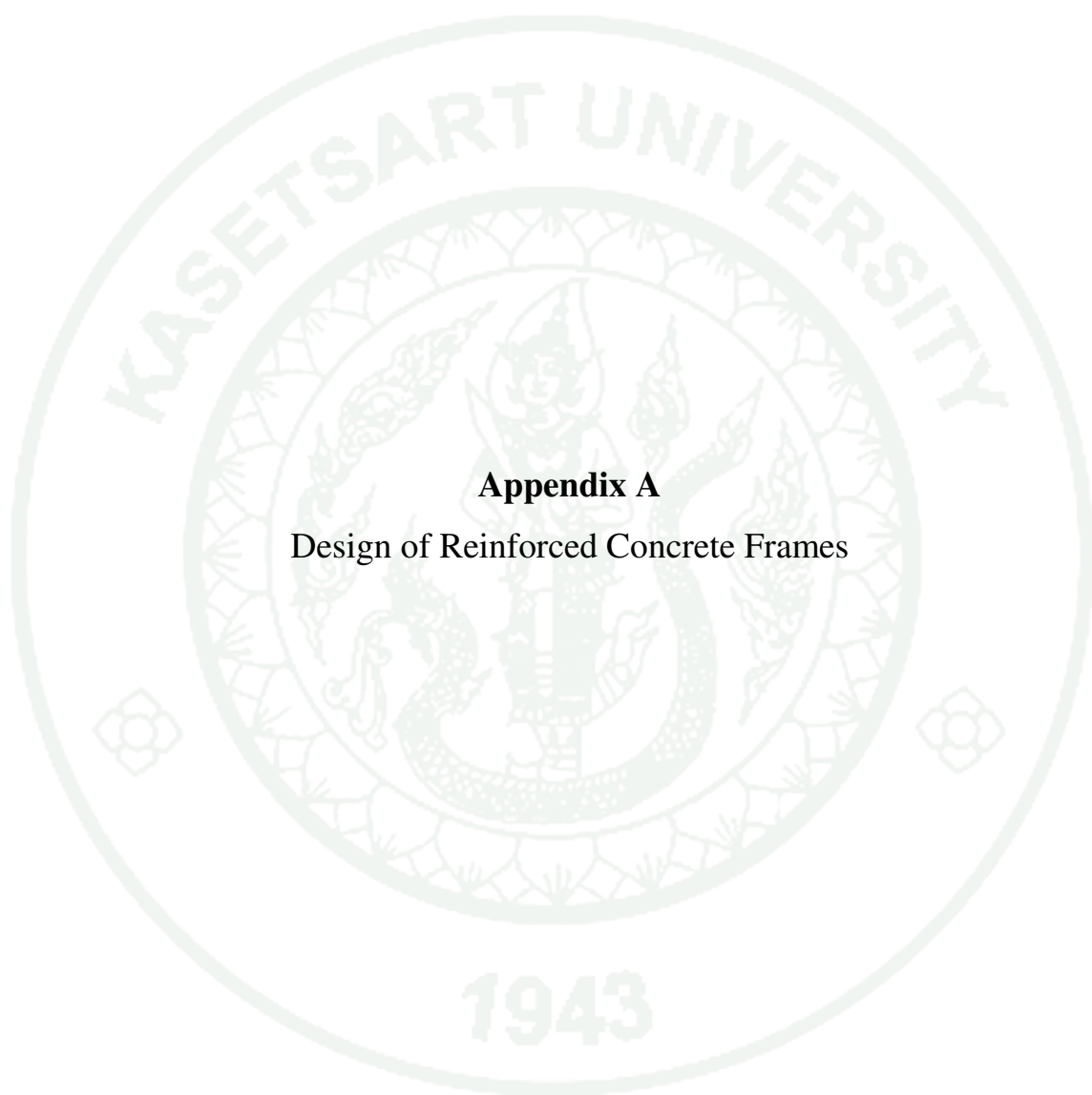
- Pauley, T. and M.J.N. Priestley, 1991 . **Seismic Design of Reinforced Concrete and Masonry Buildings**. John Wiley & Sons, New York.
- Penelis, G. G. and Kappos, A. J. 1997. **Earthquake Resistant Concrete Structures**. St. Edmundsbury Press Limited, Bury St. Edmunds, Suffolk.
- Phatiwet, P. 2002. **Seismic evaluation of beam-column frame building with non-ductile reinforced concrete details**. M.Eng. Thesis, Asian Institute of Technology.
- Phuentsho Choden. 2009. Earthquake hits Bhutan. Available Source: <http://www.kuenselonline.com>. September 23, 2009.
- Pinho, R., Casarotti, C. and Antoniou, S. (2007). A comparison of single-run pushover analysis techniques for seismic assessment of bridges. **Earthquake Engineering and Structural Dynamics** 36: 1347-1362.
- Robert R. Schneider and Walter L. Dickey. 1980. **Reinforced Masonry Design**. Prentice-Hall, INC. Englewood cliffs, New Jersey.
- Smith, B.S. 1962. Lateral Stiffness of Infilled Frames. Proceeding of the American Society of civil Engineering, **Journal of Structural Engineering** ASCE, 88 (ST6): 183-199.
- Smith, B.S. and A. Coull. 1991. **Tall Building Structures: Analysis and Design**. John Wiley & Sons, New York.
- Tassios, T.P., 1984. Masonry infill and R/C walls under cyclic actions. **CIB Symposium on Wall Structure**, State-of-the- Art Report, Warsaw.

Yong, L. 2002. Comparative Study of Seismic Behavior of Multistory Reinforced Concrete Framed Structures. **Journal of Structural Engineering** ASCE, 128: 0733-9445





**APPENDICES**



**Appendix A**  
Design of Reinforced Concrete Frames

### **Design of Reinforced Concrete Frames**

The reinforced concrete structures that were treated in this thesis were designed to IS 456-2000 and IS 1893-2002, which are the existing codes, used in the country. A limit state design concept has been used to proportion the structural members.

The concrete material with Young's Modulus of elasticity of  $22.36 \text{ N/m}^3$  and Poisson ratio of 0.2 has been considered in this design. The structural system under considerations were two dimensional models with live load of  $3 \text{ kN/m}^2$  assumed on an average tributary area of  $25 \text{ m}^2$ . The density of concrete and brick masonry was considered as  $24 \text{ KN/m}^3$  and  $20 \text{ KN/m}^3$  which were used for the seismic weight calculations.

The source of structural mass are from structural members, infill walls, floor slabs, floor finishes and imposed load. Here, since the structural system under consideration was two dimensional, a tributary width of 2.5 meters is assumed to exist and used to calculate the imposed load and dead load from the slab. All loads were applied uniformly throughout the beam elements at every level of the floor height. The uniform dead load of  $18.75 \text{ KN/m}$  had been calculated to act on the beams where as a live load of  $15 \text{ KN/m}$  was applied.

### **Building structures designed to IS 1893-2002**

The loads defined above were used to find the total seismic weight which in turn was used to obtain the total base shear of the building models under static conditions. Table A1 shows the seismic weight calculation of 8-storey building. The total seismic weight was 100% of dead loads and 25% of live loads acting on the structure according to IS 1893-2002.

The fundamental natural period of the building structure was found to be 0.878 seconds by using the empirical formulae specified in the code.

$$T = 0.075h^{0.75}$$

$T$  = fundamental period of the reinforced concrete building structures without infill walls

$h$  = Height of the building structures in meters

**Appendix Table A1** Seismic weight calculation of 8-storey building

Storey level	Storey Height (m)	Slab (KN)	Infill Weight (KN)	Column & Beam (KN)	Total Dead Load (KN)	Live Load (KN)
1	1	140.625	81	141.45	363.075	112.5
2	4.2	140.625	81	141.45	363.075	112.5
3	7.4	140.625	81	141.45	363.075	112.5
4	10.6	140.625	81	141.45	363.075	112.5
5	13.8	140.625	81	141.45	363.075	112.5
6	17	140.625	81	141.45	363.075	112.5
7	20.2	140.625	81	141.45	363.075	112.5
8	23.4	140.625	81	141.45	363.075	112.5
9	26.6	140.625	27	93.225	260.85	112.5
Total					3165.45	1012.50

The total seismic weight

$$W = DL + 25\% LL$$

$$= 3165.45 + 0.25 \times 1012.50$$

$$= 3165.45 + 253.125 = 3418.575 \text{ KN}$$

The design horizontal seismic coefficient is given by the following expression (IS 1893, 2002):

$$A_h = \frac{ZI}{2R} \left( \frac{S_a}{g} \right) \quad (A1)$$

Where,

Z = Zone factor for the Maximum Considered Earthquake (MCE)

I = Importance factor, depending upon the importance of the building structure

R = Response reduction factor

$S_a/g$  = Average response acceleration coefficient corresponding to the period

$\frac{1}{2}$  = the factor used to convert MCE to Design Basis Earthquake (DBE)

A zone factor Z = 0.36, I = 1, R = 5 and  $S_a/g$  = 2.5 (from figure 2, IS 1893-2002, for medium soil condition corresponding to the fundamental period of 0.878 seconds) was used.

Based on the above assumption, the lateral seismic coefficient was found as

$$A_h = (0.36 \times 1 \times 2.5) / (2 \times 5) = 0.09$$

The total base shear is given by the following equation from the code;

$$V_b = A_h W$$

Where,

W = total seismic weight of the building

Thus the total base shear was;

$$\begin{aligned} V_b &= 0.09 \times 3418.575 \\ &= 307.67 \text{ KN} \end{aligned}$$

The total base shear was distributed to storey levels using the formulae given in the code and the corresponding lateral forces was applied at the storey levels as shown in Figure A1. The formulae for the code;

$$Q_i = V_B \frac{W_i h_i^2}{\sum_{j=1}^n W_j h_j^2} \quad (A2)$$

Where;

$W_i$  = the seismic weight of a particular floor

$h_i$  = height of a particular floor from the base

**Appendix Table A2** Distribution of lateral forces

<b>Height (m)</b>	<b>Weight (KN)</b>	<b><math>Wh_i^2</math></b>	<b><math>F_x</math> (KN)</b>
1	363.075	363.075	0.145
4.2	363.075	6404.64	2.55
7.4	363.075	19881.98	7.91
10.6	363.075	40795.11	16.24
13.8	363.075	69144.00	27.52
17	363.075	104928.67	41.76
20.2	363.075	148149.12	58.96
23.4	363.075	198805.35	79.12
26.6	260.85	184567.03	73.46
<b>Total</b>		<b>773038.975</b>	

To calculate the lateral load, primary load cases were used. The primary load cases considered for the design of buildings were live load (LL), dead load (DL) and earthquake load (EL). These loads were combined algebraically and the maximum analysis results were used for proportioning the members.

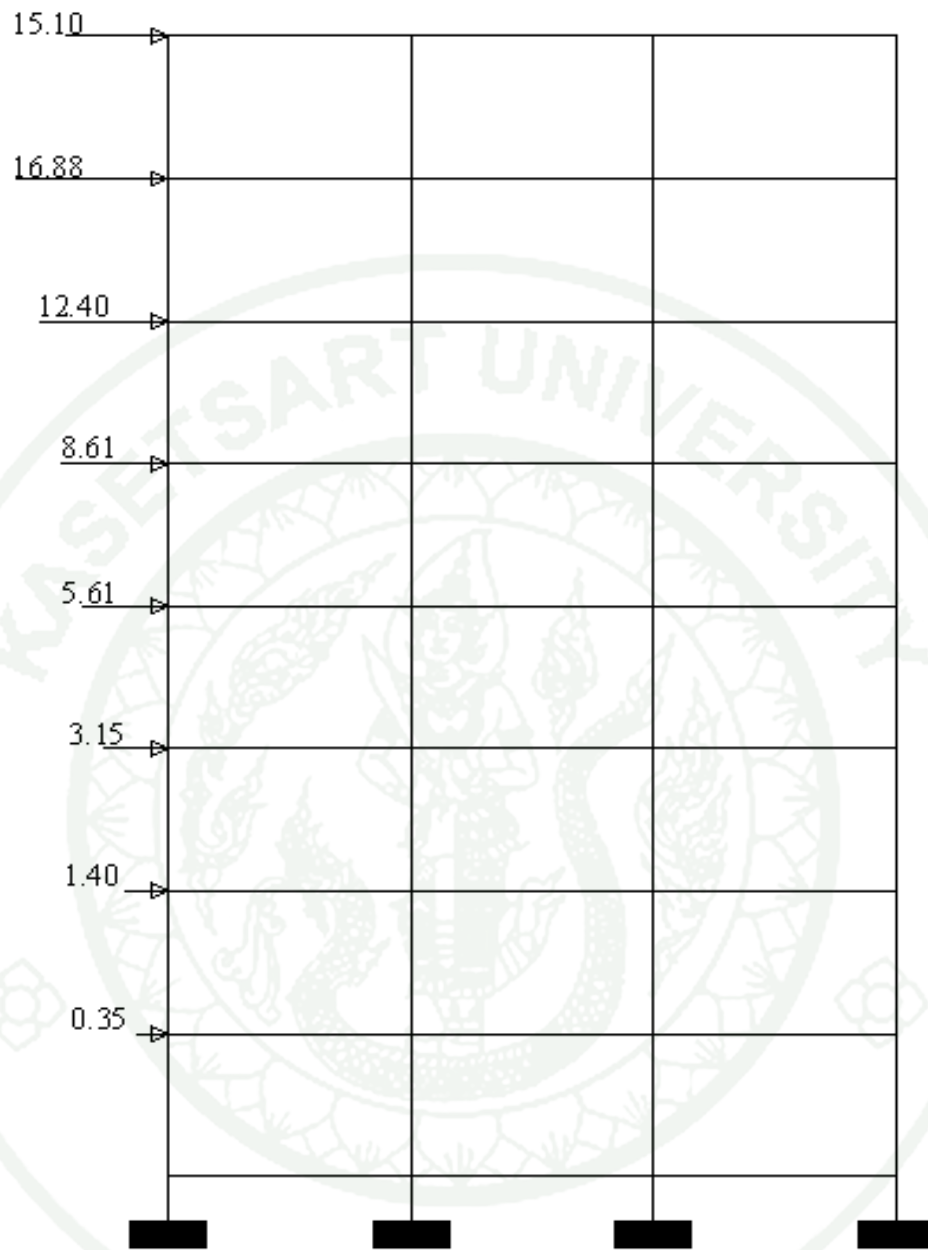
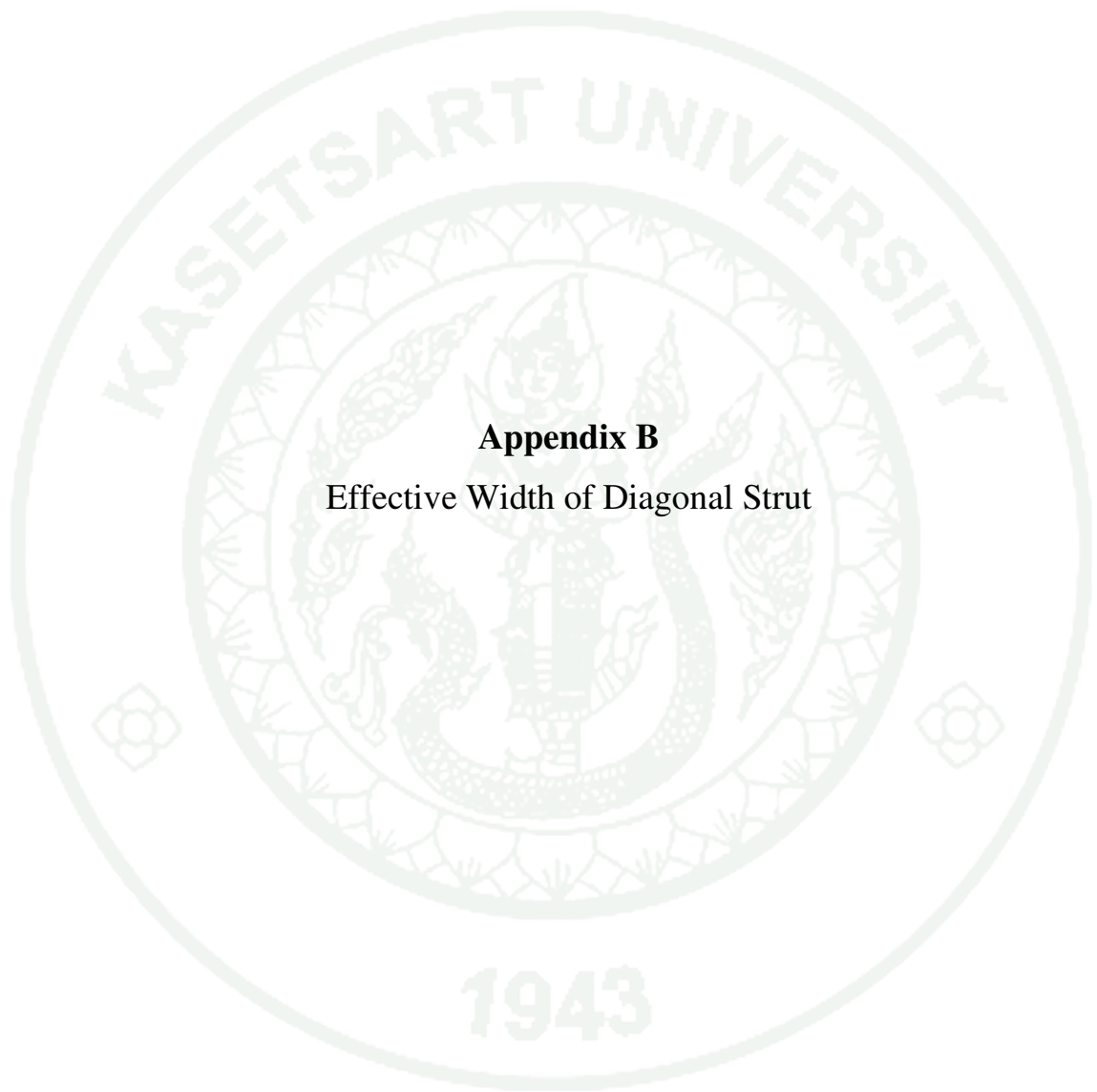


**Figure A1** Lateral load application to the structure



**Appendix B**  
Effective Width of Diagonal Strut

## Effective Width of Diagonal Strut

### 1. Calculation of width

It has been a usual practice around the world to provide masonry infill walls in a moment resisting reinforced concrete frame as partitions, exterior walls and walls around the stairs, elevators and service shafts. Masonry infill walls were considered as non-structural elements and are not considered in analysis and design. However, many research studies has recognized that it serve structurally. Masonry infill walls interact with the frame members when subjected to horizontal or lateral earthquake loading modifying the structural behavior of the moment resisting frames. When the frame is subjected to lateral loading, a translation of the upper part of the column in each storey and shortening of the leading diagonal of the frame cause the column to lean against the wall as well as compress the wall along its diagonal (Shrestha, 2008). This behaviour is analogous to the braced frame system as shown in Figure 2. Accordingly to model an infilled frame, the masonry panel is replaced by an equivalent diagonal strut whose thickness is same as that of the masonry panel and the length is the diagonal length of the compression side of the panel. However, different researcher had proposed different values for the effective width.

An original work on the investigation of the interaction between the infill panels and frames began in 1950s in Russia (Polyakov, 1956). In the United States Benjamin and Williams in 1958 (Benjamin et al, 1958) reported the first research on the lateral load behavior of infilled frames.

In 1961 Holmes proposed replacing the infill by an equivalent pin jointed diagonal strut of the same material and thickness with a width equal to one-third of its diagonal length. Mainstone (1971) proposed as relation which relates the width ' $a$ ' of infill to parameter  $\lambda$  given by equation (B2) and diagonal length  $r_{inf}$  as shown in the equation (B1). FEMA 273 use the relation proposed by Mainstone.

$$a = 0.175(\lambda h_{col})^{-0.4} r_{inf} \quad (B1)$$

$$\lambda = \left[ \frac{E_{me} t_{inf} \sin 2\theta}{4E_{fe} I_{col} h_{inf}} \right]^{1/4} \quad (B2)$$

Where;

$h_{col}$	=	Height of the column
$t_{inf}$	=	Thickness of infill wall
$r_{inf}$	=	Diagonal length of the infill wall
$E_{me}$	=	Modulus of elasticity of infill
$E_{fe}$	=	Modulus of elasticity of frame
$L_{inf}$	=	Length of infill
$h_{inf}$	=	Height of infill

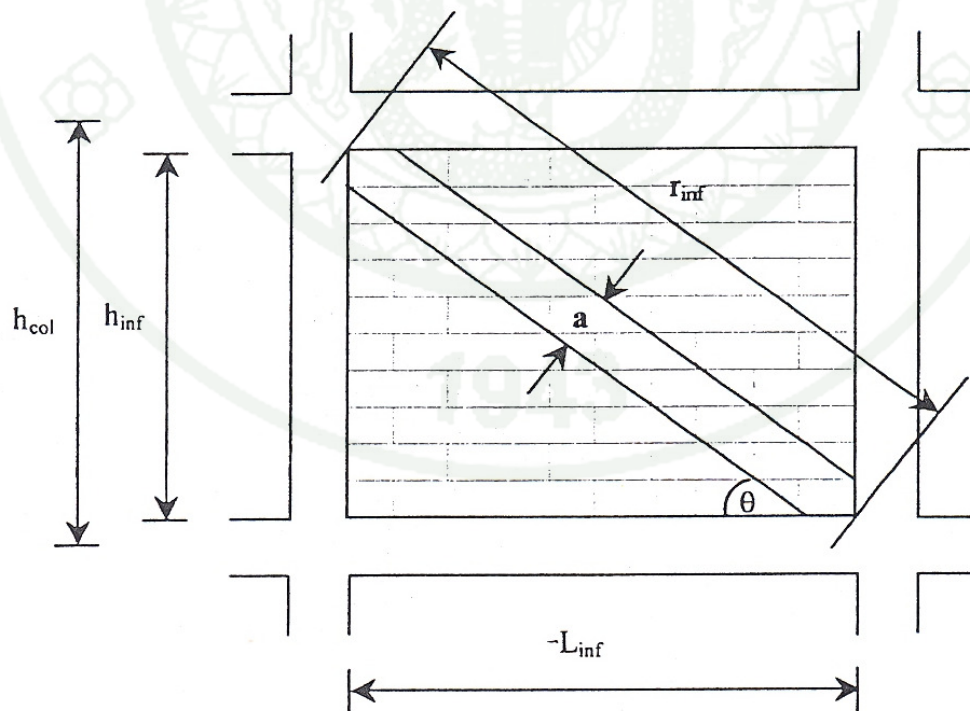


**Figure B1** Equivalent Diagonal Compression Strut Model

For 8-storey building model, following dimensions were used:

Beam depth = 0.5 m

Beam width = 0.3 m

Column width = 0.45 m

Column depth = 0.65 m

Length of beam = 5.0 m

Height of column ( $h_{col}$ ) = 3.2 m

Modulus of elasticity of infill ( $E_{me}$ ) =  $2.2 \times 10^6$  KN/m<sup>2</sup>

Modulus of elasticity of frame ( $E_{fe}$ ) =  $22.36 \times 10^6$  KN/m<sup>2</sup>

Thickness of infill ( $t_{inf}$ ) = 100 mm = 0.1 m

Height of infill ( $h_{inf}$ ) =  $h_{col}$  – depth of beam =  $3.2 - 0.3 = 2.7$  m

Length of infill ( $L_{inf}$ ) = length of beam – depth of column =  $5 - 0.65 = 4.35$  m

Diagonal length of infill ( $r_{inf}$ ) =  $\sqrt{h_{inf}^2 + L_{inf}^2} = \sqrt{2.7^2 + 4.35^2} = 5.12$  m

Moment of inertia ( $I_{col}$ ) =  $bd^3/12 = 0.45 \times 0.65^3/12 = 0.010298437$  m<sup>4</sup>

The parameter  $\lambda$  is calculated as shown below:

$$\lambda = \left[ \frac{E_{me} t_{inf} \sin 2\theta}{4E_{fe} I_{col} h_{inf}} \right]^{1/4}$$

$$\lambda = \left[ \frac{2.2 \times 10^6 \times 0.1 \times \sin 2\theta}{4 \times 22.36 \times 10^6 \times 0.010298 \times 2.7} \right]^{1/4} = 0.5306$$

The diagonal strut width is calculated using

$$a = 0.175(\lambda h_{col})^{-0.4} r_{inf}$$

$$a = 0.175(0.5306 \times 3.2)^{-0.4} \times 5.12 = 0.725 \text{ m}$$

The width of the diagonal strut for 8-storey building model = 725 mm

## 2. Calculation of lateral yield force and displacement

The lateral force capacity, for infill wall in the compression failure mechanism, can be calculated from equation (B3):

$$V_c = at_{\text{inf}} f'_m \cos \theta \quad (\text{B3})$$

Where

$$\begin{aligned} f'_m &= \text{Masonry compression strength} \\ &= 4000 \text{ KN/m}^2 \text{ (used in this study)} \end{aligned}$$

$$\frac{V_c}{t_{\text{inf}} l_{\text{inf}}} = \frac{at_{\text{inf}} f'_m \cos \theta}{t_{\text{inf}} l_{\text{inf}}} = \frac{0.725 \times 0.1 \times 4000 \times 0.85}{0.1 \times 4.35} = 566.67$$

The lateral force capacity, for infill wall in the sliding failure mechanism, can be calculated from equation B4:

$$\frac{V_f}{t_{\text{inf}} l_{\text{inf}}} = \frac{\tau_o}{(1 - \mu \tan \theta)} \quad (\text{B4})$$

Where

$$\begin{aligned} \tau_o &= 3\% \text{ of } f'_m \\ &= 0.3 \times 4000 = 120 \text{ KN/m}^2 \end{aligned}$$

$$\frac{V_f}{t_{\text{inf}} l_{\text{inf}}} = \frac{\tau_o}{(1 - \mu \tan \theta)} = \frac{120}{(1 - 0.3 \times 0.6207)} = 147.458$$

Selecting the minimum shear strength from the two mechanisms we get the maximum lateral force capacity of the infill.

$$\begin{aligned} V_m &= 147.458 \times t_{\text{inf}} \times l_{\text{inf}} \\ &= 147.458 \times 0.1 \times 4.35 \\ &= 64.144 \text{ KN} \end{aligned}$$

For the maximum lateral force, the maximum lateral displacement can be calculated from equation B5:

$$U_m = \frac{\varepsilon'_m r_{\text{inf}}}{\cos \theta} \quad (\text{B5})$$

Where

$U_m$  = maximum displacement

$\varepsilon'_m$  = masonry compression strain at the maximum compression stress

$$\begin{aligned} &= \frac{f'_m}{E_{me} \cos \theta} = \frac{4000}{2.2 \times 10^6 \times 0.85} \\ &= 0.00214 \end{aligned}$$

Therefore, the maximum displacement

$$\begin{aligned} U_m &= \frac{\varepsilon'_m r_{\text{inf}}}{\cos \theta} = \frac{0.00214 \times 5.12}{0.85} \\ &= 0.012895 \text{ m} \end{aligned}$$

The initial stiffness ( $K_o$ ) can be estimated as (equation B6):

$$K_o = 2 \left( \frac{V_m}{U_m} \right) \quad (\text{B6})$$

$$\begin{aligned} K_o &= \frac{2 \times 64.144}{0.012895} \\ &= 9948.66 \text{ KN/m} \end{aligned}$$

The lateral yielding force  $V_y$  and displacement  $U_y$  are (equations B7 and B8):

$$V_y = \frac{V_m - \alpha K_o U_m}{1 - \alpha} \quad (\text{B7})$$

$$U_y = \frac{V_y}{K_o} \quad (\text{B8})$$

$$V_y = \frac{64.144 - 0.2 \times 9948.66 \times 0.01285}{1 - 0.2}$$

$$= 48.11 \text{ KN}$$

$$U_y = \frac{V_y}{K_o} = \frac{48.11}{9948.66}$$

$$= 0.0048 \text{ m}$$

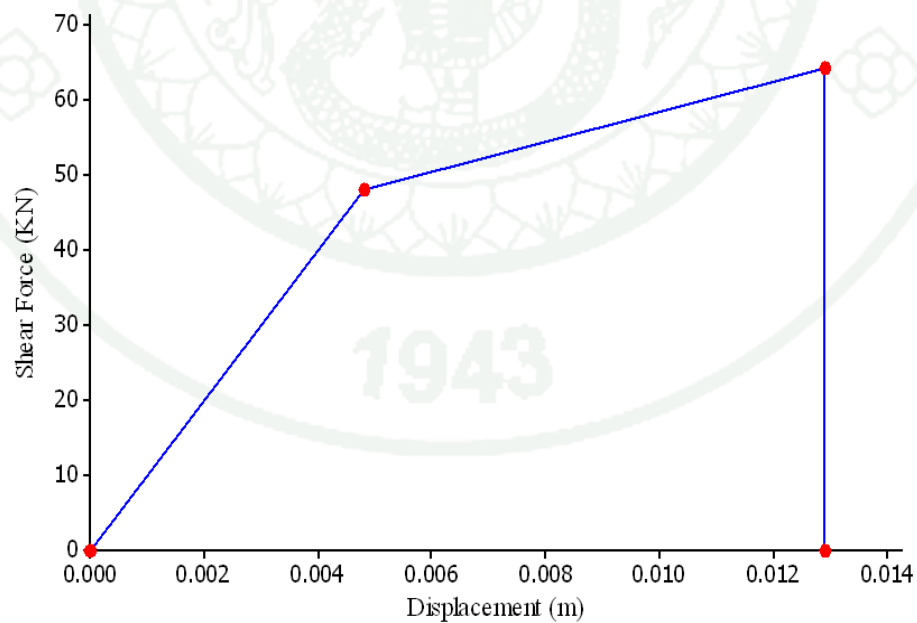


**Figure B2** Plot between displacement and shear force from the calculation

## CIRRICULUM VITAE

**NAME** : Mr. Karma Tshering

**BIRTH DATE** : May 10, 1976

**BIRTH PLACE** : Gomchu, Khaling, Tashigang Dzongkhag, Bhutan

<b>EDUCATION</b>	<b>: <u>YEAR</u> <u>INSTITUTE</u></b>	<b><u>DEGREE/DIPLOMA</u></b>
	2003 MNNIT Allahabad.	B.Tech. (Civil)
	2010 Kasetsart University	M.Eng. (Civil Engineering)

**POSITION/TITLE** : Structural Engineer

**WORK PLACE** : Phuentsholing City Corporation, Phuentsholing, Bhutan